ISSN 1028-8546

Azərbaycan Milli Elmlər Akademiyası
Fizika-Riyaziyyat və Texnika Elmləri Bölməsi
Fizika İnstitutu

2

Fizika

Cild
IX
2003

Bakı ✵ Elm

Выступление Лауреата Нобелевской премии,
Вице-Президента Российской Академии Наук

Жореса Ивановича Алферова

на Международной конференции,
посвященной 85-летию академика Гасана Багировича Абдуллаева.

Глубокоуважаемые члены Национальной Академии Наук Азербайджана, дорогие коллеги и друзья, члены семьи Гасана Багировича!

Во-первых, я сразу сказал, что я приеду на это собрание, которое посвящено 85-летию моего старшего друга и товарища, выдающегося советского, азербайджанского ученого-физика Гасана Багировича Абдуллаева.

Я рад возможности выступить на торжественном открытии международной конференции, посвященной памяти академика Г.Б.Абдуллаева. Мы сейчас посмотрели прекрасный фильм о Гасане Багировиче и очень трудно мне начинать свою речь, потому что есть такая вещь: те кого уже нет с нами, для близких людей и друзей они не умирают некогда. Они для нас всегда живы, особенно Гасана Багирович с его живым, необычайным характером, жизнерадостным, преданным идеалам – таким он был и останется в нашей памяти.

Мне посчастливилось встретиться с Гасаном Багировичем 50 лет тому назад. Я пришел в Физ-Тех, а Гасан Багирович уже второй год выполнял свою докторскую диссертацию в лаборатории профессора Дмитрия Николаевича Наследова. Мне посчастливилось очень много лет - 50 лет назад познакомиться с ним в старом здании Физ-Теха. Тогда в отделе «Физики полупроводников», руководимым Д.Н.Наследовым, существовали два сектора: сектор В.М.Тучкевича, в котором ваш покорный слуга начинал свою работу, и сектор Коломийца, где уже второй год выполнял свою докторскую диссертацию Гасан Багирович. Тогда, в 1953 году наш сектор занимался разработкой, получением и исследованием первых советских транзисторов, р-п переходов. Д.Н.Наследов и Коломиец продолжали старые традиционные исследования полупроводников. Одной из активных групп – была группа С.М.Рывкина. Академики Иоффе, Регель, Тучкевич, Рывкин, Коломиец, Стильбанс - для многих, сидящих в этом зале, это – родные имена. Гасан Багирович занимался исследованиями селена, старейшего полупроводникового материала. Он был предан селену всю жизнь и внес много интересного в исследования селена и селеновых приборов, с которых начиналась вся физика полупроводников и полупроводниковых приборов. Первый селеновый фотоэлемент был описан еще в трудах британских физиков в 1876 году. Гасан Багирович был очень любознательным. Однажды, он спросил меня: «Жорес! Вы мне объясните, как работает р-п переход?». И вот, гуляя по нашему коридору от библиотеки и дальше вглубь, я рассказывал об р-п переходе, об его электронно-дырочных частях и электрических свойствах . Выслушав мои объяснения, Гасан Багирович сказал: «Я думаю, что р-п переход – это наш коридор, справа – электроны, слева - дырки».

Гасан Багирович очень остро и быстро чувствовал новые направления в науке. Он блестяще защитил докторскую диссертацию, и после этого он уехал сюда, в Баку. Здесь раскрылся его организационный талант, и он скоро стал директором Института Физики.

В 1960-году в Баку Гасан Багирович организовал «Всесоюзное совещание по ударной ионизации и туннельному эффекту в полупроводниковых приборах» и точно оценил влияние туннелирования для понимания физики полупроводниковых приборов. Гасан Багирович сразу почувствовал, что явление туннелирования будет очень многое определять в полупроводниковых приборах. Благодаря его неутомимой энергии физическая наука в АН Азербайджана прогрессировала.

Гасан Багирович пронес через всю свою жизнь верность первому своему родному научному дому. Связь с Физико-Техническим институтом им. А.Ф. Иоффе была постоянна, он хранил верность Физ-Тех'у, его традициям. Он был исключительно великодушным ученым и добрым человеком. Свои связи с учеными Союза он поставил на служение подготовки научных кадров для родной республики. ***Все свои научные, дружеские связи он широко предоставлял своим ученикам****. Позже, когда он стал Президентом АН Азербайджана, особенно ярко проявился его талант* ***организатора науки****. Открылась возможность продемонстрировать широту своих научных взглядов. Качества, необходимые Президенту Академии Наук, которыми, несомненно, обладали Президенты Союзной Академии Вавилов, Несмеянов, Келдыш, Александров, были полностью присущи и Гасану Багировичу. Это способность понять основную идею, видеть перспективу научного направления, широта научных взглядов.*

Гасан Багировичу была присуще необычно острое чувство юмора. Когда в 1961-году он побывал в первой поездке в Америке, я спросил его о впечатлениях. Он сказал,

«Жорес, они уже построили материальную базу коммунизма, остается только изменить производственные отношения». Или, однажды он мне сказал « Жорес ты знаешь, что такое гетеропереход? Это супружеская пара, где муж и жена разной национальности».

Академик Абдуллаев широко практиковал посылку своих сотрудников на Международные конференции, во многие исследовательские центры за рубеж. В АН СССР Гасан Багирович быстро приобрел большой авторитет. К нему прекрасно относились, это я точно знаю, знаю персонально, президенты АН СССР – Несмеянов, Келдыш, Александров.

Еще одно замечательное качество Гасана Багировича-это верность дружбе! Когда я приехал в первый раз в Баку, я почувствовал еще одно замечательное качество Гасана Багировича – верность дружбе независимо от того, кто был его другом –будь это профессор и его учитель Д.Н.Наследов, или младшие научные сотрудники, без ученых степеней –А.А.Лебедев, Ж.И.Алферов, Б.Царенков

В 1972 г меня выдвинули в гл.-корр. АН СССР. Тогда я был относительно молодым человеком и поэтому не знал весь этот избирательный круг. Теперь я это хорошо знаю и могу сказать, какие надо предпринимать в данном случае действия. Перед собранием нашего отделения общей физики и астрономии, я приехал сюда, в Баку на одну из защит докторской диссертации. Я жил тогда в старом «Интуристе». После защиты мы с Гасан Багировичом, его помощником и В.И.Стафеевым поехали в номер, чтобы посидеть, поговорить – тем для разговора было много. Весь вечер мы проговорили, и уже был час ночи, когда Гасан Багирович сказал:

«Я думаю, мне надо было бы поехать на научное собрание АН. Я уверен в вас, вы пройдете. Я не поехал потому, что очень хотел посидеть с вами».

Я сказал: «Вы, знаете, Гасан Багирович, вообще-то ваше присутствие там необходимо. Будет лучше, если вы поедете».

- «Вы так считаете?»

- «Да, там один голос тоже является решающим. Так что будет лучше, если вы поедете».

Гасан Багирович обратился к своему помощнику: «Позвони в аэропорт и узнай, когда ближайший рейс». Было уже 2 ч. 10мин. ночи он сказал:

«Жорес! Зубная паста и щетка у вас найдется?»

Я сказал: «Да»

Он тут же заказал билет и мы вместе поехали провожать Гасан Багировича в аэропорт.

На следуший день, когда мы были на банкете сотрудника, раздался телефонный звонок и по телефону он попросил меня и сказал:

«Жорес, хорошо, что я поехал. Поздравляю тебя с избранием».

Гасан Багирович поздравил меня. Он сыграл очень большую роль в моей жизни.

Гасан Багирович был настоящий ученый – интернационалист. Он понимал, что наука интернациональна. Нет азербайджанской науки, русской и т.д., а есть ***Мировая наука.*** *В становлении научной общественности в Азербайджане, роль Гасана Багировича, как непревзойденного организатора науки, огромная. Он прекрасно понимал роль и значение АН СССР в развитии Академий наук всех республик, высоко ценил взаимосвязь между Академиями наук республик. Прекрасно понимал роль русской культуры, литературы, языка для прогресса национальной науки и культуры. Сегодня, когда молодое поколение имеет тенденцию пренебрегать русским языком, оно утрачивает возможность поглощать богатства одной из величайших сокровищ мировой культуры. Гасан Багирович глубоко понимал роль физики, физических открытий в общем развитии человеческой цивилизации. Гасан Багирович Абдуллаев прекрасно знал азербайджанскую литературу, искусство.*

Азербайджанский народ вправе гордиться своим замечательным сыном. Как бы он чувствовал себя, если бы он был жив? Наверно также как Келдыш или Александров. Когда мы вспоминаем своих Великих людей науки, хочется напомнить тем, от кого это зависит, насколько важна наука для развития экономики. Науку надо растить, беречь и она вернет вложенные средства сторицей.

Гасан Багирович понимал, что Наука – это гарант будущего благоденствия. Он жил во имя этого и мы не забудем его заветы.

Гасан Багирович вошел в Науку в Физ-Тех'е. Мы часто его вспоминаем. Значит, он всегда останется с нами в Физико-техническом институте им.А.Ф.Иоффе. Его портрет будет занимать достойное место в галерее академиков, выросших в стенах нашего Института.

A ROLE OF DISLOCATIONS AT PROCESSES OF THE MECHANICAL BENDING OF SILICON WAFERS

Sh.M. HASANLI, N.N. MURSAKULOV
Institute of Physics, Azerbaijan National Academy of Sciences,
Baku. Az - 1143, H. Javid av. 33

In this work, peculiarities of mechanical bending and deformation rate of silicon wafers under the influence of applied external forces have been studied. It has been shown that , for all investigated samples ,there are three characteristic sections with various slopes irrespective of the types of operation, orientation and thickness of the wafers. By increasing the applied force (F), the rate of deformation rises, reaches a maximum , and then starts to decrease not monotonically , but spasmodically by further increase of the force F. Experimental results are discussed on the base of the creation of dislocations and their corresponding plastic deformation. Furthermore we have shown that , there is a very good correlation between the density of dislocations and spasmodic decrease of the deformation rate. The analysis of the obtained results confirms the availability of plastic deformation and its inclination to localization during deformation process at room temperature .It should be added that , the spasmodic decrease of deformation rate , can be viewed as a self-organized deformable medium.

Keywords: Semiconductors, surfaces and interfaces, dislocations , deformation rate .

1. INTRODUCTION:

The bending and warping of large-diameter silicon wafers are one of the most difficult problems in manufacturing semiconductor devices and integrated circuits due to the mechanical and high-temperature treatments. In some author's [1, 2] opinion, the bending of wafers during mechanical cutting is created both by cutter displacement and occurrence of plastic deformation. According to [1], the plastic deformation of wafers during high-temperature processing is due to temperature gradient between edge and center of the wafers. Besides, it is shown, that under identical conditions of thermal processing, the wafer deformation is increased both with number of temperature cycles, and also with temperature rise. The latter can be qualitatively presented as follows: under the influence of thermal processing dislocations are created and as a result, relaxation of thermal strain occurs within the limits of the given sector. During the second thermal processing cycle, the formation of dislocations is considerably facilitated, resulting in their multiplication. The theoretical works [3-4] consider the influence of dislocations on the value of mechanical strength. The work by [4] shows the microplastic deformation in the crystals which is caused by reversible motion of dislocations. Moreover, the plastic deformation is considered to be inclined to localization at all stages of the plastic flow, and only its form changes at different stages. The works [4] slate that the nature of localization of deformation lies in self-organizing processes in deformable medium in the shapes of various sorts of waves. This is possible, because during deformation a flow of energy created by the loading device, runs through the crystal. The process of dislocations at given temperature will depend on: a)value of the applied force, b) value and allocation of local strains on the volume, c) microstructure of the crystal, availability of impurities of other phases etc.

Thus, the short analysis of the articles [1-4] shows, that the wafers' bending and warping may complicate the engineering procedures as photolithography, diffusion epitaxy and etc., and also may change the electrical characteristics of finished semiconductor devices and chips. Therefore, the questions connected with the problem of mechanical strength, and improving semiconductor devices production technology of devices, still remain topical and need to be further investigated.

The present work deals with study of the peculiarities of mechanical bending (W) and bending rate of silicon wafers under the applied force (F), and also their structures after various manufacturing operations.

2. EXPERIMENTAL TECHNIQUE and SAMPLES FOR INVESTIGATION

The investigations were carried out on both n and p-type silicon wafers having diameters of 100 mm and various surface orientations (see table 1). It should be note that, there are different testing methods for investigation of mechanical strength of semiconductor materials such as, torsion's, squeezing, tension, bending etc. among which three or four point contact and axially-symmetric methods occupy a special place. Because, they do not need takings special measures for fastening the samples, and also allow - while testing at room temperature - to receive strains of big value. However, according to [5], at three or four point contact methods of sample testing, the edge effect caused by cutting and grinding can greatly influence on the value of mechanical strength. To avoid this, the work [5] offered the axially symmetric method of plate bending, which is widely used by various researches. In the given work, the experimental results of mechanical bending and deformation rate of silicon wafers were determined by a semi-automatic apparatus designed and made on the base bending methods of hard plates, having symmetrical axis [6]. This method was chosen because it, first, allows to directly test the wafers which are used in the semiconductor devices and large scale integrated circuits production, second, allows to exclude the influence of edge effects on the value of mechanical strength. The experiments were conducted at the room temperature.

3. EXPERIMENTAL RESULTS AND DISCUSSIONS

The experimental results of dependency of mechanical bending *(W)* and rate of deformation *V* on the applied force *(F)* after various technological operations are presented in fig. 1-4. The figures 1-4 show that for all investigated samples, three characteristic sections with various slopes can

be observed irrespective of types of operations, orientation and thickness' of the wafers (dependence $W=f(F)$ for other processes given in the table are observed wears analogous character):

1) the first section (1) – a linear proportionality exists between applied force and bending value. As it is apparent from the figures, the linear dependency for different samples is maintained in the interval of the plate thickness from 0.30 to 0.50(μm).

2) the second section (2) - the increase in bending of plates has a monotonic character with increasing of the applied force. 3) the third section (3) - by increasing the applied force, the bending value increases up to destruction. 4) the slopes angles in these section(1,2,3) differ from each other. For example, after grinding process; the value of slopes are: 1) $arctg\alpha_1 = 25$, 2) $arctg\alpha_2 = 11$ and 3) $arctg\alpha_3 = 26.5$ (see fig.1). The comparison of these values indicates that the least slope is observed in the section of monotonic dependency $W = f(F(N))$ (section 2). 5) by increasing the applied force (F), the rate of deformation (V) rises, reaches a maximum, and then starts to decrease not monotonically, but spasmodically by further increase of the force F. 6) At various technological operations, the value of V varied in the interval $(1.5*10^{-4}$-$2.2*10^{-4})$m/sec.(see fig.1-4).

Table 1

Process	Orientation	Thickness(μm)
After grinding	100	475
After P diff. .	111	480
After B diff.	111	470
After epitax.	100	475
After oxidation	111	500
.After Al contact	111	505

Theoretical dependence of bending value on applied external force calculated by the formula (1) is also presented on the figures:

$$W=3P(1-\nu^2)r^2/(2\pi Eh^3)*\{a^2/r^2[1+(1-\nu)(a^2-r^2)/(2(1+\nu)b^2)]-(1+Ln(a/r))\} \quad (1)$$

where a -is the radius of fulcrum, b- is the radius of around wafer which is related to the sides of an square wafer with the relation $b=b'(1+2^{0.5})/2$,r,P,h,ν, and E are the radius of puanson, the applied load, the thickness of the wafer, Poisson coefficient and Young modulus, respectively. The comparisons of theoretical and experimental values of bending presented in figures (1-4) show that in sections (1) they agree quite well with each other. However, in the second and third sections, strong deviations are observed. From the plots, it is seen that the experimental dependencies $W=f(F(N))$ are well-approximated polynomials of 5-th order of form $W=B_0+B_1F+B_2F^2+B_3F^3+B_4F^4+B_5F^5$, where, B_0, B_1, B_2, B_3, B_4 and B_5 are constants and F is the applied load. There deviations can be due to the existence of dislocations which are created in the wafers during their bending process which have not been taken into account in the theory. The similar regions are found at squeezing of Si and Ge single crystals and also at tension of various polycrystalline materials [7-9]. In the work by [7], the obtained results are explained by the concept of heterogeneous dislocations created at squeezing of the samples.

It is shown in the work [4] that between the rate of deformation and density of dislocations created during deformation process, these exists the following dependency: $V \cong \sigma Vm\ (Q/E)$ (2) where, σ - internal stress of the wafers ,Vm is the velocity of testing machine and $Q \cong \sigma\ L\ b\ \rho_1$ (3) is heat scattering energy of mobile dislocations in unite volume, L is the average distance between dislocations, b is the Buguer's vector and ρ_1 is the density of mobile dislocations, E the energy of fixed dislocations in unit volume is given by $E \cong Gb^2\rho_2$ (4). Where, G is the shear modulus, ρ_2 is the density of fixed dislocations.

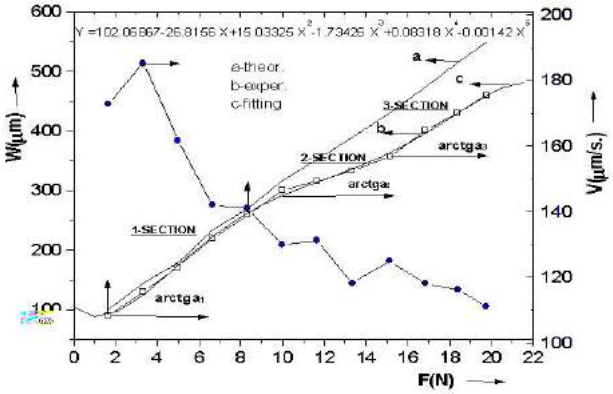

Fig.1. Dependence of the wafer bending and deformation rate on the applied laod after grinding process

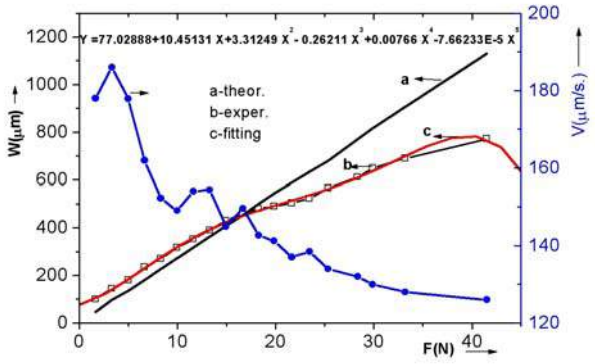

Fig.2. Dependence of the wafer bending and deformation rate on the applied laod after oxidation process.

The following is an explanation of the experimental data mentioned above from the standpoint of buildup and motion of dislocations under influence of the applied force F. In the first section (1), under the external force F, the wafer bends and deforms, resulting in the creation of dislocations. They move on various slip planes and then are unorderly situated on them. Increasing the value of F further, results in an increase in both concentration and density of mobile dislocations on these planes. Therefore, according to the formula (3), the increase in density of the mobile dislocation will give rise to the increase in Q energy scattering into heat, and as a result, the wafer will heat up. Heating the wafer, in turn, will promote a rise of new dislocations and an increase of their density. In this case according to the formula (2) the wafer's deformation rate will also increase. The given idea is confirmed by experimental results of dependencies of deformation raate on the value of the applied force (see fig. 1-4). Due to the easy and reversible motion of dislocation at

large distances, the observed resilient deformation of wafers takes place in order words, the linear proportionality W= f *(F)* is consistent in section (1). In section (2) with a further increase of the applied force, the number of dislocations and simultaneously, their motions rate will increase in different crystallographic directions. For this reason, in certain crystallographic directions, an accumulation of dislocations occurs. Stored dislocations elastically interact between themselves, creating obstacles for the motion of other dislocations. The further movement of dislocations is impeded and as a result, the density of fixed dislocations is enlarged. Thus, the obstacle experience major pressure and the wafer is plastically deformed. Apparently, the availability of a plastic deformation is the reason for observed monotonic enlargement of the wafer's bending (see fig.1-4). It should be underlined, that in accordance with the formula (4), with the increase of fixed dislocations density, their energy *E* also increases, and according to the formula (2), the rate of wafer's deformation should also decrease. This statement is confirmed by the experimental results shown in fig.(4). As it is seen from the figures, despite increasing the value of F, both the slope of the second section and the wafer deformation decrease. Thus, the decrease in the rate of deformation is not monotonous but it is in spurts. The saltatory change in deformation rate is apparently, connected with the fact that part of dislocations stored at hindrances, under certain conditions are able to overcome their barrier and move further. As a result, the saltatory motion of dislocations takes place resulting in the saltatory change of the wafer's deformation rate. It should be noted that, the hindrance to the motion of dislocations and saltatory change in deformation rate might be caused by the availability of impurities and other defects in the wafer and thereby inhibit the motion of dislocations and promote formation of dislocation avalanches. In the third region, by increasing the external force further, the number of dislocation is increased and the process of dislocation accumulation is continued. At the same time, part of dislocations having opposite sign may annihilate which causes a partial relaxation of the internal stresses. Besides a part of dislocations may move from one slip plane to the other one, and then, the number of dislocations on the latter maybe increased, resulting in the hardening of the wafer and increase of its bending and consequently in the decrease of deformation rate. The increase of accumulation of the dislocations in certain crystallographic direction and their interaction through the neighboring slip planes may cause stresses in separate directions. At values of stress larger than the wafer's breaking point, some cracks may be formed in it. However, the process of a crystal fracture will depend on the kinetics of the cracks growth.

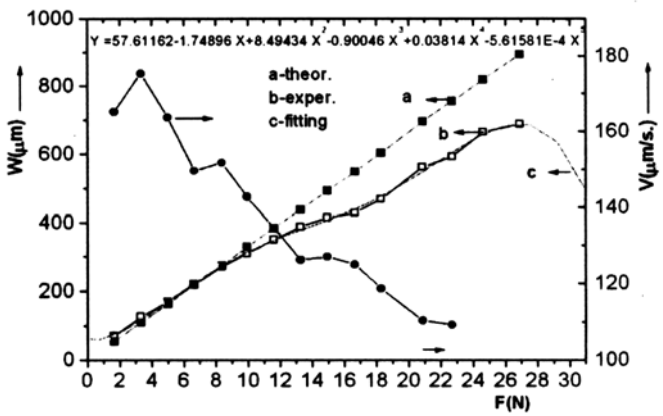

Fig.3. Dependence of the wafer bending and deformation rate on the applied load after epitaxy process

From the analysis of experimental results are revealed the following peculiarities of mechanical bending and rates of deformation of silicon wafers after diverse manufacturing operations:

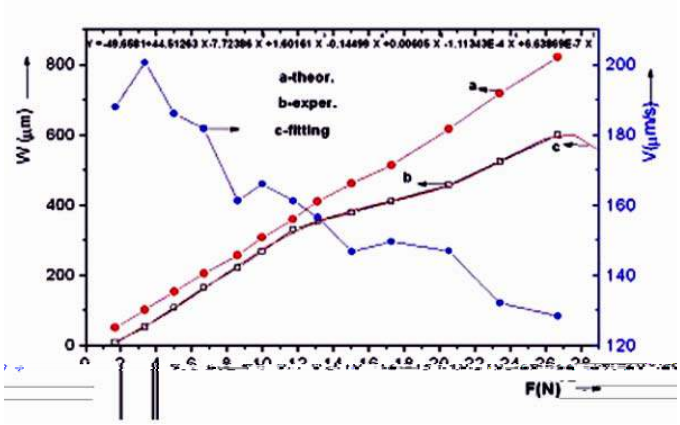

Fig.4. Dependence of the wafer bending and deformation rate on the applied load after phosphor(P) diffusion process.

1) Irrespective of the type of operation, orientation and tickness of wafers on curves *W=f(F)* are observed. three characteristic section with various slopes, a) the section (1)-a linear proportionality exists between *W* and *F*. б) the section(2) of monotonic dependence *W=f(F)*, c) the third section (3) by increasing the applied force, the bending value increases up to destruction.

By increasing the applied force *F*, the rate of deformation rises, reaches a maximum, and then starts to decrease not monotonically, but spasmodically by further increase of the force *F*.

Experimental results are discussed on the base of the creation of dislocations and their corresponding plastic deformation.

[1] *Y.Trau.* Basis of technology superlager integrated circuits. 1985, p. 246-250.

[2] *D. Thelbaut and L. Jastrebski*. RGA Review, 1980, v.41, p.592.

[3] *E.S. Aifantis.* J. Eng. Mat. Techn., 1984, v.106,p.326.

[4] *L.B. Zuev, V. I. Danilov*. Theor. and Appl. Fracture mech., 1998, v. 30 , p.175.

[5] *Yu. A. Kontsevoi et al*. Plasticity and durability of semiconductor materials and structures, 1982, p. 139.

[6] *Sh. M. Gasanly and E. K. Guseynov*. Turkish Journal of Physics, 1995, 19, N1 p.644

[7] *V. P. Alechin.* Physics of strength and plasticity of surface layers of materials. 1983,p. 54-60.

[8] *M. B. Mejenniy, M. G. Milvidski et al*. Fizika tverdogo tela, 2001, v.43, №1, p. 47.

[9] *N.N. Peschanskaya, P.N. Yakushev et al*. Fizika tverdogo tela, 2002, v.44. №9, p.1609

Ş.M. Həsənli, N.N. Mursakulov

SİLİSİUM LÖVHƏSİNİN MEXANİKİ ƏYİLMƏSİ PROSESİNDƏ DİSLOKASİYALARIN İŞTİRAKI

Bu məqalədə xarici qüvvələrin təsiri altında silisium lövhəsinin mexaniki əyilmə və əyilmənin deformasiya sürətinin xüsusiyyətləri tədqiq edilmişdir. Göstərilmişdir ki, bütün tədqiq edilən nümunələr üçün texnoloji proseslərin növündən, kristalloqrafik orientasiyasından və lövhələrin qalınlığından asılı olmayaraq müxtəlif meyilli üç xarakterik oblast müşahidə edilir. Tətbiq edilmiş qüvvənin (F) qiyməti artdıqca deformasiya sürəti artır, maksimuma çatır və qüvvənin sonrakı artmasına müvafiq olaraq sıçrayışla azalır.

Eksperimental nəticələr əyilmə deformasiyası zamanı dislokasiyaların yaranması ilə izah edilir. Bundan başqa dislokasiyaların sıxlığı ilə deformasiya sürətinin sıçrayışla azalması arasında yaxşı korrelyasiya olmasını göstərmişdir. Alınmış nəticələrin analizi plastik deformasiyanın otaq temperaturunda mümkünlüyünü və deformasiya prosesi zamanı onun lokallaşmaya meylli olmasını təsdiq edir. Bu mülahizələrə onu əlavə etmək lazımdır ki, deformasiya sürətinin sıçrayışla azalmasına deformasiyaya uğrayan mühitin öz-özünü tənzimləməsi kimi baxmaq olar.

Ш. М. Гасанли, Н.Н.Мурсакулов

РОЛЬ ДИСЛОКАЦИЙ В ПРОЦЕССАХ МЕХАНИЧЕСКОГО ИЗГИБА КРЕМНИЕВЫХ ПЛАСТИН

В этой работе изучались особенности механического изгиба и скорости деформации кремниевых пластин под действием приложенных внешних сил. Показано, что для всех исследованных образцов, независимо от вида технологических операций, кристаллографической ориентации и толщины пластин наблюдаются три характерных областей. При увеличении приложенной силы (F), скорость деформации растет, достигает максимума, и затем начинает уменьшаться не монотонно, а скачкообразно с дальнейшим увеличением приложенной силы F. Экспериментальные результаты объясняются на основе зарождения дислокаций в процессе изгиба. Кроме того, показано, что, имеется хорошая корреляция между плотностью дислокаций и скачкообразным уменьшением скорости деформации. Анализ полученных результатов подтверждают возможность при комнатной температуре пластической деформации, и стремление ее к локализации в течение процесса деформации, а также скачкообразное уменьшение скорости деформации, может рассматриваться как самоорганизация деформируемой среды.

Received: 19.05.03

GROUND REMOTE SENSING OF BACKGROUND AIR POLLUTION LAYER ON THE CITY OF BAKU BY THE DAY SKY BRIGHTNESS

F.I. ISMAILOV
Azerbaijan National Aerospace Agency Institute of Ecology
370106 Baku, Azerbaijan, 159

Remote sounding of air pollution by scattered sun light has proved to be useful for analysis background level in conditions of the city smoke. This paper deals with the investigation of the space characteristics of altitude air pollution layer on Baku from the day sky light measurements.

Introduction

The background air pollution layer in conditions of Baku smoke has been formed during many years. Study of modern state of this layer is one of the cardinal problems of ecological monitoring of background level of anthropogenic impact on all Absheron Peninsula.

It is known that the intensity of background air pollutions is determined by the number of background aerosol particles which are very optically active at effective wavelength λ=0.55μm of solar radiation [1-3]. Ground remote sensing of air pollution by incoming solar radiation is of great interest. This method is very informative and technically simple [2, 3].

The present work includes the information about the results of research of space situated and different characteristics of background air pollution layer on Baku from the day sky light measurements which carried out with actinophotometric device [4].

Methods of the research and results

The day sky light brightness depends on changes of optical depth τ and scattering functions $f(\theta)$ of background aerosol particles; where θ is the scattering angle [2, 3]. The determination of these parameters is based on measurements of illumination of direct radiation S and the sky brightness $B(\theta)$ in solar almucantar for any time:

$$\tau = \ln p = \frac{1}{m_0} S / S_0 \qquad (1)$$

$$f(\theta) = \frac{1}{m_0} B(\theta) / S_0 \qquad (2)$$

where S_0 is the solar constant, P is the atmosphere transmittance, m_0 is the optic mass of atmosphere.

The scattering angle is determined according to formula [2]:

$$\cos\theta = \cos Z \cos Z_0 + \sin Z \cdot \sin Z_0 \cdot \cos\Phi \qquad (3)$$

where Z_0 is the solar zenith angle, Z is the sensing zenith angle, ϕ is the sensing azimuth angle.

The background level of air pollution can be estimated from the following empirical expression [3]

$$\upsilon = 2{,}2 \cdot 10^{-11} \cdot \sigma \qquad (4)$$

where υ is the volume concentration of background aerosol, σ is the scattering coefficient at wavelength ∂=0.55μm.

Experiment has been carried out on the actinophotometer [4] which were constructed specially for research of atmospheric transparency. Figure 1 shows the medium Bouger curves for the west and east of Baku. These curves derived from observations data by Bouger – Lambert long method [2] and averaged over the period from the sunrise to the afternoon (curve 1) or from the afternoon to the sunset (curve 2).

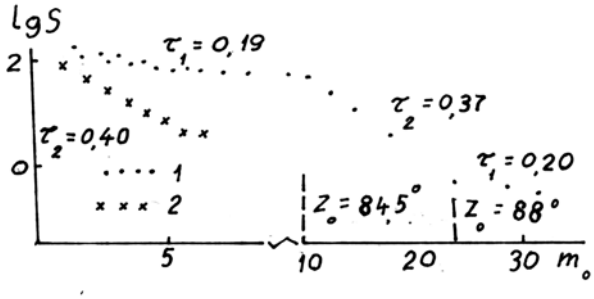

Fig.1. Medium Bouger curves for observed points:
1 - Mushvigabad settlement; 2 - Ahmadli settlement.
τ - optical thickness in directions to the pollution layer (τ_2) and in other directions (τ_1) in $\frac{w}{m^2 \cdot sr \cdot pm}$.

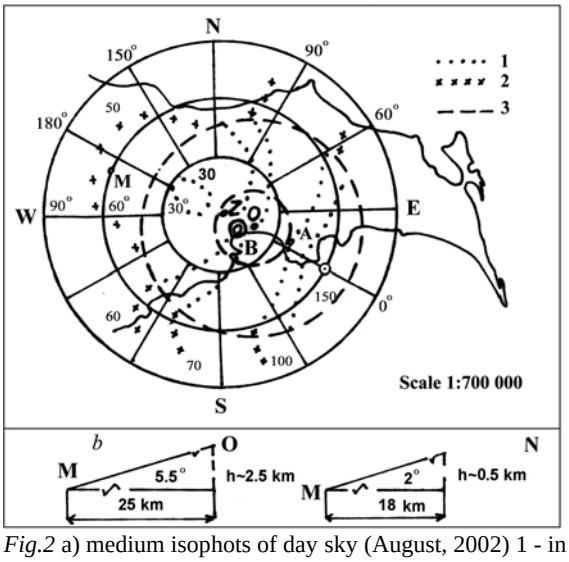

Fig.2 a) medium isophots of day sky (August, 2002) 1 - in region (3) of pollution layer, 2 - out of this region, M – Mushvigabad, A - Ahmadli, Z - zenith, O - center of pollution layer, B - Baku. b) h_2 - upper and h_1 - low altitude of boundaries of pollution layer.

As seen from figure 1 the Bouger curves in the region m_0=10÷29 have been observed the "anomaly" which apparently is connected with the background pollution layer. Therefore, dependence of optic thickness from relative air mass can apply to study background air pollution on city in detail.

The angular dependence of the scattered sky light are shown on the figure 2. This dependence is represented by day sky light measurements in different almucantars and verticals on territory o the institute of Ecology.

The results of measurements were graphed in the form of maps of the radiance on sky sphere. Figure 2a show high values for the forward scattering directions from zenith to horizon, a minimum at the scattering angle about $(Z=20^\circ, \Phi=180^\circ)$ and slightly increasing values towards the backscatter azimuth angle of 180°. This behavior is typical for background aerosol scattering.

Angular dependence of diffuse light from the day sky contains information about the geometry of distribution of background air pollution layer. For estimate space size of this layer we determine relative values of the scattered solar radiation in different angles region $(\theta_i, \theta_i - \pi/6$ as follows:

$$\Gamma_i = \int_{\theta_i - \Delta\theta_i}^{\theta_i} f(\theta)\sin\theta d\theta \Big/ \int_0^{\pi} f(\theta)\sin\theta d\theta \qquad (5)$$

In table 1 there have been presented values of ratio the (5) for $\Delta\theta = \pi/6$ and $i = 1 \div 6$.

Values of quantity (5) in per cent (%)

Table 1

θ_i in degrees	30	60	90	120	150	180	- 30	- 60	- 90	- 120	- 150	- 180
Γ_i, in %	13	10	9	7	5	4	13	11	10	6	6	4

As it is seen from table 1 isophots have very asymmetric structure on direction perpendicular to the solar vertical. Figure 2a shows that the center of pollution layer is observed at point 0 with the spherical coordinates about $z = 22{,}5^\circ, \Phi = -5^\circ$.

It was impossible to evaluate altitude propagation of air pollution layer. In the following figure 2b it has been found altitudes of upper and low boundary of pollution layer for angles of view (figure 1) and distances on the earth (figure 2a) from observed point M.

Values of average parameters of air pollution layer on Baku are given in table 2.

Conclusion

1. The day sky brightness and direct solar radiation measurements were carried out with actinophotometric device [4] in conditions of Baku smoke. It is found that the strongly background air pollution layer on Baku have place.
2. The results of calculations of mean characteristics of background air pollution layer are given.
3. It is shown that the method of ground remote sensing of air pollution layer by the incoming solar radiation may be used to receive the most capacious information in conditions of the city smoke in view of their regularity.

Characteristics of background air pollution layer on Baku.

Table 2

Parameter	Value
Thickness	$\Delta h = h_2 - h_1 = 2$ km
Radius of cross section	$R = 17$ km
Space volume	$V = \pi R^2 \cdot \Delta h = 1{,}8 \cdot 10^3$ km^3
Optical thickness	$\Delta\tau = \tau_2 - \tau_1 = 0{,}2$
Optical density (scattering coefficient)	$\upsilon = \frac{\Delta\tau}{\Delta h} = 0{,}1$ km^{-1}
Volume concentration	$v = 2{,}2 \cdot 10^{-11}$
Mass concentration (density of particles $p = 2\,g/sm^3$ [3])	$M = p \cdot V = 44 \frac{mg}{m^3}$
Mass of layer's pollution	$m = M \cdot v = 80t$

[1] *K.T. Whitby*. The physical characteristics of sulfur aerosols. Atmospheric Environment, v. 12, p. 135 - 159.

[2] *G.P. Guchin.* Methods, instrumentation and results of atmospheric spectral measurements. L.: Gidrometeoizdat, 1988, p. 32 (in Russian).

[3] *F.I. Ismailov*. Parameterization of effects of light scattering by submicronic aerosol. Baku, 1992, Cand. dis., p. 103-108 (in Russian).

[4] *F.I. Ismailov*. Method and technical solutions of informativity increase of actinometric measurements, - Journal "Fizika", Baku, 2002, v. 8, №1, p. 47-49.

F.İ. İsmayılov

BAKI ŞƏHƏRİ ÜZƏRİNDƏ HAVANIN FON ÇİRKLƏNMƏSİ QATININ SƏMANIN GÜNDÜZ PARLAQLIĞINA ƏSASƏN YER ÜSTÜ MƏSAFƏDƏN TƏDQİQİ

Böyük sənaye şəhəri şəraitində fon səviyyəsinin analizi üçün Günəşin səpələnən şüalanmasına əsasən havanın çirklənməsinin məsafəli öyrənilməsi faydalı olduğu aşkar edilir. İşdə Bakı şəhəri üzərində səmanın gündüz işığına əsasən havanın çirklənməsinin yüksək qatının fəza xüsusiyyətləri öyrənilir.

GROUND REMOTE SENSING OF BACKGROUND AIR POLLUTION LAYER ON THE CITY OF BAKU BY THE DAY SKY BRIGHTNESS

Ф.И. Исмаилов

НАЗЕМНОЕ ДИСТАНЦИОННОЕ ИССЛЕДОВАНИЕ ФОНОВОГО СЛОЯ ЗАГРЯЗНЕНИЯ ВОЗДУХА НАД ГОРОДОМ БАКУ ПО ЯРКОСТИ ДНЕВНОГО НЕБА

Дистанционное зондирование загрязнения воздуха по рассеянному излучению Солнца является важным для анализа фонового уровня в условиях крупного промышленного города. В работе исследуется пространственные характеристики высотного слоя загрязнения воздуха над городом Баку по измерениям света дневного неба.

Received: 19.05.03

PHOTOELEMENT WITH SCHOTTKY BARRIER ON THE BASE OF THE MAGNESIUM PHTALOCYANINE ORGANIC SEMICONDUCTOR

M.M. PANAHOV, S.A. SADRADDINOV, J. H. JABBAROV, B.SH. BARKHALOV

Baku State University,

Z. Khalilov str.,23, Baku, 370145

In this work the results of the study of the influence of the thermal processing in oxygen atmosphere on photoelectric properties of the Al/MgPc Schottky barrier in SnO_2 /MgPc/Al thin film structures are presented.

At present the great variety of film structures with the Schottky barrier on the base of inorganic semiconductors is used in microelectronics [1, 2]. At last years similar structures are created and broadly investigated also on the base of the organic semiconductors (OS), in particular, on the base of phthalocyanine and its complexes with metals [3, 4]. Development of the doping technology for OS will enable these compounds to form a serious competition to inorganic materials used now, and possibly, fabricating the semiconductor devices with qualitatively new characteristics.

By choosing respective electrode material one can form ohmic [5, 6], as well as rectifying [3, 6, 7] electrical contacts to semiconducting metal-organic compounds of the phthalocyanine class.

The investigation of the current characteristics of "sandwiches", in which OS magnesium phthalocyanine (MgPc) layer was equipped by Al or Ag electrodes have been conducted elsewhere [7]. Non-symmetrical volt-ampere characteristics (VAC) were explained by the formation of the p-n-junction in MgPc as the result of substitution of Mg atoms by Al ones during the heat treatment. The further study of the similar structures have shown the presence of the Schottky barrier in the Al/MgPc interface.

In this work the results of the study of the influence of the heat treatment in oxygen atmosphere on photoelectric properties of the Al/MgPc Schottky barrier in SnO2/MgPc/Al thin film structures are presented.

VAC of the Al/MgPc/Al thin film structures studied elsewhere [7], were symmetrical, while current in the Al/MgPc/Ag structure depended on polarity of the applied voltage. The fact that MgPc is a p-type semiconductor [7], and forward direction corresponds to the positive potential on Al-electrode, evidenced for the presence of the Schottky barrier in the Al /MgPc interface.

MgPc used by us in studies was additionally cleaned by the double sublimation in the vacuum. The SnO_2 /MgPc/Al thin film structures have been obtained by the thermal evaporation in the vacuum (~10^{-6} Torr) consistently MgPc and second Al electrode onto the quartz substrate, on which beforehand was deposited the transparent SnO_2 electrode. The thickness of the layer was 0,2÷2,0μm. The doping by the oxygen was produced by endurance of the film in the oxygen atmosphere at 390÷420K. All measurements have been conducted in the vacuum ~10^{-5} Torr.

The presence of the Schottky barrier in Al/MgPc interface determines main electrical as well as light characteristics of the element, which are described below.

Study of the dark current characteristics of the "sandwich" structures on the base of the *SnO_2 /MgPc/Al* structures shows, that the doping by oxygen essentially changes all electrophysical characteristics of the system. The height of the Schottky barrier, determined from the slope of the temperature dependence of the current, for the sample processed in the oxygen atmosphere (Φ=0.5eV) in two times is less, than for the sample processed in the high vacuum (Φ=1.0eV).

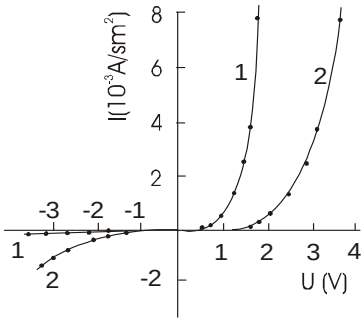

Fig. 1. Volt-ampere characteristics of the SnO_2 /MgP_c/Al structures, annealed in oxygen atmosphere: 1-dark, 2-under constant illumination L=5·10^4Lx.

On the fig. 1 the dark and light VAC are presented for the photoelement on the base of the SnO_2 /MgPc/Al, processed in the oxygen atmosphere at room temperature. It is seen from VAC that the dependence *I* on *U* is essentially non-symmetrical, which is connected with the effect of the Schottky barrier. At the illuminating the structure, non-equilibrium charge carriers form which influence on all characteristics of the structure.

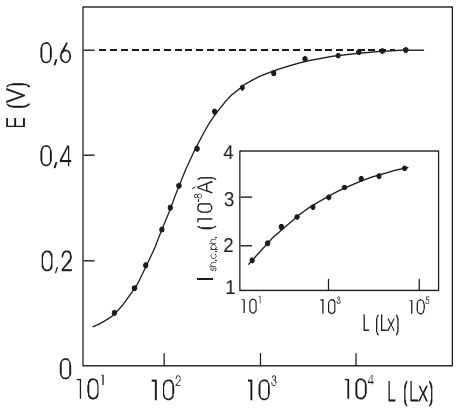

Fig. 2. The dependence of the photo e.m.*f.* on the illumination. Insert- short circuited photo-e.m.*f.* versus illumination.

Under the illumination the separation of the charge carriers between the *Al* and *MgPc* occurs and the photovoltaic effect is observed. On the fig. 2 the dependence of the photo-e.m.f. on illumination intensity *L* has been shown. As one can

see from the fig. 2, at great L the resistance of the barrier layer decreases so, that photo-e.m.f. approaches to the saturation – limiting value 0.5-0.6eV for the samples with the doped MgPc layer.

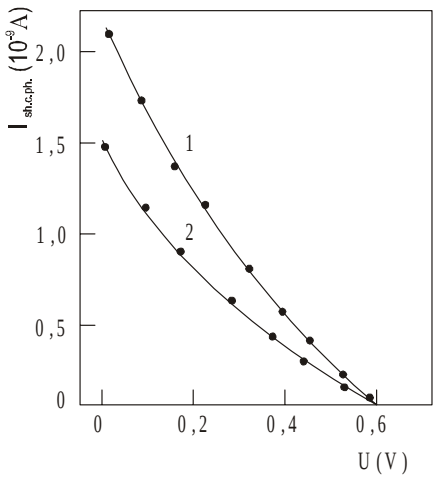

Fig 3. The dependence of the short circuited photo current $I_{sh.c.ph.}$ on the reverse bias voltage U, under illumination: -$8 \cdot 10^3$Lx, 2-10^4Lx.

This value corresponds to the Schottky barrier height, obtained from the analysis of the dark volt-ampere characteristics. On the insertion of fig.1 the dependence of the short circuit photocurrent I_{sc} on the light intensity L is shown. It is seen that the short circuit photocurrent I_{sc} increases with growing of the light intensity L.

The height of the Schottky barrier also can be determined from the dependence of I_{ph} versus the bias voltage under constant illumination. The dependence of the short circuit photocurrent on the inverse bias voltage is shown in fig.3. As would be expected, at the positive potential on the transparent SnO_2 electrode with the increase U the I_{sc} current decreases, and at $U \approx 0.6$ V for the MgPc layer doped by oxygen ($U \approx 0.1$V for source, which is determined from the dependence I versus $1/T$) $I_{sc}=0$, i.e. at $U \approx 0.6$V the short circuit current disappears. The determined value 0,6eV corresponds to a height of the potential Schottky barrier for the SnO_2/MgPc/Al structure doped by the oxygen. At the positive potential on Al-electrode, with the growing U only increase of the current in the structure occurs, what is also explained by the influence of U on the Schottky barrier in Al/MgPc interface.

[1] *Yu.A. Goldberg.* Mikroelektronika, 1982, v.11, p.3 (in Russian).

[2] *G.B. Petrov.* Zarubezhnaya elektronika, 1977, No. 4, p.77 (in Russian).

[3] *Yu.A. Vidadi, K.Sh. Kocharli, B.Sh. Barkhalov, S.A. Sadraddinov*. Phys. Status Solidi (a), 1976, v. 33, k. 67; v. 34, k. 77.

[4] *Yu. A. Vidadi, S.A. Sadraddinov.* Abstracts of the V Republic Inter-High school Scient. Conference, Baku, 1992, p.2.

[5] A. *Sussman.* Space - charge - limited currents in copper phthalocyanine thin films. J.Appl.Phys., 1967, v. 38, № 7, p. 2738.

[6] *A.P. Martinenko.* Phtalocyanines - perspective microelectronics material. Moscow: CSRI "Electronics", 1982 (Dep.) (in Russian).

[7] *M.I. Fedorov, V.A. Benderski.* Characteristics of thin-film photocells on the base of magnesium phthalocyanine . FTP, 1970, v. 4, No. 7, p. 1403 (in Russian).

[8] *A.K. Ghosh, D.H. Moser, T. Feng*. J. Appl. Phys., 1974, v. 45, p. 230.

M.M. Pənahov, S.Ə. Sədrəddinov, C. H. Cabbarov, B.Ş. Barxalov

MAQNEZİUM FTALOSİANİN (MgPc) ƏSASLI ŞOTTKİ BARYERLİ STRUKTURLARIN DÜZLƏNDİRİCİ XASSƏSİNƏ OKSİGENİN TƏSİRİ

Nazik təbəqəli SnO_2/MgPc/Al strukturunda maqnezium ftalosianinin oksigen atmosferində istilik emalının Şottki çəpərinin fotoelektrik xassələrinə təsiri tədqiq olunmuşdur. Alınan nəticələr göstərir ki, MgPc nazik təbəqəsini oksigenlə aşqarlamaqla onun əsasında düzəldilən strukturun xassələrini idarə etmək olar.

М.М. Панахов, С.А. Садраддинов, Дж.Г. Джаббаров, Б.Ш. Бархалов

ФОТОЭЛЕМЕНТ С БАРЬЕРОМ ШОТТКИ НА ОСНОВЕ ОРГАНИЧЕСКОГО ПОЛУПРОВОДНИКА - ФТАЛОЦИАНИНА МАГНИЯ

В настоящей работе приводятся результаты исследования влияния термообработки MgPc в кислородной атмосфере на фотоэлектрические свойства барьера Шоттки Al/MgPc в пленочных структурах Al/MgPc. Полученные результаты показывают, что легированием пленки MgPc кислородом можно управлять свойствами структур на основе MgPc.

Received: 19.05.03

LONGITUDINAL MAGNETORESISTANCE OF SEMICONDUCTIVE FILM WITH THE PARABOLIC POTENTIAL IN QUANTIZING MAGNETIC FIELD

Kh.A. GASANOV
Scientific-technical complex "Informatika"

In this work longitudinal magnetoresistance in semiconductive films with parabolic potential in strong magnetic field are investigated. It is shown that longitudinal magnetoresistance is nedative at certain value of the magnetic field. Its magnitude is determined by spin splitting.

The account of quantiation the electron motion in the magnetic field unlike the classic theory leads to different from zero the longitudinal magnetoresistance. The change of the longitudinal magnetoresistance is caused by the fact that in the quantum magnetic field the possibility of the charge carriers scattering and Fermi level depend essentially on the magnetic field [1-3]. The longitudinal magnetoresistance in some region of the magnetic field may be negative, it has been experimentally observed in the wide range of semiconductors [4, 5]. The magnetoresistance sign, its value, the nature of the temperature and field dependence have been determined by m any factors, the band structure, the relaxation mechanism and size of sample. In paper [6] the existence of the negative magnetoresistance in the multilinear semiconductors in the fixed region of the magnetic field both for three and two-dimensional electron gas when has been theoretically predicted, the sample thickness has been compared with the diffusion length, which is connected with the account of the spin-orbit scattering of the current carriers on the impurities. It has been also noted, that in the same region of the magnetic fields in the non-degenerate case the main contribution in to the anomaly magnetoresistance gives the quantum correction to the magnetoresistance without the account of the electron interaction, caused by the spin-orbit interaction. Suggested in the present paper theoretically research gives the alternative explanation to the negative magnetoresistance of the semiconductive film with the parabolic potential in the strong magnetic field, placed in the film plane with the account of the spin-orbit interaction. It has been established, that in some region of the magnetic fields, the magnetoresistance of the non-degenerated electron gas has the negative values. Besides the behavior of the electron gas depends essentially on the spin splitting.

The electron energy spectrum of the conductivity in the parabolic quantum well in the longitudinal quantizing magnetic field has the form [7]:

$$\varepsilon_{N,k_y,k_z,\sigma} = \left(N+\frac{1}{2}\right)\hbar\omega + \frac{\hbar^2 k_Z^2}{2m} + \frac{\omega_0^2}{\omega^2}\frac{\hbar^2 k_y^2}{2m} + \sigma g \mu_B H \qquad (1)$$

Here Landaus gauge is chosen for the vector-potential $\overline{A}(0, x\cdot H, 0)$; ω_0 characterizes the parabolic potential of the film:

$$U = \frac{m\omega_0^2 x^2}{2}$$

$$\omega = \sqrt{\omega_o^{\ 2} + \omega_C^{\ 2}},\ \omega_c = \frac{eH}{mc}$$

is the cyclotron frequency, μ_B is Bohr magneton, g is the factor of the spin splitting, $\sigma = \pm\frac{1}{2}$, N is the number of the quantum level. The coordinate wave function, corresponding to the energy eigenvalue (1) has the form:

$$\varphi_{N,k_y,k_z}(r) = \varphi_N(x - x_0)exp\left(ik_y \cdot y + ik_z \cdot z\right) \qquad (2)$$

where

$$\varphi_N(x-x_0) = \frac{1}{\pi^{\frac{1}{4}} a_0^{\frac{1}{2}} \sqrt{2^N N!}} exp\left(-\frac{(x-x_0)^2}{2a_0^2}\right) H_N\left(\frac{x-x_0}{a_0}\right)$$

where

$a_0 = \sqrt{\frac{\hbar}{m\omega}}$; $x_0 = -\frac{\omega_c}{\omega}\frac{\hbar k_y}{m\omega} = -\frac{\omega_c}{\omega}a_0^2 k_y$, H_N is the Ermitte polynomial.

The current density in the direction of the magnetic and electric fields (H//j) is given by the following expression:

$$j_z = -e\frac{L_y L_z}{(2\pi)^2}\sum_{N,\sigma}\int\int_{-\infty}^{\infty}\frac{\hbar k_z}{m} f_1(\varepsilon)dk_y dk_z \qquad (3)$$

where $f_1(\varepsilon)$ is the non-equilibrium addition to the Fermi Derek spreading function, $f_1(\varepsilon)$ is presented in the form:

$$f_1(\varepsilon) = \frac{\hbar k_z}{m}\tau_H(\varepsilon)\left(\frac{\partial f_0}{\partial \varepsilon}\right)eE_z \qquad (4)$$

where $\tau_H(\varepsilon)$ is relaxation time in the quantizing magnetic field. In the case of the scattering in the short-acting potential, the relaxation time m ay be present ed in the form [1]:

$$\tau_H^{-1}(\varepsilon) = \tau_0^{-1} g_H(\varepsilon) \qquad (5)$$

where $g_H(\varepsilon)$ is the density of states, which for the charge carriers in the parabolic well in the longitudinal quantizing magnetic field has the form:

$$g_H(\varepsilon) = \frac{L_y L_z}{2\pi\hbar^2} \cdot \frac{m\omega}{\omega_0} \sum_{N,\sigma} \Phi(\varepsilon - \varepsilon_{N,\sigma}) \Phi(-\varepsilon + \varepsilon_{N,\sigma} + \frac{\beta L_x^2}{4}) \qquad (6)$$

Here $\varepsilon_{N,\sigma} = \hbar\omega\left(N + \frac{1}{2}\right) + \sigma g \mu_B H$

$\Phi(x)$ is the Heaviside function, $\beta = \frac{m\omega_0^2}{2\omega_c^2} \cdot \omega^2$

At the real concentration Fermi levels are located much below $\frac{\beta L_x^2}{4}$, therefore in the case of the weak filling in the expression for the density of states (6) $\Phi\left(-\varepsilon + \varepsilon_{N,\sigma} + \frac{\beta L_x^2}{4}\right)$ may be considered equal to 1.

Applying formulae (3-6) and passing to the polar coordinates for the conductivity σ_{zz} we obtain

$$\sigma_{zz} = \frac{e^2 L_y L_z}{2\pi\hbar^2} \cdot \frac{\omega}{\omega_0} \sum_{N,\sigma} \int_{\varepsilon_{N,\sigma}}^{\infty} (\varepsilon - \varepsilon_{N,\sigma}) \tau_H(\varepsilon) \left(-\frac{\partial f_0}{\partial \varepsilon}\right) d\varepsilon \qquad (7)$$

In order to calculate y_{zz} we should divide the integration region on the energy from the region $\frac{\hbar\omega}{\kappa_0 T} r$ to $\frac{\hbar\omega}{\kappa_0 T}(r+1)$ and then performing the summation over r from 0 to ∞. Thus, after the integration on the energy and the summation on the spin we obtain:

$$\begin{aligned}
\sigma_{zz} = \frac{\sigma_0}{2} \sum_{N=0}^{\infty} \sum_{r=0}^{\infty} \Bigg\{ & \frac{1}{N+r+1/2} \Bigg[arf_0\left(a\left(N+r+1/2\right) - \frac{b}{2}\right) - (ar+b) f_0\left(a\left(N+r+1/2\right) + \frac{b}{2}\right) + \\
& + \ln \frac{1+e^{\eta - a\left(N+r+1/2\right) + \frac{b}{2}}}{1+e^{\eta - a\left(N+r+1/2\right) - \frac{b}{2}}} \Bigg] + \frac{1}{N+r+1} \Bigg[(2ar+b) f_0\left(a\left(N+r+1/2\right) + \frac{b}{2}\right) - \\
& - \left(2a(r+1)+b\right) f_0\left(a\left(N+r+3/2\right) - \frac{b}{2}\right) + \ln \frac{1+e^{\eta - a\left(N+r+1/2\right) - b/2}}{1+e^{\eta - a\left(N+r+3/2\right) + b/2}} + \\
& + \ln \frac{1+e^{\eta - a\left(N+r+1/2\right) - b/2}}{1+e^{\eta - a\left(N+r+3/2\right) + b/2}} \Bigg] + \frac{1}{N+r+3/2} \Bigg[a(r+1) f_0\left(a\left(N+r+3/2\right) + \frac{b}{2}\right) - \\
& - \left(a(r+1) - b\right) f_0\left(a\left(N+r+3/2\right) - \frac{b}{2}\right) + \ln \frac{1+e^{\eta - a\left(N+r+3/2\right) + b/2}}{1+e^{\eta - a\left(N+r+3/2\right) - b/2}} \Bigg] \Bigg\}
\end{aligned} \qquad (8)$$

where

$$a = \frac{\hbar\omega}{k_0 T},\ b = \frac{g\mu_B H}{k_0 T},\ \eta = \frac{\xi}{k_0 T},\ \sigma_0 = \frac{e^2 n \tau_0}{m} \qquad (9)$$

here *n* is the two-dimensional concentration.

This formula is true for the arbitrary degree of the electron gas degeneracy.

It is possible to sum N and r for the non-degenerated electron gas, and this formula (8) can be presented the form

$$\sigma_{zz} = \sigma_0 \frac{e^{-\frac{a}{2}}}{4} \frac{sh\frac{a}{2}}{ch\frac{b}{2}} \left[(2-b) + a\, sh\frac{b}{2} + \frac{a\, ch\frac{b}{2}}{(1-e^a)} + \frac{1}{2}(2b-a) e^{\frac{a}{2}}\ sh\frac{b}{2} \ln cth\frac{a}{4} \right] \qquad (10)$$

From the formula (10) it is possible to show, that the region of the magnetic field and temperature exist, where $\rho(H)<\rho(0)$, $(\rho(0))$ is the resistance in the absence of the magnetic field, i.e it has been establish negative magnetoresistivity, magnitude of which depend on the value of the spin splitting, unlike the negative magnetoresistance, revealed for the three-dimensional case in the paper [3], where the spin splitting can not done into account. It is shown that longitudinal magnetoresistance is negative at certain value of the magnetic field.

Supposing $a>1$, $a>b$, $b<1$, for the magnetoresistance $\frac{\Delta\rho}{\rho}=\frac{\rho(H)-\rho(0)}{\rho(0)}$, we receive from (10):

$$\frac{\Delta\rho}{\rho}=-\frac{b^2(H)}{4}=-\left(\frac{g\mu_B H}{2k_0 T}\right)^2 \qquad (11)$$

Using the above-indicated formulae and numerous calculations, it is possible to determine such physical characteristics as the factor of the spin split, the parameter of the quantum well ω_0.

[1] *B.M.Askerov.* Kinetic effects in semiconductors, L. Nauka ,1970, p.303.

[2] *P.N. Argyres, E.N.Adams*. Phys.Rev, 104, 900 (1956)

[3] *L.S.Dubinskaya.* FTT, 1965, 7, 2821.

[4] *A.I.Dmitriev, Z.D.Kovalev, V.I.Lazorenko and G.V.Lashkarev* Phys. Stat. Sol.(b), 1990, 162,213.

[5] *E.G.Gwinn, R.M.Westervelt, P.F. Hopkins, A.J.Rimberg, M.Sundaram, and A.C.Gossard*. Phys. Rev. B 39, 1989, 6260.

[6] *V.L. Altshuler, A.G. Aronov, A.I.Larkin, D.E.Khmelnitskiy.* JETP, 1981, v.81, issue2, 768.

[7] *F.M. Gashimzade, A.M.Babayev, Kh.A.Gasanov* FTT,2001, 43, 1776.

X.A.Həsənov

KVANTLAYIJI MAQNİT SAHƏSİNDƏ PARABOLİK POTENSİALLI YARIMKEÇİRİCİ TƏBƏQƏNİN UZUNUNA MAQNİT MÜQAVİMƏTİ

Bu işdə güclü maqnit sahəsində parabolik potensiallı yarımkeçirici təbəqənin uzununa maqnit müqaviməti tədqiq edilmişdir. Təyin edilmişdir ki, maqnit sahəsinin müəyyən oblastında maqnit müqavimətinin dəyişməsi mənfi olur və bu spin parçalanması ilə bağlıdır.

Х.А. Гасанов

ПРОДОЛЬНОЕ МАГНИТОСОПРОТИВЛЕНИЕ ПОЛУПРОВОДНИКОВОЙ ПЛЕНКИ С ПАРАБОЛИЧЕСКИМ ПОТЕНЦИАЛОМ В КВАНТУЮЩЕМ МАГНИТНОМ ПОЛЕ

В работе исследовано продольное магнитосопротивление полупроводниковой пленки с параболическим потенциалом в сильном магнитном поле. Установлено, что сушествует область магнитного поля, где магнитосопротивление отрицательно, причем величина магнитосопротивления определяется спиновым расщеплением.

Received: 19.05.03

THE INFLUENCES OF THE SURFACE EFFECTS ON THE MECHANISMS OF THE CURRENT PASSAGE IN THE SILLICON PHOTOELEMENTS WITH OPTICAL COVERINGS

R.S. MADATOV, V,G, GASUMOVA
Baku State University
Z. Khalilov st., 23, Baku, 370143

N.A. SAFAROV, G.M. AKHMEDOV
Institute of Physics, Azerbaijan National Academy of Sciences,
Baku. Az - 1143, H. Javid av. 33

The influence of two-layer superface coverings of $ZnS+Nd_2O_3$ on the volt-ampere characteristic (VAC) of sillicon photoelements is investigated. It is established that in a result of the penetration of zinc atoms in the near-surface region of the silicon the compensation degree of recombination centres increases. It leads to the bending of the band edges on the semiconductor surface. It, in turn, promotes the creation of the fitted electric field of the directed *p-n* transition. It is supposed that the increase of photocurrent is caused by the decrease of the velocity of the surface recombination in the result of the passivation of the surface levels.

The number of works [1-4] of the investigation of the influence of the surface coverings on the collection coefficient and efficiency of the sun elements is considered in the ref (1-4). The results of these works allow to make some preliminary conclusions on the effectivity of the application of the optical coverings with the different indexes of reflaction. However, the choice of the materials for the optical layers is so limited that it is possible to solve the given problem so that to obtain the minimum value of the reflection coefficient. Among perspective materials for using by the way of the antireflection coverings in the silicon sun elements are SiO_2, Ti_2O_5, ZnS and e.t.c., which have the high transparency in the operating region of the spectrum. Indisputably that the optimal optical characteristics should go with the light resistance and ability to save unchangeable the initial characteristics of the sun element. But, analogous way of the decrease of the reflection coefficient has the some disadvantages: the textured surface, obtained after the treatment, is the absorbing for the absorption edge, in the result of that the non-photoactive part of the sun light increases; the presence of the high-speed surface states, which are the recombination centers [4]. The given disadvantages lead to the worsening of the volt-ampere and spectral characteristic forms of the sun elements. In this regard the investigation of the influence of the optical coverings on the ascilation-recombination, and the surface channels also in the sillicon *p-n* transitions can give the information on the nature of the mechanisms of current passage. In this paper the influences of the surface covering on the volt-ampere characteristics of the sillicon sun elements with the optical coverings $ZnS+Nd_2O_3$, relieved at the different temperatures are studied.

The experiment methodology

The p-n transition have been prepared by the diffusion of the phosphor in the *p*- type sillicon with the specific resistance 2Om·cm. The depth of the deposition of *p-n* transition, the thickness of the sample and surface concentration are 0.2mkm, 350mk and $10^{20}cm^{-3}$ correspondingly. The obtained elements have the short circuit current is 0,52V and efficiency is 11%.

The antireflection coverings of ZnS and Nd_2O_3 were heated up after the purification by the plasma etching of the top layer of the doped area of the element. The first layer of the covering was the film of ZnS with thickness 70Å, heated up by the thermal way in the vacuum, the second layer is film of Nd_2O_3, obtained by the ion-plasma evaporation with the following thermal relieving at 400-450°C. The surface layer resistance of the obtained films for the double-layer covering (120Å) was from 70 to 100Om/m^2.

The results and discussion

The spectral curves of the reflection from the element surfaces with double-layer covering $ZnS+Nd_2O_3$ after the stickness of the protective glass plate are presented on the fig1.

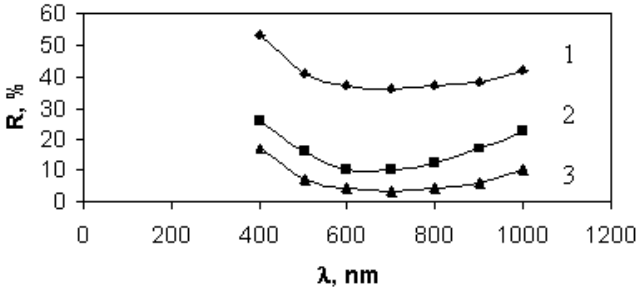

Fig.1. Spectral dependences of light reflection coefficient from the surface of silicon photoelements with coverings: 1. SiO_2 (1); 2. Nd_2O_3 (2); 3. $ZnS+Nd_2O_3$.

The reflection curves from pure silicon (1) and the sillicon with single-layer covering Nd_2O_3, SiO_2 for comparison of the experimental curves shows that the more wide area of low reflection can be obtained with the help of double-layer covering of $ZnS+Nd_2O_3$ in the visible region of spectrum. This result well agrees with experiment dates on the measured values of the short circuit photocurrent. As it is shown from fig.2 the photocurrent increase for the elements with the covering $ZnS+Nd_2O_3$ (curve2) is the 60% approximately. The output power of 1cm^2 of the sun element and the filling factor VAC for the double-layer covering are 1.62mVt and 0.62, and for SiO_2 10.1mVt and 0.65. The values I(0), A andRn calculated from load VAC by the

method (5), are 10^{-9}A/cm^2, 1.2 and 0.2 correspondingly for the covering of ZnS+Nd_2O_3 and 10^{-7}A/cm^2, 1.7 and 0.5 for SiO_2.

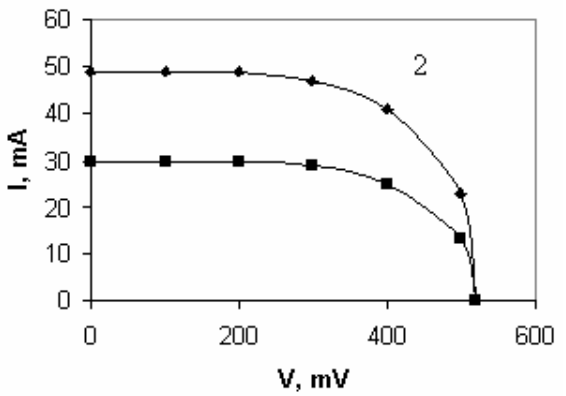

Fig.2. The load volt-ampere characteristics of silicon photoelements with coverings:1. . SiO_2; 2. ZnS+Nd_2O_3

It followes to note that the character pecularity of the obtained results is that ih them the nonload photoelectromotive force doesn't depend on the covering nature, although можно было бы ожидать the increaseof photoelectromotive force after heating up the covering of the surface by the layer ZnS+Nd_2O_3 because of photocurrent increase. However, this isn't observed. It means that in the real elements the photocurrent is defined by the mechanism of the inverse current through the p-n transition (3). The more essential contribution, besides of the warm generation and recombination, leading to the increase of the diffusion current, give the generations and recombinations in the quazineutral parts of the *p-n* transition, and the leakages trough the surface channels also.

For the calculation of the diode parameters I_0, A, R_n (where A is the recombination coefficient in the *p-n* transition region, I is the diffusion saturation current, R_n is the shunt resistance) the experimental VAC measured in the darkness in the diode mode and the nonload mode are used (fig 3). The calculation of VAC is made by the following formulae (1).

$$J = J_f - J_o(exp\frac{q(u + JR_{II})}{AKT} - 1) - \frac{u + JR_{II}}{R_{III}} \qquad (1)$$

This calculation allows to present visually the influence of the consequetive and shunt resistances on the sun elements propertie. This generation (1) is applied in the calculations in case of the big currents only ($J_d > J_0$, where J_d~10^{-7}A/cm^2, J_0=10^{-9}A/cm^2, and of the recombination mechanism of the inverse saturation current passage through the *p-n* transition also [5]. The calculation VAC of the sillicon photoelement with coverings SiO_2 (1) and ZnS+Nd_2O_3 (2) are shown in the fig. 3.

It was revealed that the plating of the surface layer resistance 75 Om/m^2 leads to the decrease R_n from 0,6Om to 0.2Om and the improvement of the form VAC of the *p-n* transition. In addition, the shunt resistance of the elements changes insignificantly.

Thus, the plating the optical covering of ZnS+Nd_2O_3 on the surface of the sillicon photoelement decreases the consequative resistance value and expresses the appreciable influence on the coefficients J_0 and A. In addition, J_0 and A are 10A/cm^2 and 1.3 correspondingly.

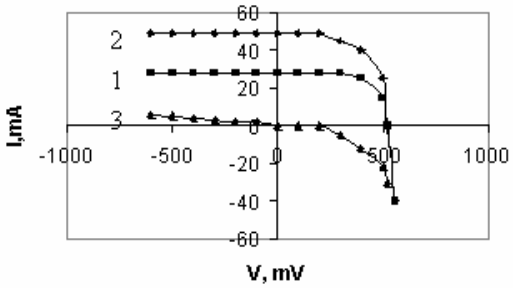

Fig.3. Calculated volt-ampere characteristics of silicon photoelements with coverings, light – 1. . SiO_2; 2. ZnS+Nd_2O_3; dark- 3.

The calculation on the light volt-ampere characteristics allows to define the values of parameters J_0 and A, for those values namelt, which are the character for the sun elements in the operating mode. The calculation is made with the linear dependence J_{sc}~$f(U_{xx})$, where $tg\alpha$~(q/AKT), and the value lgJ_0 is cutted on the axis of ordinates (fig4).

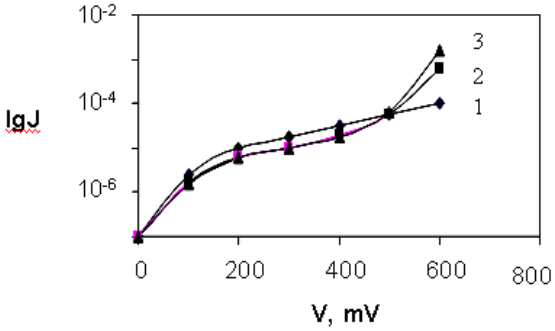

Fig.4. Dark (1) and light (2.3) Characteristics of silicon photoelements with coverings: 1. . SiO_2; 2.3. ZnS+Nd_2O_3

As it is seen from the fig 4 and dependence ?

The calculated values J and A for the samples at the low voltages are 10^{-6}A/cm^2 and 2.5, 10^{-5}A/cm^2 and 2.5; and at the high voltages are 10^{-9}A/cm^2 (and 1.2, 10^{-6}A/cm^2 and 2 correspondingly. The comparison of the values J_0, A and Rn shows that plating the optical double-layer covering of ZnS+Nd_2O_3 leads to the decrease of J_0, R_n and A, which mainlydepend on properties of the interface metal-semiconductor [1]. It is need to take into consideration that volt-ampere characteristics of the photoelement with the wide transition is true only for the definite voltage value (i.e. near the operating point of the photoelement). However, the influences of the surface recombination on the photoelements' characteristics don't take into consideration in it. The comparison of the values J_0, A and R_n for the photoelements with the optical coverings SiO_2 and ZnS+Nd_2O_3 shows that the dark VAC differ insignificantly at the low voltages, (J_{in}...J_0), but light characteristics differ strongly at the high levels of lightening. The such significant change of VAC structure at the plating of the layer ZnS+Nd_2O3 can show that atoms of the zinc, ionized by the lightening action diffuse intensively into the sillicon near lighted surface.

Aaaaathe combination of the obtained dates on the base of the electric, photoelectric and optical measurements bear on that in the sillicon photoelements with the optical

coverings $ZnS+Nd_2O_3$ the creation of the electro-compensated layer in the surface area of the sillicon is the one of the possible reason of the observed changes of the recombination parameters of *p-n* transition. At the lightening the balance brakes and the photostimulated diffusion of the zinc occures, in the result of which the compensation degree of the recombination centres increases that in turn leads to the bend of the edges of the band on the semiconductor surface. In addition, the surface recombination velocity increases from 10^5 to 10^3cm/c [6].

Judging by the investigations of VAC and effect of the field also, carried out in [4], the increase of the efficiency with the covering $ZnS+Nd_2O_3$ is caused by the decrease of J_0 and A in the area of the average voltages, where the sun element works. Thus, at the plating of $ZnS+Nd_2O_3$ on the sillicon sun element surface in distinction of SiO_2 the thin isolating layer occures with the polarized states on the Si surface accordingly. This layer, in turn, can promote to the acceleration of the zinc ions migration in the Si volune and the creation of the fitted electric field of the directed *p-n* transition.

In the result of the made investigation it can make the following conclusions:

1) The efficiency can be increased from 10 to 15% because of the decrease of the reflection in the spectrum region 0.4-0.8mkm at the plating of the double-layer covering $ZnS+Nd_2O_3$ on the surface of the sillicon photoelements.
2) The experimental photoelements have the low consequent resistance and the well volt-ampere characteristics in comparison with the photoelements with SiO_2 coverings, having the same depth of the deposition of p-n transition.

[1] *A.M. Vasilyev, A.P. Landsman0*. Poluprovodnikoviye fotopreobrazovateli. M. Sov. radio, 1971, p.246 (in Russian).

[2] *M.M. Koltun.* Selektivniye opticheskiye poverkhnostniye preobrazovateli, M. Nauka, 1979, p.104 (in Russian).

[3] *V.A. Rodzkov, A.I. Petrov, M.B. Shalimova*. Pisma v DzTF, 1994, v.20 v.12, p.c.43-46 (in Russian).

[4] *G.B. Abdullayev, M.Ja. Bakirov, G.M. Akhmedov, N.A. Safarov*. Geliotekhnika, 1994, №1, p.14-16 (in Russian).

[5] *V.M. Yevdokimov*. Geliotekhnika, 1972, №6, p. 16-20 (in Russian).

[6] *I.P. Gavrilova*. Geliotekhnika, 1972, №6, p. 23-27 (in Russian).

[7] *R.S. Madatov, N.A. Safarov, G.M. Akhmedov*. Конф.ТРЕ-2002, 23-25 апрель, 2002, с.439-441(in Russian).

R.S. Mədətov, V.Q. Qasımova, N.A. Səfərov, Q.M. Əhmədov

OPTİK ÖRTÜKLÜ SİLİSİUM GÜNƏŞ ELEMENTLƏRİNDƏ CƏRƏYANKEÇMƏ MEXANİZMİNƏ SƏTH EFFEKTLƏRİNİN TƏSİRİ

Silisium fotoelementi üzərinə çəkilmiş $ZnS + Nd_2O_3$ səth örtüyünün VAX-na təsiri öyrənilmişdir. Müəyyən edilmişdir ki, sink atomlarının silisiumun səthinə diffuziyası nəticəsində rekombinasiya mərkəzlərinin kompensasiya dərəcəsi artır. Bu isə, yarımkeçiricinin səthində zonanın əyilməsinə və keçidə doğru yönəlmiş elektrik sahəsinin yaranmasına səbəb olur. Fərz edilir ki, fotocərəyanın artmasına səbəb, səth səviyyələrinin passivləşməsi nəticəsində rekombinasiya sürətinin azalmasıdır.

Р.С. Мадатов, В.Г. Гасумова, Н.А. Сафаров, Г.М. Ахмедов

ВЛИЯНИЯ ПОВЕРХНОСТНЫХ ЭФФЕКТОВ НА МЕХАНИЗМЫ ТОКОПРОХОЖДЕНИЯ В КРЕМНИЕВЫХ ФОТОЭЛЕМЕНТАХ С ОПТИЧЕСКИМИ ПОКРЫТИЯМИ

Исследовано влияние двухслойных поверхностных покрытий из $ZnS+Nd_2O_3$ на вольт-амперную характеристику (ВАХ) кремниевых фотоэлементов. Установлено, что в результате проникновения атомов цинка в приповерхностную область кремния возрастает степень компенсации рекомбинационных центров, что приводит к изгибу краев зоны на поверхности полупроводника. Это, в свою очередь способствует созданию встроенного электрического поля направленного p-n перехода. Предполагается, что рост фототока обусловлена уменьшением скорости поверхностной рекомбинации в результате пассивизации поверхностных уровней.

Received: 22.05.03

ABOUT DOMAIN WALL MOTION IN A SURFACE STABILIZED FERROELECTRIC LIQUID CRYSTAL

H. F. ABBASOV
Baku State University
370145, Baku, Z. Khalilov str, 23.

The domain wall motion was investigated in «the semiconductor – ferroelectric liquid crystal – metal» structure, occurring under action of an electrical field in the surface stabilized ferroelectric liquid crystal.

Due to unique properties the ferroelectric liquid crystals [1] are widely applied in engineering that, in turn, has caused wide research of these materials. Such properties are the best threshold and time characteristics of the surface stabilized ferroelectric liquid crystal (SSFLC), which strongly depend on surface conditions of electrodes, with which the liquid crystal contacts.

In the given work the domain wall motion was investigated in «the semiconductor – ferroelectric liquid crystal - metal» structure occurring under an electrical field in SSFLC.

As a liquid crystal the mixture having the ferroelectric phase in a wide temperature interval, consisting of:

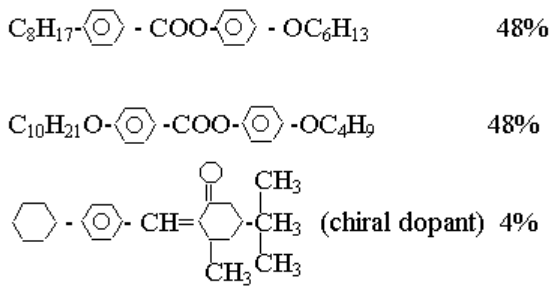

and with the following phase transition temperatures:

$$C \xleftarrow{30^0\,C} S_C \xleftarrow{62^0\,C} S_A \xleftarrow{66^0\,C} Ch \xleftarrow{70^0\,C} I$$

has been used.

In structure as the semiconductor was used *p*-type Si, and as the metal electrode was used SnO_2.

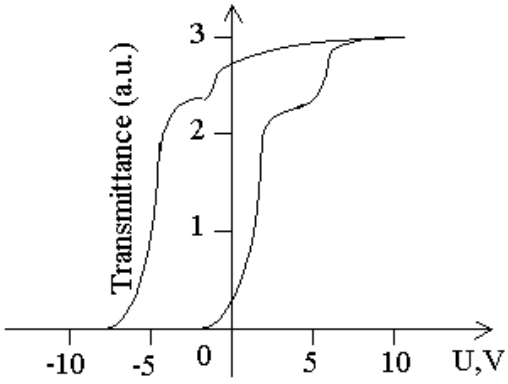

Fig.1. Light transmittance in an arbitrary units as a function of an applied voltage for the switching process under a bipolar rectangular voltage wave at the frequency $\nu = 0.01$ Hz and amplitude U_0=10 V.

To obtain a homogeneous orientation of SSFLC the surface of electrodes was preliminary treated by polyimide lacquer and subsequently rubbed in one direction [2]. It must be noted that the semiconductor essentially improves the quality of orientation. The cell thickness is about 4,8 μm, an effective area is 152mm^2. The tilt angle of molecules measured at temperature 39°C by polarizing microscope is 18°. The spontaneous polarization has been measured by the triangular pulse method [3] and at above mentioned temperature it is 0.5 $\frac{nCl}{sm^2}$.

The experiment was carried out in the set up on the basis of polarizing microscope. The light transmittance of the cell was measured by the photo multiplier, the signal from which was registrated by the oscilloscope. Under an electrical field action the Clark-Lagerwall transition takes place [4]. As well as known, the electrooptic effect occurs in two stages: at first at low voltage the bulk switching (I) takes place, and then at high voltage the surface switching – the domain wall motion (II) takes place (fig.1). From this oscillograms, which are received at different values of the applied voltage, the switching time was determined (fig. 2).

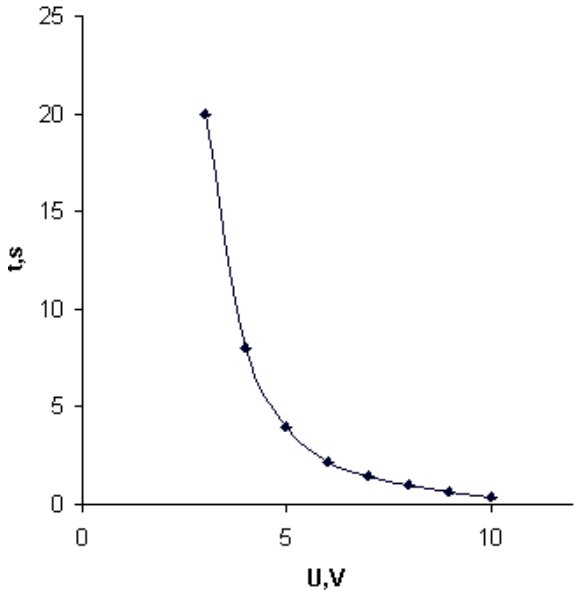

Fig.2. The dependence of the switching time on the applied voltage.

As seen from figure 2, the switching time decreases with increasing of the applied voltage. By drawing this dependence in logarithmic scale we have established, that the dependence $\tau(U)$ has the form $\tau \sim U^{-2}$

In order to explain the obtained results, we propose the following model. Let S_0 is an effective area, where we observe the domain wall motion, $n(t)$ is a number of domains

in this area and *S(t)* is the area which is occupied by domains at the given moment, *dS* is the increment of the area of all domains. It is clearly that *dS* is proportional to the domains' free area *(S_0-S)*, to the total increment of the all domains area *ndS'* and inversely proportional to the already occupied by domains area *S*, i.e.

$$dS = c\frac{S_0 - S}{S} ndS' \tag{1}$$

where C is a coefficient of proportionality.

Let's take into account, that the area increment of the domain having the circular form of radius *r* looks as

$$dS' = 2\pi rdr = 2\pi\overline{\upsilon}t \cdot \overline{\upsilon}dt = 2\pi\overline{\upsilon}^2 tdt$$

The domain wall velocity depends on a direction. Therefore the averaged domain wall velocity determined as $\overline{\upsilon} = \sqrt{\upsilon_{||} \cdot \upsilon_{\perp}}$ is used at the calculations, where the signs $||$ and $\perp$ belong to the case of motion in the direction parallel and perpendicular to the smectic layers, accordingly.

It is obviously also, that the number of domains is inversely proportional to the time, as they covered each other: $n \approx \frac{c'}{t}$. After the integrating of (1) we obtain:

$$\int_0^S \frac{S}{S_0 - S} dS = \int_0^t 2\pi\overline{\upsilon}^2 t \cdot \frac{C'}{t} dt \tag{2}$$

$$ln\left(1 - \frac{S}{S_0}\right) + \frac{S}{S_0} = -\frac{2\pi C'\overline{\upsilon}^2 t}{S_0} \tag{3}$$

where, $C'=c \cdot c'$.

The expanding of the expression $ln\left(1 - \frac{S}{S_0}\right)$ in a series at $S=0$ and neglecting of the high order members gives:

$$\frac{S_0}{2}\left(\frac{S}{S_0}\right)^2 = 2\pi C'\overline{\upsilon}^2 t \tag{4}$$

At complete switching, when the domains occupy all effective area, i.e. $S=S_0$ and $t=\tau$, we obtain

$$\tau = \frac{S_0}{4\pi C'} \cdot \frac{1}{\overline{\upsilon}^2} \tag{5}$$

The theoretically predicted dependence of the domain wall velocity on the applied voltage *U* is linear [5-7]:

$$\overline{\upsilon} = \frac{2P}{\eta N} U \tag{6}$$

where, *P* is the spontaneous polarization, η is the rotational viscosity, *N* is the parameter that describe the surface.

Then we obtain the following expression for switching time

$$\tau = C\frac{\eta^2}{U^2} \tag{7}$$

where, $C = \frac{S_0 N^2}{16\pi C'}$ is a coefficient which depends on the surface state.

Thus, the proposed model correctly explains the dependence *τ(U)* obtained experimentally.

[1] *J.C.Rhoo*. Liquid crystals: physical properties and nonlinear optical phenomena. Wiley Interscience, New-York, 1994

[2] *A.A.Sonin*. The surfase physical of liquid crystals, 1995.

[3] *K. Miyasato, S.Abe, H.Takezoe, A.Fukyda, F.Kuze.* Jpn. J.Appl. Phys. 1983, v.22, p.1661.

[4] *N.A.Clarc, S.T.Lagerwall.* Appl. Phys. L. 1980, v.36, p.879.

[5] *M.A.Handschy, N.A.Clark*. Ferroelectrics, 1984, v.59, pp.116.

[6] *Y.Ishibashi.* Jpn. J.Appl. Phys. 1985, v.24, pp.126-129.

[7] *J.Ouchi, H.Takano, H.Takezoe, A.Fukuda*. Jpn, J.Appl. Phys, 1987, v.26, №1, pp. 21-24.

H.F. Abbasov

SƏTHLƏ STABİLLƏŞMİŞ SEQNETOELEKTRİK MAYE KRİSTALDA DOMEN SƏRHƏDLƏRİNİN HƏRƏKƏTİ HAQQINDA

«Yarımkeçirici-seqnetoelektrik maye kristal-metal» strukturunda səthlə stabilləşmiş seqnetoelektrik maye kristalda elektrik sahəsinin təsiri altında Klark-Lagervol effekti baş verdikdə muşahidə olunan domen sərhədlərinin hərəkəti öyrənilmişdir.

Х.Ф. Аббасов

О ДВИЖЕНИИ ДОМЕННЫХ ГРАНИЦ В ПОВЕРХНОСТНО СТАБИЛИЗИРОВАННОМ СЕГНЕТОЭЛЕКТРИЧЕСКОМ ЖИДКОМ КРИСТАЛЛЕ

В работе было изучено движение доменных границ в структуре «полупроводник-сегнетоэлектрический жидкий кристал-металл», происходящее под действием электрического поля в поверхностно стабилизированном состоянии сегнетоэлектрического жидкого кристалла при осуществлении в нем эффекта Кларка-Лагервола.

Received: 22.05.03

OPTICAL MODEL ANALYSIS OF NEUTRON ELASTIC SCATTERING ON CARBON

Kh.Sh. ABDULLAYEV, M.Sh. MAMEDOV
Baku State University, Baku 370145, Z. Khalilov st., 23

The calculation of the optical model of neutron scattering for C^{12} nucleus in the energy region of 4-14MeV has been carried out. To estimate a compound elastic scattering at low energies, the Hauser-Feschbach formalism has been used. A good agreement is obtained at higher energies.

In the present paper in order to explain the neutron scattering on the C^{12} nuclei, the prediction of optical model of nucleus has been investigated more thoroughly. The obtained results are in a good agreement with the experimental data in the neutron energy region of 6.5-14MeV.

Recently the estimation of sections of neutron interactions with nuclei by different model predictions is of great interest. For average neutron energies and for medium and heavy nuclei, the use of the nucleus optical model gives rather reasonable results [1, 2]. However, to estimate the neutron data for relatively light nuclei, the use of such a model needs additional investigations. This is attributed to different experimental data for supporting points on the one hand, and also to necessity for improvement of the optical potential on the other hand. In the present paper to determine the neutron energy region and to obtain the appropriate optical parameters, the estimation of the data on C^{12} by the nucleus optical model has been carried out.

For neutron energies lower than 4MeV, the optical parameters account the experimental data on light nuclei insufficiently indicating a low energy limit for the optical model. A good data agreement at neutron energies of 6.5-14MeV can be used to compensate for missing experimental data as the optical parameters in this energy region smoothly vary with energy. However, the obtained optical parameters are somewhat inaccurate due to a lack of the experimental data in the energy region considered.

The optical potential has been used in the following form [3]:

$$V(r) = -V_{CR} v_{cr}(r) - iV_{IM} v_{im}(r) - V_{SO} v_{so}(r)(\vec{\sigma}.\vec{e}) \quad (1),$$

where

$$v_{cr}(r) = \frac{1}{1 + exp[r - R_1/a]} \text{ (Woods-Saxon form)} \quad (2)$$

and $v_{lm}(r)$ is the surface absorption form factor

$$v_{lm}(r) = exp\left\{-\left(\frac{r - R_2}{b}\right)^2\right\} \text{ (the Gaussian form)} \quad (3)$$

The spin-orbit term is

$$v_{SO}(r) = -\left(\frac{h}{m_\pi C}\right)^2 \frac{1}{r}\frac{d}{dr} v_{cr}(r) \text{ (the Thomas form)} \quad (4)$$

$$R_1 = r_{or} A^{1/3}; \quad R_2 = r_{oi} A^{1/3} \quad (5)$$

where A is the mass number of the target nucleus.

In the present paper r_{or} and r_{oi} are equal to the value of r_0. The $R=r_0A^{1/3}$ is equated to the nuclear radius. Using the above potential (1), a following set of optical parameters i.e. V_{CR}, V_{IM}, V_{SO}, a, b and $r_{0,}$ has been obtained.

The slight parameters changes are explained by different values of experimental cross-sections. However, to reveal the dependence of optical parameters on neutron energy is difficult due to interrelation between the optical parameters themselves. Moreover, at different neutron energies the change of optical parameters is not the same.

For calculation, a special computer programme was used. In this programme the search of parameters was realized by minimization of the following function:

$$\chi^2 = \sum_i \left(\frac{\sigma_i^{cal} - \sigma_i^{exp}}{\Delta\sigma_i^{exp}}\right)^2 + \frac{1}{N}\sum_{j=1}^{N}\left(\frac{\sigma(\theta_j)^{cal} - \sigma(\theta_j)^{exp}}{\Delta\sigma(\theta_j)^{exp}}\right)^2$$

where $\Delta\sigma$ is the experimental error of the σ value.

The given programme also contains the Hauser-Feschbach formalism where the cross-section data are assumption of compound neutron elastic scattering.

The fitting process for obtaining the optical parameters was carried out at neutron energies of 4.50; 7 and 13MeV. The data for the other energies were obtained at linear interpolation. The fact that for the carbon nuclei the experimental data on the total cross-section strongly vary at the neutron energies of 4.8; 5.3 and 8MeV indicates that the corresponding optical parameters should not be considered as absolute.

For neutron energies lower than 7MeV the Hauser-Feschbach formalism with the following energy levels for C^{12} was used [4].

E (MeV)	J^π	MeV	J^π
0	0^+	-6.134	3^-
6.052	0^+	6.916	2^+
6.047	1^+	7.121	1^-

The calculated cross-section values and the experimental data are shown in Table 1. It is seen from the Table 1 that there is a good agreement for values at neutron energies more or equal to 6MeV.

A significant variation of near 8MeV indicated that the optical model prediction for this energy cannot be considered sufficient. However, as seen in table 1, the given data are in a good agreement.

Table 1.

E_n, MeV	σ_T^{exp}, δ	σ_T^{cal}, δ	σ_{el}^{exp}, δ	σ_{el}^{cal}, δ
4,50	1,43 ± 0,05	1,43	1,55	1,42
5,00	1,45 ± 0,07	1,45	1,12±015	1,18
5,50	1,50 ± 0,07	1,50	0,97	1,25
6,00	1,41	1,41	1,35	1,33
7,00	1,39 ±0,04	1,39	0,97	0,86
8,00	1,37 ±0,06	1,37	0,95	0,84
9,00	1,45 ±0.04	1,45	1,05	0,93
10,00	1,42 ±0,06	1,42	1,03	0,89
11,00	1,46 ±0,03	1,46	1,01	0,87
12,00	1,47 ± 0,05	1,47	0,97	0,83
13,00	1,51 ±0,07	1,51	0,89	0,87

For the purpose of calculation, the experimental data on inelastic cross-sections were obtained in the following form:

$$\sigma_{nonel} = \sigma_T - \int \sigma_{el}(\theta) d\Omega ,$$

These data, as compared to σ_t, are inaccurate due inaccuracy of the σ_{el} values.

The optical parameters obtained for different neutron energies are tabulated in table 2.

In calculation the interpretation of $R=r_0A^{1/3}$ as the nuclear radius is somewhat inaccurate the as r_0 value slightly changes for different neutron energies. It should be noted that if r_{oi} slightly differs from r_0, the obtained parameters values are practically unchangeable.

Table 2.

E_n, MeV	V_{CR}, MeV	V_{im}, MeV	V_{SO}, MeV	*a, f*	*B, f*	r_0, *f*
4,5	32,2	1,9	8,3	0,72	0,90	1,10
5,0	34,5	2,0	7,6	0,50	0,98	1,27
5,5	35,3	2,2	8,5	0,51	0,97	1,35
6	38,1	2,2	8,1	0,53	0,99	1,41
7	41,0	2,1	7,3	0,52	0,95	1,38
8	40,3	2,2	8,0	0,53	0,91	1,37
9	42,1	2,1	4,8	0,55	0,86	1,28
10	43,2	2,2	4,4	0,61	0,83	1,25
14	50,4	7,4	5,1	0,65	0,78	1,20

The neutron size as compared to that of nucleus can be neglected in the case of heavy nucleus nuclei, while for the light C^{12} nucleus it is unreasonable. Probably, this fact can explain the energy dependence of V_{CR} and r_0 parameters (table 2). It has been found that with increase of neutron size relative to the target nucleus the r_0 value also increases, while the value of V_{CR} decreases.

The increase of V_{IM} with neutron energy conforms with theoretical predictions, on the base of the exclusion principle.

[1] *D.M.Annand, R.F.Finlay.* Nucl. Phys., 1985, v. A443, p.249.
[2] *G.V.Anikin, I.I.Kotukhov.* Atomnaya Energiya, 1986, 54. (in Russian)
[3] *Vu L.L., Overley J.C.* Nucl. Phys., 1979, v.A324, p.160.
[4] *W.Hauser, H.Feschbach.* Phys. Rev., 1952, v.37, p.366.

X.Ş.Abdullayev, M.Ş.Məmmədov

KARBON NÜVƏSİNDƏN NEYTRONLARIN SƏPİLMƏSİNİN OPTİK MODELƏ GÖRƏ TƏHLİLİ

C^{12} nüvəsi üçün neytronların səpilməsinin optik modelə görə hesablanması yerinə yetirilmişdir. 4-14 MeV energi intervalı götürülmüşdür. Aşağı enercilər üçün kompaund elastiki səpilməni qiymətləndirmək məqsədilə Hauzer-Feşbah formalizmindən istifadə olunmuşdur. Yaxşı uyğunluq halları yüksək enercilər üçün alınır.

Х.Ш. Абдуллаев, М.Ш. Мамедов

АНАЛИЗ УПРУГОГО РАССЕЯНИЯ НЕЙТРОНОВ НА АТОМАХ УГЛЕРОДА ПРИ ПОМОЩИ ОПТИЧЕСКОЙ МОДЕЛИ

Проведено вычисление по оптической модели рассеяния нейтронов для ядра C^{12}. Рассматривался энергетический интервал 4-14МеВ. При низких энергиях для оценки компаундного упругого рассеяния применялся формализм Хаузера-Фешбаха. Хорошее согласование получается при высоких энергиях.

Received: 22.05.03

$TlInS_2$ <Mn> - NEW RELAXOR FERROELECTRIC

O.A. SAMEDOV
Institute of Radiation Problems of Azerbaijan National Academy of Sciences
31a, H.Javid av., Baku - 1143

It was shown $TlInS_2$ doped 0,1at.% Mn displays all idiosyncrasies of relaxor ferroelectric. The temperature range of a steady relaxor (nanodomain) state and temperature of phase transition in a ferroelectric (makrodomain) state attended by anomalies of polarization and pyroelectric properties was defined.

1. Introduction

The analysis of the dielectric constant temperature dependence $\varepsilon(T)$ in the phase transitions region of $TlInS_2$ crystal shows that this dependence has different forms for the samples taken from various technological batches. It is found in [1] that the different forms of $\varepsilon(T)$ result from the fact that $TlInS_2$ crystals relate to the berthollide class, i.e. the compounds with composition rearrangement occurring during the growth process. However, this peculiarity does not lead to smearing of the phase transitions, and the dependence $\varepsilon^{-1}(T)$ obeys the Curie-Weis law [2, 3] with a constant of $\approx 10^{-3}$ in the large frequency range going from kilohertz to submillimeter lengths. The neutron-diffraction research has also established [4] that $TlInS_2$ compound is an improper ferroelectric with incommensurate phase.

The temperature region, where instability of $TlInS_2$ crystal lattice is observed, is very sensitive to the trivalent cationic impurities of different ionic radius and coordination numbers. Moreover, for some impurities one observes the increase of phase transition temperatures while for others one obtains the decrease of them (the results of this comparative research have now been submitted for publication). It is also interesting to investigate the nature of these phase transitions in $TlInS_2$ crystals. The transition metals of iron group are the multicharged impurity ions and can form the deep centers of strong localization that are capable to strong interaction with highly polarizable $TlInS_2$ crystal lattice.

In this paper we present the results of study on dielectric, polarization and pyroelectric properties of $TlInS_2$<Mn> crystals.

2. Experimental Technique

The $TlInS_2$ crystals were grown by the modified Bridgman-Stockbarger method. It was not observed any anisotropy of dielectric properties in the plane of layer. The measurements have been carried out on the crystal faces cut out perpendicularly to the polar axis. The crystal faces were planished, polished and then covered by the silver paste. The dielectric constant ε and the tangent $tg\delta$ of the dielectric losses angle were measured by the alternating current bridge E7-8, E7-12, P5058 and Tesla BM560 at the frequencies 1kHz, 1MHz, 10kHz and 100kHz accordingly in the temperature region 150–250K.

The velocity of temperature scanning was 0.1 K/min. The dielectric-hysteresis loops have been studied at the frequency of 50Hz using modified Soyer-Tauer scheme. The pyroeffect has been investigated by the quasistatic method using universal voltmeter V7-30.

3. Results

The dielectric constant temperature dependencies $\varepsilon(T)$ of both $TlInS_2$ (curves 1, 2) and $TlInS_2$<Mn> crystals (curves 3, 4) are presented in fig. 1. The curves 1, 3 correspond to the cooling regime; the curves 2 and 4 are obtained at the heating regime. As it is seen from Figure 1, the well-known [3] typical sequence of the phase transitions was observed on $TlInS_2$ crystals (curves 1, 2). One sees the paraelectric-commensurate phase transitions at 216K, and two additional transitions at 200 and 204K. Last two transitions were most likely caused by the rearrangement of the modulated structure; their nature was widely discussed in [5]. The final transition to the polar phase occurs at 196K.

The dependence $\varepsilon(T)$ can be described by the Curie-Weis law with the Curie constant of $C^+=5.3\cdot10^3$K in the temperature region $T-T_1$ (216)≤50°. The anomaly at 196K appears during the crystal cooling where all peaks are strong enough and there is no any signs of smearing. As one can see from the Figure 1, the dielectric hysteresis for $TlInS_2$ crystals is observed only at the temperature about 196K (and not at the maximum of the curves). The thermal hysteresis of the doped samples is situated at the temperature T_m, corresponding to the maximum of $\varepsilon(T)$ curve) and is about 2K (curves 3 and 4 in Figure1).

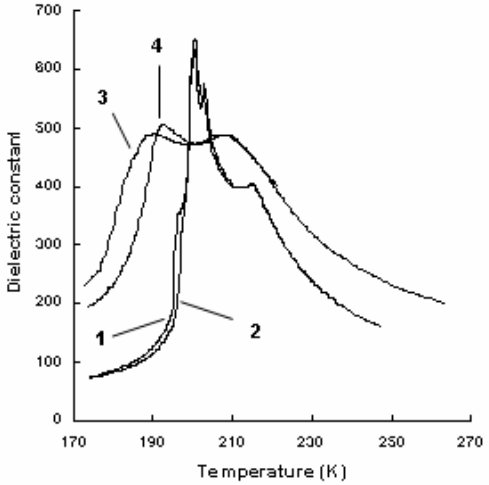

Fig.1. The dielectric constant $\varepsilon(T)$ temperature dependencies. Curves 1, 2 - the dependencies $\varepsilon(T)$ of $TlInS_2$ crystal (1-cooling; 2-heating); Curves 3, 4 – the dependencies $\varepsilon(T)$ of $TlInS_2$<Mn> crystal (3-cooling; 4-heating).

The dielectric constant temperature dependence $\varepsilon(T)$ is significantly different in this temperature region for $(TlInS_2)_{1-x}(Mn)_x$ crystals, where x=0.001. The dependence is strongly blurred, and the phase transitions move by 10K towards the

lower temperature region. The region of incommensurate phase with two anomalies at 190K and 209K becomes wider. It is natural in this case to explain the reason of such radical change of the dependence $\varepsilon(T)$ for 0.1-mol% Mn doping.

It is known [6, 7] that the composition fluctuation is the main reason of smearing of phase transition temperatures. However, not all kind of defects and increase of their concentration can cause the smearing. According to [8] the smearing is determined by the defects having dipole moments that create the electric fields and electric field gradient in the adjoining regions of the crystal. In addition, since $TlInS_2$ is a semiconductor, the doping of impurities creates the corresponding centers of charge carrier localization that can create the local electric fields stimulating generation of the induced polarization near the phase transitions [9-11]. An important peculiarity of the ferroelectrics with smearing phase transitions is the fact that the dielectric constant at temperatures higher than T_m changes not in agreement with the Curie-Weis law of $\varepsilon^{-1}(T)=C^{-1}(T-T_0)$ but in accordance with the law of $\varepsilon^{-1}(T)= = A+B(T-T_0)^2$.

In $TlInS_2$<Mn> crystals was observed significant frequency dispersion and growth T_m with growth of frequency f. The increase T_m with growth of frequency is well described by the Vogel-Fulcher law (fig.2), interpretive as temperature of static freezing electrical dipoles or transition in a condition of dipole glass [12, 13].

The investigation of polarization properties of $TlInS_2$<Mn> shows that the dielectric hysteresis loops are observed below 175K and the maximum value of spontaneous polarization, P_s, for such loops reaches $4\cdot10^{-8}$C/cm^2. The value of P_s for non-doped $TlInS_2$ crystals is equal to $1.8\cdot10^{-7}$ C/cm^2. The value of Ps in the temperature region from 175 to 210K is $1.5\cdot10^{-8}$C/cm^2.

The investigation of the dielectric constant frequency dispersion has been carried out at the frequencies of 1kHz-1MHz. No temperature shift for the maximums of $\varepsilon(T)$ curves in $TlInS_2$ crystals was observed, while the shift of the smeared maximums of $\varepsilon(T)$ curves for $TlInS_2$<Mn> crystals is equal to 3K.

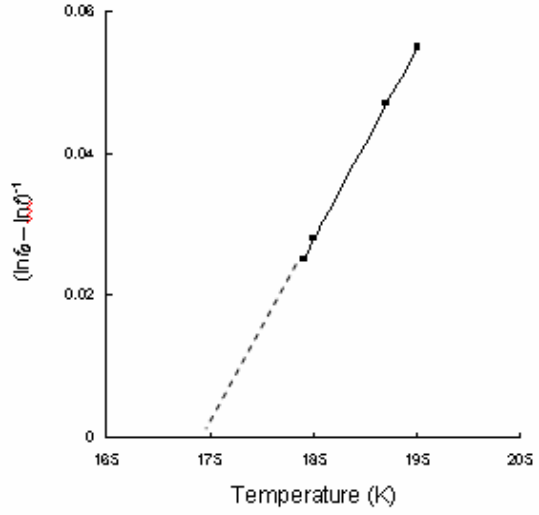

Fig.2. The dependence $(\ln f_0 - \ln f)^{-1}$ from T_m for $TlInS_2$<Mn>, illustrating performance of the Vogel-Fulcher law.

The temperature dependencies of the pyroelectric coefficient $\gamma(T)$ of $TlInS_2$ (curve 1) and $TlInS_2$<Mn> crystals (curve 2) are presented in fig.3. The measurements were carried out in the quasistatic regime and the pyroelectric coefficient was calculated using the following equation: $\gamma=J/A_0\cdot dT/dt$, where J is the pyroelectric current, A_0 is the area of the electrodes, dT/dt is the heating rate. The measurements were carried out on the samples, which were preliminary polarized in the external electric field. The dependence $\gamma(T)$ for the pure $TlInS_2$ crystal has one peak only with the maximum value of $1.4\cdot10^{-7}$ C/K·cm^2 at 196K. Two anomalies at 190K and 174K are observed for $\gamma(T)$ of $TlInS_2$<Mn> crystal.

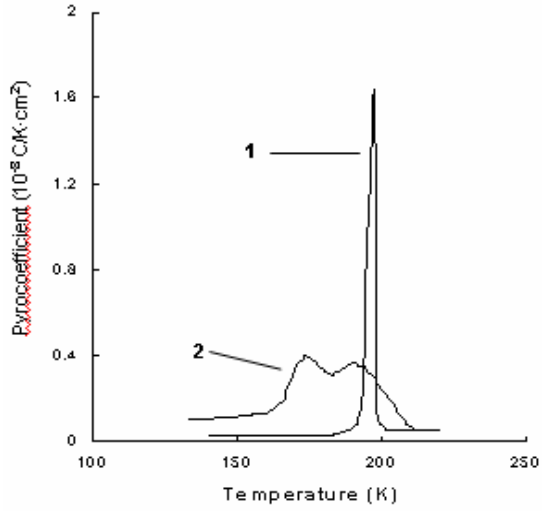

Fig. 3. The temperature dependence of the pyroelectric coefficient. Curve 1 - $TlInS_2$ crystal; Curve 2 - $TlInS_2$<Mn> crystal.

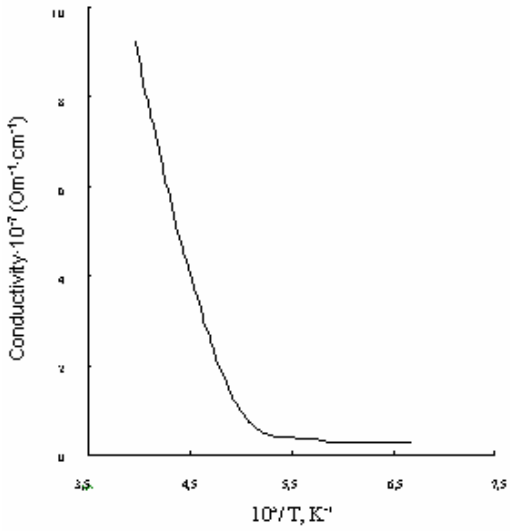

Fig. 4. The dependence of conductivity σ from $1/T$ for $TlInS_2$<Mn> crystal.

The temperature dependence of conductivity on frequency 1 kHz is shown in fig. 4. It is visible, that the conductivity has thermoactivated character, and can be described by the Mott law: $\sigma=\sigma_o exp[-(U/kT)^v]$, where U - the energy of activation, k–Boltzmann constant, v-parameter depending on the mechanism of conductivity. It is known, that the parameter v is approximately equal 1 at the zoned mechanism of conductivity, and in a case of hopping conductivity it lays within the limits of $0,2<v<0,5$.

In an 175-190K interval of temperatures conductivity has thermoactivated character, is satisfactorily described by the above-stated Mott law with a parameter v equal 0,25, that

corresponds thermoactivated hopping to the mechanism of conductivity. Thus on dependence fig.4 it is possible to pick out 3 temperature areas described by various mechanisms of conductivity. The high-temperature area corresponds to the zoned mechanism of conductivity. The temperature area 175-190K- thermoactivated hopping, and area is lower 175K– hopping to the mechanism of conductivity. The estimation of length of a jump shows, that this distance is approximately equal 100A^o that corresponds to jumps of carriers between nanodomain by inclusions.

4. Discussion and Conclusion

The analysis of figures 1-4 allows one to state that $TlInS_2$<Mn> crystals reveal all peculiarities that are typical for the relaxor ferroelectrics. The doping of $TlInS_2$ crystal by Mn cations leads to smearing of phase transitions, and the frequency dispersion of dielectric constant is observed. Moreover, the elongated dielectric hysteresis loop is observed in the smearing region of the phase transition, and the temperature dependence of the dielectric constant in the region of high temperatures is described not by the Curie-Weis law but according to the $(\varepsilon')^{-1}=A+B(T-T_0)^2$ functional form.

The smearing of phase transitions and other ferroelectric peculiarities of $TlInS_2$<Mn> crystal are undoubtedly caused by the structure disorder that leads to the appearance, in a wide temperature region, of local symmetry distortions and internal electric field. Although the phase transitions in $TlInS_2$ crystals are under investigation for a long period of time the satisfactory understanding of physical mechanisms of the processes taking place in the crystals and the unambiguous interpretation of the observed phenomena does not exist. It may be caused by the fact that, during the investigations of phase transitions in $TlInS_2$ crystals, not enough attention was paid to the semiconductor properties of these crystals. This is especially valid for the crystals doped by the cationic impurities. These impurities can form the capture levels (traps) at the bottom of the conduction band. One has to consider two processes: charge carrier localization on the local centers, and their influence on the phase transitions. This issue was considered by Mamin [9-11], where it was shown that the thermal filling of traps could lead to an intricate sequence of phase transitions as well as to the appearance of an unstable boundary state between the phases (incommensurate-commensurate).

The dependence $\gamma(T)$ shows the peak at 175K, and there is no peak of $\varepsilon(T)$ at this temperature (compare figures 1 and 3). According to [11] this peculiarity is typical for the relaxors. It may be explained by an assumption that the oscillation frequency of the induced polarization is determined by the characteristic relaxation time not only of the lattice subsystem as it takes place in usual ferroelectrics but also by the relaxation time of the electronic subsystem. Naturally, the characteristic time τ_η for the change of the order parameter η and the characteristic time τ_m for the change of the electron concentration m in the traps are significantly different $(\tau_\eta/\tau_m<<1)$. Using this assumption the author of [11] investigated the mentioned above problem by separation of fast and slow processes. As a result it has been established that the effective temperature T_{cm} of the phase transition is shifted to lower temperatures due to thermal filling of the capture levels. In our experiments this temperature corresponds to 175 K for the crystals of $TlInS_2$<Mn>. When the localized charges create the local electric fields the spontaneous polarization in the weak external fields in the separate microfields will be directed to the different directions in compliance with space distribution of the localized charges. Therefore, the hysteresis loop in the temperature region 175–190K is observed as narrow and stretched. And according to the same reason, we did not observe the peculiarities in the dependence $\varepsilon(T)$ connected with phase transition at the temperature T_{cm}.

Thus, the doping of $TlInS_2$ crystals by Mn leads to the appearance of the temperature region in which the crystals show all peculiarities that are typical for the relaxors. The phase transition from the relaxor (nanodomain) to the macrodomain (ferroelectric) state occurs at the temperature 175K. The jump in the temperature dependence $\gamma(T)$ corresponds to this transition.

[1] *R.M. Sardarly, O.A. Samedov, I.Sh. Sadykhov, A.I. Nadzhafov, N.A. Eyubova, T.S. Mamedov*, Inorganic Materials, 2003, v.39, No.4, p.327.

[2] *A.A. Volkov, Yu.G. Goncharov, G.V. Kozlov, K.R. Allakhverdiev and R.M. Sardarly*, Soviet Phys. Solid State, 1983, 25, 2061.

[3] *R.A. Aliev, K.R. Allakhverdiev, A.I. Baranov, N.R. Ivanov, R.M. Sardarly*, Soviet Phys. Solid State, 1984, 26, 775.

[4] *S.B. Vakhrushev, V.V. Zdanova, B.E. Kvyatkovski, N.M.Okuneva, K.R. Allakhverdiev, R.A. Aliev, R.M. Sardarly*, JETP letters, 1984, 39, 291.

[5] *R.A. Suleymanov, M.Yu. Seidov, F.I. Salaev, R.F. Mikailov*, Phys. Solid State, 1993, 35, 177.

[6] *I.P. Raevski, V.V. Eremkin, V.G. Smotrakov, E.S. Gagarina, M.A. Malitskaya*, Phys. Solid State, 2000, 42, 161.

[7] *M.D. Glinchuk, E.A. Eliseev, V.A. Stefanovich, B. Hilger*, Phys. Solid State, 2001, 43, 1299.

[8] *L. Benguigai, K. Bethe*, J.Appl.Phys., 1976, 47, 2728.

[9] *R.F. Mamin*, Phys. Solid State, 1991, 33, 1473.

[10] *R.F. Mamin*, JETP letters, 1993, 58, 538.

[11] *R.F. Mamin*, Phys. Solid State, 2001, 43, 1314.

[12] *F. Chu, I.M. Reaney, N. Setter*, Ferroelectrics, 1994, 151, 1-4, 343.

[13] *D. Viehland, S.J. Jang, L.E. Cross, M. Wutting*. J. Appl. Phys., 1990, 68, 2916.

O.Ə.Səmədov

$TlInS_2$ <Mn> – YENİ RELAKSOR SEQNETOELEKTRİK

Göstərilmişdir ki, 0,1 at.% Mn aşkarlanmış $TlInS_2$ kristalı relaksor seqnetoelektriklər üçün xarakterik olan bütün xüsusiyyətlərə malik olur. Dayanıqlı relaksor (nanodomen) halının varlıq temperatur intervalı və seqnetoelektrik (makrodomen) halına keçid temperaturu piroelektrik xassələrində alınan anomaliya görə müəyyən edilmişdir.

О.А. Самедов

$TlInS_2$ <Mn> - НОВЫЙ РЕЛАКСОРНЫЙ СЕГНЕТОЭЛЕКТРИК

Показано, что $TlInS_2$, легированный щ,1 ат.% Mn проявляет все характерные особенности релаксорного сегнетоэлектрика. Установлена температурная область существования устойчивого релаксорного (нанодоменного) состояния и температура фазового перехода в сегнетоэлектрическое (макродоменное) состояние, сопровождаемое аномалиями поляризационных и пироэлектрических свойств.

Received: 24.05.03

REACTIVE CHARACTERISTICS OF OPTONEGATRON ELEMENTS ON THE BASE OF LOCAL POLYCRYSTALLINE SILICON FILMS

F.D. KASIMOV
Azerbaijan National Aerospace Agency,159 av. Azadlig, 370106 Baku
e-mail: ssddb@azerin.com, tel: (99412) 621736

A.A. MAMEDOV
Azerbaijan Technical University, 370073, Baku, H.Javid ave. 25

Abstract. The capacitance-voltage characteristics of local polycrystalline silicon films were investigated in the frequency range 0,465-10 MHz. A transition in the character of reactive conductivity from capacitance to inductive behavior was discovered under influence the illumination the inductance transformed back into a capacitance and the negative resistance region disappeared from the current-voltage curve, consequently local polysilicon films are the optonegatron elements.

It is shown that inductivity phenomena in polycrystalline silicon films occur by processes of recharging of deep levels.

Optonegatronics, polycrystalline silicon films, reactive conductivity, inductivity, capacitance, deep level.

1. Introduction

Recently disordered structures have received much attention from designers of active devices as they offer an increase in functional possibilities per unit volume of electronic devices without an increase in the packing density of integrated circuits. Among the structures under consideration are amorphous semiconductors in which a phase transition takes place because of the action of different modes of excitation. This is followed by negative resistance and phase transition phenomena [1] by a transition of capacitive reactivity into inductive behavior [2] and possibility to form the optonegatron elements [3].

Of particular interest is the investigation of such phenomena in polycrystalline silicon (poly-Si) films, because silicon is the basic semiconductor material in microelectronics. Use of the technique of local growth of poly-Si films during the epitaxial formation of monocrystalline silicon [4] makes it possible to form elements with data processing circuits on the same chip. For example, according to [5], locally grown poly-Si films can be considered as distributed RC structures for integrated circuit filters. As shown in [6], locally grown poly-Si films exhibit a memory switching effect.

In this paper we report some inductive phenomena which were first observed in switching poli-Si films during capacitance-voltage measurements.

2. Experimental results

The poly-Si films (200μm×20μm) were formed on locally oxidized silicon-substrates of *p*-type conductivity with a resistivity of 10Ω·cm during the process of epitaxial growth of a 5μm monocrystalline film of *n*-type conductivity with a dopant concentration (phosphorus) of 10^{16} cm^{-3}. Epitaxial growth was performed in a heated (by high frequency power) vertical-type reactor using the high temperature (1200°C) chloride process. The waters were oxidized to obtain a pyrolytic oxide of thickness 3.5μm, and aluminum ohmic contacts were formed using photolithography and vacuum deposition techniques. The sample construction is presented on the Fig. 1.

The capacitance-voltage (C-V) characteristics were measured with an L2-7 impedance bridge at room temperature over the frequency range 0,465-10MHz using an ac signal of low voltage (25mV).

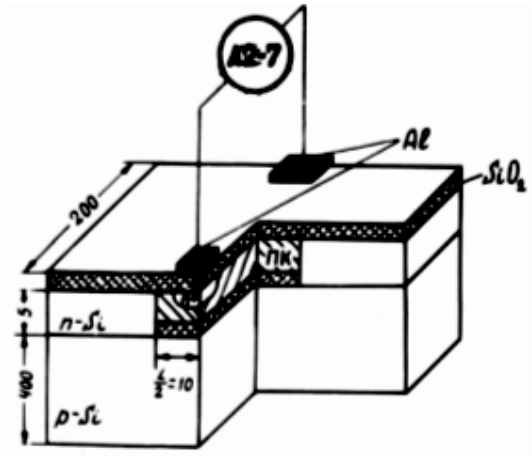

Fig. 1. Construction of the element on the base of a local poly-Si film

Typical C-V characteristics of poly-Si films in the OFF state at different frequencies of the ac signal are presented in fig.2,a. As can be seen, at definite voltage values for both bias polarities the capacitance changes from positive to negative, the phenomenon showing a purely inductive behaviour. With increasing frequency of the ac signal the voltage corresponding to this inversion of sign also increased. The capacitance of poly-Si films in the ON state was negative over the full frequency range (fig. 2,b).

From a comparison of the characteristics shown in fig. 2,a and fig. 3,a it appears that the sign inversion of the capacitance takes place at voltages near the threshold voltages of switching. The volt-ampere (I-V) characteristics of poly-Si films were measured on the waters by probes. When a microscope lamp with a power of 20 W was switched on, the negative resistance region disappeared from the I-V curve while the rest of the curve was almost unchanged (fig. 3,b). C-V measurements performed with and without illumination showed that under illumination the capacitance changed from negative to positive values simultaneously with the disap-

pearance of the negative resistance region from the I-V curve.

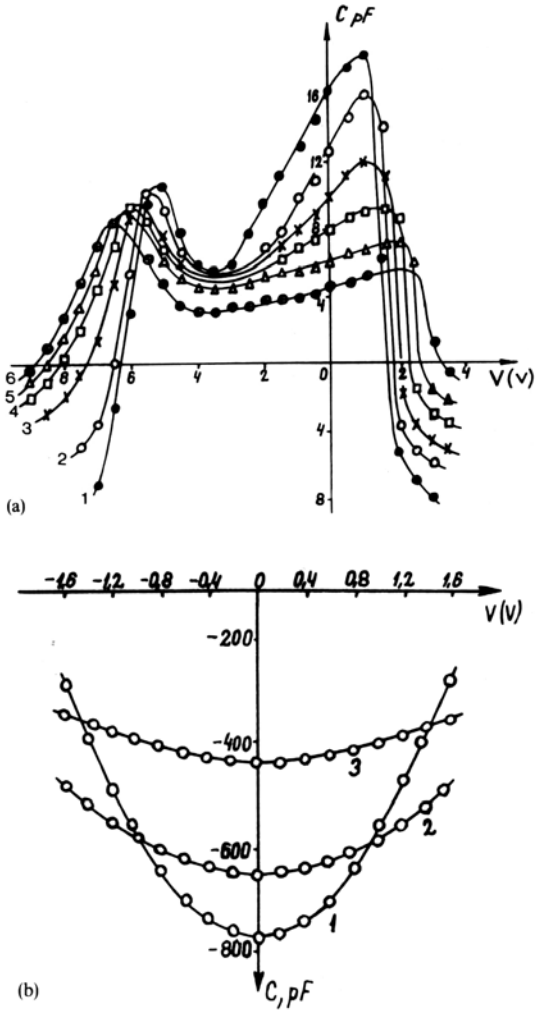

Fig. 2. Capacitance-voltage characteristics of a poly-Si film at various frequencies: (a) OFF state (curve 1 - 0.465 MHz; curve 2 - 1 MHz; curve 3 - 3 MHz; curve 4 - 5 MHz; curve 5 - 7 MHz, curve 6 - 10 MHz, (b) ON state (curve 1 -0.465 MHz, curve 2 - 5 MHz, curve 3 - 10 MHz)

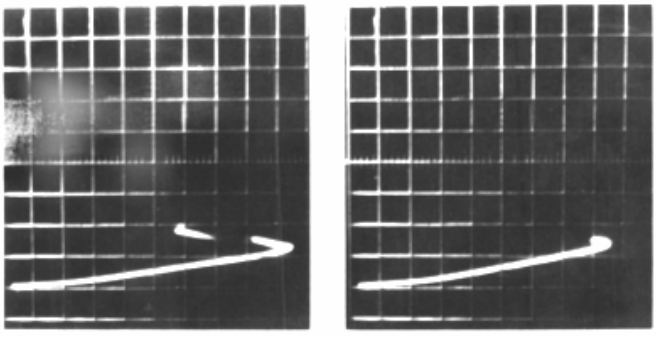

Fig.3. I-V-characteristics of a poly-Si film under reverse bias (a) without illumination and (b) under illumination (horizontal axis - 1V/division; vertical axis - 5 mA/division)

3. Discussion and conclusions

The capacitance transition observed in the OFF state could be explained in terms of carrier trapping by deep levels at the grain boundaries. In fact in the OFF state the capacitance of a poly-Si film is determined by depletion layers at the grain boundaries and must decrease with increasing reverse bias because of the widening of these layers (fig. 2,a, left side).With a further increase in bias a sequential breakdown of potential barriers takes place resulting in an of capacitance due to the contribution of free carriers injected into the depletion region.

Then, as seen from fig. 2,a, an abrupt decrease in the capacitance and its transition to negative values take place. The asymmetry of the C-V characteristics relative to the bias polarity is explained by the fact that, according to [6], in switching poly-Si films the potential barriers exist only on one side of the grain. Thus under forward bias the capacitance instantly increases the carrier injection (fig. 2,a, right side).

As has been shown [7] for the breakdown region of p-n junctions containing deep levels, the capacitive behavior of the reactive conductance changes into an inductive behavior as a result of carrier generation and capture. The presence of deep levels and barrier layers suggests that the observed transition of the capacitance to negative values in poly-Si films is also due to processes of recharging of their deep levels.

As the result of the breakdown, free carriers are injected into depletion layers where they are captured by deep traps at the grain boundaries. At a low injection level the relaxation time of deep levels is sufficiently long and satisfies the condition $1/\tau<\omega$ where ω is the cyclic frequency of the ac signal. Therefore the traps cannot follow the changes in the ac signal and do not participate in reactive conductance. The capacitance is positive. With increasing bias the injection level also increases. This is followed by an increase in the probability of free-carrier capture by deep traps, which results in a decrease in their relaxation time. At a definite injection level the condition $1/\tau=\omega$ is satisfied and the reactive conductance becomes zero. With a further increase in the bias voltage the ac signal frequency becomes lower than the frequency $1/\tau$ of free-carrier capture. Thus, while the ac signal is changing, the deep traps manage to capture and generate carriers. This results in a lagging phase shift between the current and the voltage, i.e. the films exhibit inductive behavior. The decrease in current due to illumination, which is shown by the disappearance of the S-shaped region, indicates that the poly-Si films exhibit negative photoconductivity. Similar phenomena are also connected with deep traps.

As known from [8], the deep level centers in semiconductors can have several charge states with corresponding different degrees of localization of the wave-function. The center charge states with $n>1$ may be shown on an electron band structure by the insertion of the correlated electron level which can exist in a conduction band. In this case it is possible for a conduction electron which traps a photon to jump from a zone into a local state, thus creating a negative photoconductivity.

In the ON state there are no potential barriers, the film resistance is low and the injection level is high. In this case the limiting factor of the capture and generation of free carriers is the intrinsic relaxation time of deep traps. This time corresponds to the intrinsic transition time from the OFF to the ON state, which according to [6] is of the order of 10 ns. Consequently, in poly-Si films in the ON state the transition of the capacitance to positive values, according to the condi-

tion $\omega>1/\tau$, can take place at ac signal frequencies higher than 15 MHz.

Thus, from the investigations carried out we concluded that a locally grown poly-Si film is a functional element with non-linear C-V-characteristics, having two stable conduction states with voltage-and light-controlled parameters, therefore it is possible to use them as the optonegatron elements.

[1] *P.E. Schmidt, R.C. Callaroti*. Study of the operation of ovonic switches in the relaxation oscillation mode. J. Appl. Phys., 1984, v..55, №8. p. 3144-3147.

[2] *A.S. Deshevoy, L.S. Gasanov*. Tverdotelnaya induktivnost v amorfnikh i compensirovannikh poluprovodnikakh Fizika I tekhnika poluprovodnikov. 1977, t.11, №10, s.1995, 1999.

[3] *M.A. Filinyuk*. Optonegatronika - istorichnii shlyakh rozvitku ta percpectivi. Optoelectronic information-power technologies (Vinnitza). 2001, №1, p.251-259.

[4] *A.G. Abdullayev, F.D. Kasimov, V.M. Mamikonova.* Simultaneous growth of mono- and polycrystalline silicon films. Thin. Solid Films. 1984, v.115, №3, p..237-243.

[5] *C.Y. Lu, N.C. Lu*. Current transport across a grain boundary in polycrystalline semiconductors // Solid-State Electron. 1983. –v.26, №6, p..549-557.

[6] *A.G. Abdullayev, F.D. Kasimov, V.A. Vetkhov*. Memory switching in locally grown polycrystalline silicon films // Thin Solid Films. 1984, v.112, №2, p.121-125.

[7] *G.M. Avakyantz*. Primesnaya teoriya aktivnikh i reaktivnikh svojstv electronno-dirochnikh perekhodov // Radiotekhnika i Elektronika. 1965, №4, s.693-699.

[8] *F.F. Kasimova, N.G. Javadov*. Stimulirovannoye svetom otritzatelnoye soprotivleniye v kremnievikh p-n-perekhodakh s polikristallicheskoi bazoi. Izvestiya Vuzov.Elektronika (Moskva). 1999, №1-2, s..47-51.

F.C. Qasımov, Ə.A. Məmmədov

POLİKRİSTALLİK SİLİSİUMUN LOKAL PLYONKALARI ƏSASINDA OPTONEQATRON ELEMENTLƏRİN REAKTİV XASSƏLƏRİ

0,465÷10MHs diapazonunda monokristallik plyonkaların epitaksial yetişdirmə prosesində becərdilmiş polikristallik silisium lokal plyonkasının volt-tutum xarakteristikaları tədqiq edilmişdir. Reaktiv keçiriciliyin xarakterinin tutumdan induktivliyə inversiya effekti aşkar edilmişdir. İşıqlanmanın təsiri ilə induktiv xarakter əksinə tutuma keçir, VAX-dakı mənfi müqavimət hissəsi yox olur, deməli, polikristallik silisium lokal plyonkaları optoneqatron elementləridir. Göstərilmişdir ki, polikristallik silisium plyonkalarındakı induktiv hadisələri, dərin səviyyələrin yenidən yüklənməsi ilə əlaqədardır.

Ф.Д. Касимов, А.А. Мамедов

РЕАКТИВНЫЕ СВОЙСТВА ОПТОНЕГАТРОННЫХ ЭЛЕМЕНТОВ НА ОСНОВЕ ЛОКАЛЬНЫХ ПЛЕНОК ПОЛИКРИСТАЛЛИЧЕСКОГО КРЕМНИЯ

В диапазоне 0,465÷10 МГц исследованы вольт-емкостные характеристики локальных пленок поликристаллического кремния, выращенных в процессе эпитаксиального наращивания монокристаллических пленок. Был обнаружен эффект инверсии характера реактивной проводимости из емкостного в индуктивный. Под влиянием освещения индуктивный характер переходил обратно в емкостный, а участок отрицательного сопротивления на ВАХ исчезал. Следовательно, локальные пленки поликремния являются оптонегатронными элементами.

Показано, что индуктивные явления в поликремниевых пленках обусловлены процессами перезарядки глубоких уровней.

Received: 16.06.03

BASES OF THE THEORY OF CAPACITY AND ENERGY OF DISTORTION IN ELECTRICAL CIRCUITS WITH NONLINEAR POWER

E.M. FARKHADZADE, H.B. GULIYEV
Scientific-Research Institute of Power Engineering and Energy Design
Az1012, Zardabi str., 94

Increase of sensitivity of modern technologies to sinusoidal distortion of a power requires perfection of the mechanism, responsibility of the consumers generated high harmonic component (HHC), where level exceeds normative values. An integrated parameter of quality of electrical energy is the energy of distortion.

However theory of capacity and energy of distortion in networks of an alternating current is not developed. The results of researches allowing to establish essence energy of distortion and to calculate it for any spectrum HHC are given.

Despite of significant number of works devoted to a problem of definition of capacity and energy of distortion, the difficulties of its decision are known. The urgency of a problem grows in connection with the varied relations of the participants of the market of the electric power, by increase of the requirements to quality of the electric power on the part of the consumers [1].

Let's distinguish power *(U)* and current in a circuit (I), having:

- Identical frequency. Let's name as their same harmonics (SH) of power and current. Private, but, it is obvious most important case is U_1 and I_1 of the basic harmonic;
- Various frequency. Let's name them different-name harmonics (DNH) of a power and current.

The variable making of capacities of SH and the capacity DNH as a matter of fact is exchange capacity (EC) and between its complete (S_n), active (P_n) and reactive (Q_n) components the square-law dependence, i.e. $S_n^2 = P_n^2 + Q_n^2$ takes place. To distinguish EC of the basic harmonic from EC HHC it is accepted to name last as capacity of distortion (CD), and energy, appropriate to it by energy of distortion (ED).

Before to define capacity *(S)* and energy *(W)* HHC with the purposes of comparison we shall refer to known results of definition S_1 and W_1, including their active (P_1) and reactive (Q_1) parameters for the basic harmonic [2]. Let

$$u_1(t) = U_{1,m} \sin \omega t \qquad (1)$$

$$i_1(t) = I_{1,m} \sin(\omega t + \varphi_1) \qquad (2)$$

$$S_1(t) = P_1(t) + Q_1(t) \qquad (3)$$

where $P_1(t) = P_1(1 - \cos 2\omega t)$, $Q_1(t) = Q_1 \sin 2\omega t$

EC of the basic harmonic consists from:

By active component with a maximum equalled $P_{1,m} = |P_1|$, where $P_1 = 0{,}5U_{1,m}I_{1,m}\cos\varphi_1$ and with energy, which for the period T_1 is equalled

$$W_{P,1}^{(+)} = \left|W_{P,1}^{(-)}\right| = P_1 T_1 \pi^{-1} \qquad (4)$$

where the marks (+) and (-) designate a direction of flows *SE*. In the subsequent statement the mark *W* with the purposes of simplification will be specified only if it is necessary.

By reactive component with a maximum equal $Q_{1,m} = |Q_1|$, where $Q_1 = 0{,}5U_{1,m}I_{1,m}\sin\varphi$ and with energy, which for the period T_1 is equal

$$W_{Q,1} = Q_1 T_1 \pi^{-1} \qquad (5)$$

Similarly

$$S_{1,m} = |S_1|, \text{ where } S_1 = 0{,}5U_{1,m}I_{1,m}$$

$$W_{S,1} = S_1 T \pi^{-1} \qquad (6)$$

Generally, when in a linear circuit a power

$$u(t) = \sum_{n=1}^{n_m} U_{n,m} \sin n\omega t \qquad (7)$$

The current is equalled

$$i(t) = \sum_{n=1}^{n_m} I_{n,m} \sin(n\omega t + \varphi_n) \qquad (8)$$

The instant value of complete capacity *S(t)* on sine not wave curves *u(t)* and *i(t)* would seem equally to product of instant values $u(t_i)$ and $i(t_i)$ by analogy to sine wave curves of a power and current. Let's show on a simple example, that such calculation is erroneous. Let at a circuit with linear loading in curves *u(t)* and *i(t)* alongside with the basic harmonic there are the third and seventh harmonic, i.e.

$$u(t) = U_{1m} \sin\omega t + U_{3m} \sin 3\omega t + U_{7m} \sin 7\omega t$$

$$i(t) = I_{1m} \sin(\omega t + \varphi_1) + I_{3m} \sin(3\omega t + \varphi_3) + I_{7m} \sin(7\omega t + \varphi_7)$$

At the moment t_1 at the marked approach

$$S(t_1) = u(t_1) \cdot i(t_1),$$

and the product includes six components, which are deprived physical meaning, since under action of n^{th} of a harmonic of a power in a linear circuit the harmonics of a current can not proceed, where order is differed from *n*. The accounts *S(t)* must make under the formula

$$S(t)=\sum_{n=1}^{n_m}U_{n,m}I_{n,m}\sin n\omega t\sin(n\omega t+\varphi_n)=\sum_{n=1}^{n_m}P_n-\sum_{n=1}^{n_m}P_n\cos 2n\omega t+\sum_{n=1}^{n_m}Q_n\sin 2n\omega t=P_{\Sigma,cp}+S_{1,1}(t)+D_{oc}(t) \quad (9)$$

where, n_m- greatest number HHC; $S_{1,1}(t)$ -EC at $n=1$; $D_{oc}(t)$- CD *SH*; $U_{n,m}$, $I_{n,m}$ and φ_n are calculated by the results of the Furye-analysis of curves $u(t)$ and $i(t)$.

$$P_n=0{,}5U_{n,m}I_{n,m}\cos\varphi_n=P_1K_{Un}K_{I(n)}\frac{\cos\varphi_n}{\cos\varphi_1}=S_1K_{U(n)}K_{I(n)}\cos\varphi_n \quad (10)$$

$$Q_n=0{,}5U_{n,m}I_{n,m}\sin\varphi_n=Q_1K_{U(n)}K_{I(n)}\frac{\sin\varphi_n}{\sin\varphi_1}=S_1K_{U(n)}K_{I(n)}\sin\varphi_n \quad (11)$$

$$S_n=0{,}5U_{n,m}I_{n,m}=S_1K_{U(n)}K_{I(n)} \quad (12)$$

Accordingly, parameters ED SH of a power and current for n^{th} of a harmonic with $n=\overline{2,n_m}$ Can be calculated under the formulas:

$$W_{P,n}=W_{P,1}K_{U(n)}K_{I(n)}\frac{\cos\varphi_n}{\cos\varphi_1}=W_{S,1}K_{U(n)}K_{I(n)}\cos\varphi_n \quad (13)$$

$$W_{Q,n}=W_{Q,1}K_{U(n)}K_{I(n)}\frac{\sin\varphi_n}{\sin\varphi_1}=W_{S,1}K_{U(n)}K_{I(n)}\sin\varphi_n \quad (14)$$

$$W_{S,n}=W_{S,1}K_{U(n)}K_{I(n)} \quad (15)$$

If CD (ED) is compared for n^{th} HHC ($n=\overline{2,n_m}$) (9-15) and EC (EE) of the basic harmonic (3-6), then it is uneasy to notice, that their relation is defined with factors n^{th} HHC of a power ($K_{U(n)}$) and current ($K_{I(n)}$). If $K_{U(n)}$ and $K_{I(n)}$ is as much as possible allowable values then it is possible to conclude, that CD (ED) make from EC (EE) of the basic harmonic no more than one percent.

Let's consider now definition CD and ED for DNH of a power and current. Let in a circuit of a current power source (PS) with a sine wave power is included NP (ventil converters, arc steel-smelting of the furnace and etc.). The current in circuit will be equal a circuit (8), and capacity at n=2, n_m.

$$S_{1,n}(t)=u_1(t)\,i_n(t)=P_{1,n}(t)+Q_{1,n}(t) \quad (16)$$

where

$$P_{1,n}(t)=P_{1,n}\left[\cos(n-1)\omega t-\cos(n+1)\omega t\right] \quad (17)$$

$$Q_{1,n}(t)=Q_{1,n}\left[\sin(n+1)\omega t-\sin(n-1)\omega t\right] \quad (18)$$

$$P_{1,n}=P_1K_{I(n)}\frac{\cos\varphi_{1,n}}{\cos\varphi_1}=S_1K_{I(n)}\cos\varphi_{1,n} \quad (19)$$

$$Q_{1,n}=Q_1K_{I(n)}\frac{\sin\varphi_{1,n}}{\sin\varphi_1}=S_1K_{I(n)}\sin\varphi_{1,n} \quad (20)$$

$$S_{1,n}=S_1K_{I(n)} \quad (21)$$

From the equations (21) and (12) it is visible, that the capacity contains only variable (pulsing) part and on the order more, than $S_n(t)$.

Let's define the moments of time ($t_{1,n,m}$) at which $P_{1,n}(t)$, $Q_{1,n}(t)$ and $S_{1,n}(t)$ reach the maximal values designated, accordingly $P_{1,n,m}$, $Q_{1,n,m}$ and $S_{1,n,m}$. Having calculated derivative of functions $P_{1,n}(t)$, $Q_{1,n}(t)$ and $S_{1,n}(t)$, equate them to zero and having generalized results for n, we have:

1. For function $P_{1,n(t)}$ Parameter $\left|P_{1,n,m}\cdot P_{1,n}^{-1}\right|=\left|\gamma_{1,n}^{P}\right|=2$ for all odd harmonics, and for even harmonics $\left|\gamma_{1,n}^{P}\right|$ =2 practically at n≥ 8 (the divergence makes as follows $\beta_{1,n}^{P}=100\left(1-0{,}5\left|\gamma_{1,n}^{P}\right|\right)\le 1{,}5\%$). Thus, by analogy to active capacity $P_{n(t)}$, the parameter $P_{1,n(t)}$, has a maximum (under the marked conditions) equaled $2|P_{1,n}|$. However, if for $P_{n(t)}$ this maximum always positive, the maximum $P_{1,n(t)}$ can be both positive, and negative.

The modular summation of maximal of active capacity HHC gives large mistakes of calculation, since $P_{1,n,m}$ is differed with mark and for even harmonics and a moment of occurrence.

2) For function $Q_{1,n}(t)$

The parameter $\left|Q_{1,n,m}\cdot Q_{1,n}^{-1}\right|=\left|\gamma_{1,n}^{Q}\right|=2$ for all even harmonics, and for odd harmonics $\left|\gamma_{1,n}^{Q}\right|=2$ practically at $n\ge 7$ (divergence makes as follows $\beta_{1,n}^{Q}100\left(1-1{,}5\left|\gamma_{1,n}^{Q}\right|\right)\le 2{,}5\%$). Let's notice, that such change for reactive capacity of the same harmonics $Q_n(t)$ HHC is not present. $Q_{n,m}=\left|Q_n\right|$;

The modular summation of maximal of reactive capacity HHC as well as for active capacity gives large errors of calculation.

Let's define ED $W_{1,n}$ for $P_{1,n}(t)$, $Q_{1,n}(t)$ and $S_{1,n}(t)$.

Empirically by integration of the functions $P_{1,n}(t)$, $Q_{1,n}(t)$ and $S_{1,n}(t)$ and by definition accordingly $W^{(+)}_{P,1,n}$, $W^{(+)}_{Q,1,n}$ and $W^{(+)}_{S,1,n}$ we have defined what, at $n \geq 3$ for the period of the basic harmonic T_1 with an error no more than 1 %.

$$W_{P,1,n} = 2{,}56\frac{P_{1,n}}{\omega} = 8{,}1\cdot 10^{-3} P_{1,n} \qquad (22)$$

$$W_{Q,1,n} = 2{,}56\frac{Q_{1,n}}{\omega} = 8{,}1\cdot 10^{-3} Q_{1,n} \qquad (23)$$

$$W_{S,1,n} = 2{,}56\frac{S_{1,n}}{\omega} = 8{,}1\cdot 10^{-3} S_{1,n} \qquad (24)$$

If (22-24) are some transformed, we shall receive:

$$W_{P,1,n} = 10^{-2} P_{1,n,cp} = 10^{-2} U_{1,cp} I_{n,cp} \cos\varphi_{1,n} = 8{,}1\cdot 10^{-3} S_1 K_{I(n)} \cos\varphi_{1,n} \qquad (25)$$

$$W_{Q,1,n} = 10^{-2} Q_{1,n,cp} = 10^{-2} U_{1,cp} I_{n,cp} \sin\varphi_{1,n} = 8{,}1\cdot 10^{-3} S_1 K_{I(n)} \sin\varphi_{1,n} \qquad (26)$$

$$W_{S,1,n} = 10^{-2} S_{1,n,cp} = 10^{-2} U_{1,cp} I_{n,cp} = 8{,}1\cdot 10^{-3} S_1 K_{I(n)} \qquad (27)$$

where $U_{1,cp} = \frac{2}{\pi} U_{1,m}$; $I_{n,cp} = \frac{2}{\pi} I_{n,m}$.

The formulas (25-27) are simple enough and allow to define ED HHC directly by results of decomposition of function $i(t)$ in a trigonometrically number Furye.

Let's proceed to a question of definition summation (S) CD and ED of an any spectrum HHC.

At a sine not sinusoidal power in a circuit with NP the instant value of capacity can be calculated under the formula:

$$\begin{aligned} S_{\Sigma}(t) &= \sum_{n=1}^{n_m} P_n - \sum_{n=1}^{n_m} P_n \cos 2n\omega t + \sum_{n=1}^{n_m} Q_n \sin 2n\omega t + \\ &+ \sum_{n=2}^{n_m-1} P_{1,n}\left[\cos(n-1)\omega t - \cos(n+1)\omega t\right] + \sum_{n=2}^{n_m-1} Q_{1,n}\left[\sin(n+1)\omega t - \sin(n-1)\omega t\right] = \\ &= P_{\Sigma,cp} + S_{1,1}(t) + D^{(SH)}_{\Sigma,S}(t) + D^{(DNH)}_{\Sigma,S}(t) = P_{\Sigma,cp} + G_{\Sigma,S}(t) \end{aligned} \qquad (28)$$

where $D_{\Sigma,S}(t)$ - summation instant CD for SH and DNH; $G_{\Sigma,S}$- summation instant EC. In turn:

$$D^{(DNH)}_{\Sigma,S}(t) = \sum_{n=2}^{n_{m-1}} P_{1,n}(t) + \sum_{n=2}^{n_m-1} Q_{1,n}(t) = D^{(DNH)}_{\Sigma,P}(t) + D^{(DNH)}_{\Sigma,Q}(t) \qquad (29)$$

The definition of the maximal values $D^{(DNH)}_{\Sigma,S}(t), D^{(DNH)}_{\Sigma,P}(t)$ and $D^{(DNH)}_{\Sigma,Q}(t)$ at practicable in practice spectra HHC requires large analytical calculations.

Before to formulate algorithm of account CD and ED of an any spectrum HHC DNH (in subsequent the indexes DNH is omitted) we shall consider some features of calculations on a concrete example. A graphic illustration of change of an active and reactive component CD and ED, in conditions, when alongside with the basic harmonic, in a circuit the currents of thirds proceed and fifth harmonics is shown in a fig. 1a, and allows to conclude:

1. The functions $P_{1,n}(t)$ and $Q_{1,n}(t)$ are not sinusoidal characterized periodically varied by amplitude and duration of each half-cycle. Nevertheless the maximal values of this function and functions $S_{1,n}(t)$ are connected by square-law dependence. However, $\sum P^2_{1,n,m} + \sum Q^2_{1,n,m} >> \sum S^2_{1,n,m}$ and $\left(\sum P_{1,n,m}\right)^2 + \left(\sum P_{1,n,m}\right)^2 >> \left(\sum S_{1,n,m}\right)^2$.

2. The moments of occurrence of the maximal values $P_{1,n}(t)$ of odd harmonics coincided, and the marks can be opposite. The moments of occurrence of maximal $Q_{1,n}(t)$ of odd harmonics do not coincide, and the marks of the maximal values can be different. Therefore algebraic summation of maximal as $P_{1,n}(t)$ and $Q_{1,n}(t)$ results in the large mistakes of calculation.

3. ED (is shaded) on an interval $T_1/4$ $W^{(+)}_{\Sigma,P} = \left|W^{(-)}_{\Sigma,P}\right|$ and $W^{(+)}_{\Sigma,Q} = \left|W^{(-)}_{\Sigma,Q}\right|$ and is calculated as the sum of the areas limited to an interval T/2 and curves $P_{1,3}(t)$ and $P_{1,5}(t)$ (or $Q_{1,3}(t)$ and $Q_{1,5}(t)$).

4. $W_{S,P} << W_{1,3,P} + W_{1,5,P}$ and $W_{S,Q} << W_{1,3,Q} + W_{1,5,Q}$

Otherwise ED designed as the sum energy of separate harmonics exceeds essentially then the valid value. In a fig.1a, it would be visible from comparison of the areas with longitudinal (designating WS) and cross (designating the sum $W_{1,3}$ and $W_{1,5}$) shading. The basic difficulty of analytical calculation of the valid values CD and ED at an any spectrum HHC alongside with greatness of calculation, consists in formalization of definition of the moments of crossing of functions $D_{\Sigma,S}(t)$, $D_{\Sigma,P}(t)$ and $D_{\Sigma,Q}(t)$ of an axis t. The following algorithm of calculation CD and ED in the single-phase

purpose with NP on an interval T_1 is supposed. The algorithm consists of the following blocks:

1. Are entered 2 (n_m+1) discrete values $u(t)$ and $i(t)$ with an interval $\Delta t_1=T_1/2\ (n_m+1)$.

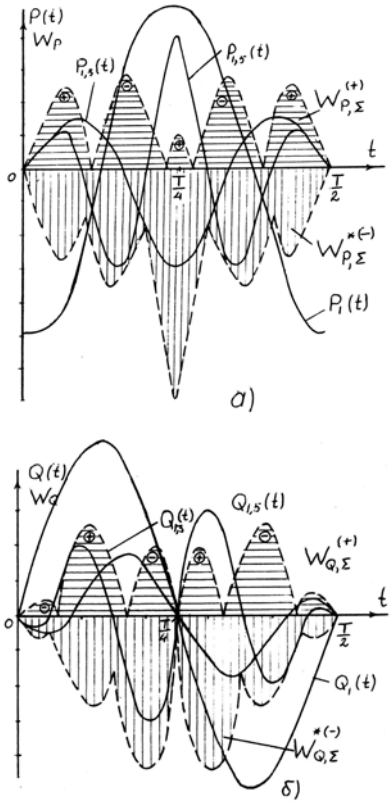

Fig.1. Comparison energies (power) of distortion

a) an active-power; b) reactive-power

2. Under the formulas Furye the amplitudes $(U_{n,m}$ *and* $I_{n,m})$ and corners of shift $\left(\psi_{\mathrm{n}}^{\mathrm{U}}\right.$ and $\left.\psi_{\mathrm{n}}^{\mathrm{I}}\right)$ of harmonics for $n=1$, nm are calculated.

3. The factors are calculated: distortions of sinusoidalness of a power K_U and n^{th} of a harmonic of a power $K_{U(n)}$ and current $K_{I(n)}$ with $n=2, n_m$.

4. The harmonics exceeding normative values are allocated. This condition is based on two situations. First ED for a spectrum of harmonics which are not exceeding normative values much less of 0,5 % from energy of the basic harmonic. Second is considered, that to payment should be subject only ED of harmonics, for which the established requirements to the parameters are not carried out. A consequence of this condition is the sharp reduction of number of calculations.

5. Under the formulas (16-21) the instant values $S_{1,n}(t_j)$, $P_{1,n}(tj)$ and $Q_{1,n}(tj)$ with $j=1, M$, $n=1, n_m$, where M=d $n_{m,n}$ are calculated; $n_{m,n}$ number of sections, at which the area sinusoid, calculated by a method of trapezes on an interval $T_1/4$ does not differ practically from the valid parameter ($d=5$); nm, n-greatest number of harmonics exceeding normative value. Let's remind, that the interval $T_1/4$ is a half-cycle of change CD.

6. Are calculated summation CD $D_{\Sigma,S}(tj)$, $D_{\Sigma,P}(tj)$ and $D_{\Sigma,Q}(tj)$ with $j=1, M$ with that difference, that it are taken into account only important of a harmonic.

7. The relative meaning of the maximal CD are defined:

$$\delta D_{\Sigma,S,m}=max\left\{D_{\Sigma,S}\left(t_j\right)\right\}_M\cdot S_{1,m}^{-1},\delta D_{\Sigma,P,m}=max\left\{D_{\Sigma,P}\left(t_j\right)\right\}_M\cdot P_{1,m}^{-1}$$

and

$$\delta D_{\Sigma,Q,m}=max\left\{D_{\Sigma,Q}\left(t_j\right)\right\}_M\cdot Q_{1,m}^{-1}$$

8. The relative meanings(importance) of a complete, active and reactive component ED by everyone important ВГС are calculated.

$$\delta W_{P,1,n}=100\frac{W_{P,1,n}}{W_{P,1}}=\frac{25\pi\sum_{j=1}^{M-1}\left[\left|P_{1,n}\left(t_j\right)\right|+\left|P_{1,n}\left(t_{j+1}\right)\right|\right]}{MP_1} \quad (30)$$

$$\delta W_{Q,1,n}=100\frac{W_{Q,1,n}}{W_{Q,1}}=\frac{25\pi\sum_{j=1}^{M-1}\left[\left|Q_{1,n}\left(t_j\right)\right|+\left|Q_{1,n}\left(t_{j+1}\right)\right|\right]}{MQ_1} \quad (31)$$

$$\delta W_{S,1,n}=100\frac{W_{S,1,n}}{W_{S,1}}=\frac{25\pi\sum_{j=1}^{M-1}\left[\left|S_{1,n}\left(t_j\right)\right|+\left|S_{1,n}\left(t_{j+1}\right)\right|\right]}{MS_1} \quad (32)$$

9. The relative values of complete ($W_{D,S}$), active ($W_{D,P}$) and reactive ($W_{D,Q}$) components ED under the formulas are calculated

$$\delta W_{D,P}=100\frac{W_{D,P}}{W_{P,1}}=\frac{25\pi\sum_{j=1}^{M-1}\left[\left|D_{\Sigma,P}\left(t_j\right)\right|+\left|D_{\Sigma,P}\left(t_{j+1}\right)\right|\right]}{MP_1} \quad (33)$$

$$\delta W_{D,Q}=\frac{W_{D,Q}}{W_{Q,1}}=\frac{25\pi\sum_{j=1}^{M-1}\left[\left|D_{\Sigma,Q}\left(t_j\right)\right|+\left|D_{\Sigma,Q}\left(t_{j+1}\right)\right|\right]}{MQ_1} \quad (34)$$

$$\delta W_{D,S}=\frac{W_{D,S}}{W_{S,1}}=\frac{25\pi\sum_{j=1}^{M-1}\left[\left|D_{\Sigma,S}\left(t_j\right)\right|+\left|D_{\Sigma,S}\left(t_{j+1}\right)\right|\right]}{MS_1} \quad (35)$$

10. The complete, active and reactive exchange energy *(G)* in a circuit with NP is calculated

$$W_{G,P} = 5 \cdot 10^{-3} M^{-1} \sum_{j=1}^{M-1} \left[\left| P_1(t_j) + D_{\Sigma,P}(t_j) \right| + \left| P_1(t_{j+1}) + D_{\Sigma,P}(t_{j+1}) \right| \right] \quad (36)$$

$$W_{G,Q} = 5 \cdot 10^{-3} M^{-1} \sum_{j=1}^{M-1} \left[\left| Q_1(t_j) + D_{\Sigma,Q}(t_j) \right| + \left| Q_1(t_{j+1}) + D_{\Sigma,Q}(t_{j+1}) \right| \right] \quad (37)$$

$$W_{G,S} = 5 \cdot 10^{-3} M^{-1} \sum_{j=1}^{M-1} \left[\left| S_1(t_j) + D_{\Sigma,S}(t_j) \right| + \left| S_1(t_{j+1}) + D_{\Sigma,S}(t_{j+1}) \right| \right] \quad (38)$$

The results of accounts, confirming the structural analysis CD and ED, allow to receive objective quantitative parameters ED at various spectra HHC NP.

Conclusions

1. The energy SH of a power and current (W_n) with $n>1$ generators of power stations is proportional to multiplication $K_{U(n)}$ and $K_{I(n)}$, 1 % from energy of the basic harmonic W_1, a rule, do not exceed. The energy DNH ($W_{1,n}$) is generated by nonlinear loading and is proportional $K_{I(n)}$.
2. The basic making energy DNH is the component caused by the basic harmonic of a power and HHC of a current. All other components are within the limits of accuracy of account and measurement.
3. The capacity DNH has pulsing character with varied amplitude and duration of waves of a pulsation.
4. The energy DNH on an interval $T_1/2$ consists from equaled on parameter of positive and negative component (by analogy with EE of the basic harmonic) and is a part of exchange energy of a circuit of an alternating current.
5. The arithmetic addition, as maximal values CD, and ED DNH results in the large error of account.
6. The influence ED DNH is shown in distortion sinusoidalness and change of parameter EE.
7. The recommended algorithm of account allows objectively to estimate ED and EE in a circuit with NP.

[1] *B.H. Belousov, Yu.C. Jelezko.* Reflection in the contracts on electrosupply of questions of quality of the electric power both conditions of consumption and generation of jet energy. - Industrial power, 1998, № 11, p. 15-22.

[2] *P.A. Ionkin, N.A. Melnikov, A.I. Darevskiy, E.C. Kukharkin.* Theoretical bases the electrical engineers, ch.1. M. "«Higher school", 1965, 734 p.

[3] GOST 13109-97. Norms of quality of electrical energy in systems of electrosupply of general purpose.

E.M. Fərhadzadə, H.B. Quliyev

QEYRİ-XƏTTİ YÜKLÜ ELEKTRİK DÖVRƏLƏRİNDƏ TƏHRİF GÜCÜ VƏ ENERJİSİ NƏZƏRİYYƏSİNİN ƏSASLARI

Müasir texnologiyanın gərginliyin sinusoidallığı təhrifinə həssaslığın artması yüksək harmoniyalar generasiya edən işlədicilərin məsuliyyəti mexanizminin təkmilləşdirilməsini tələb edir. Elektrik enerji keyfiyyətinin inteqral göstəricisi təhrif enerjisidir. Lakin dəyişən cərəyan şəbəkələrində təhrif gücü və enerji nəzəriyyəsi işlənməmişdir. Bu işdə təhrif enerjisinin mahiyyətini təyin edən və istənilən harmonik spektrin hesablanmasına imkan verən tədqiqat nəticələri verilir.

Э.М. Фархадзаде, Г.Б. Гулиев

ОСНОВЫ ТЕОРИИ МОЩНОСТИ И ЭНЕРГИИ ИСКАЖЕНИЯ В ЭЛЕКТРИЧЕСКИХ ЦЕПЯХ С НЕЛИНЕЙНОЙ НАГРУЗКОЙ

Увеличение чувствительности современных технологий к искажению синусоидальности напряжения требуют совершенствование механизма, ответственности потребителей, генерирующих ВГС, уровень которых превышает нормативные значения. Интегральным показателем качества электрической энергии является энергия искажения.

Однако теория мощности и энергии искажения в сетях переменного тока не разработана. Приводятся результаты исследований, позволяющие установить суть энергии искажения и вычислить ее для произвольного спектра ВГС.

Received: 16.06.03

THE TRANSIENT RADIATION OF THE NON-INVARIANT SOURCE IN THE PLANE-LAYERED MEDIUM

I.M. ABUTALIBOV, M.B. ASADOVA, I.G. JAFAROV
Azerbaijan Pedagogical State University
U. Gadjibekov str. 34

The process of the transient radiation of the non-invariant relativistic source of the electromagnetic field, in particularly, the magnetic dipole moment in the plane-layered medium is considered. The general expressions, describing the radiation field and change of the own field are obtained. The analysis of the obtained formulas for the ultrarelativistic velocity of the magnetic moment is done.

1. INTRODUCTION

The investigation of the transient radiation of the non-invariant relativistic source of the electromagnetic field of charge had been carried out firstly half an age ago in the work of Ginsburg and Frank [1], in which it was shown, that the so-called transient radiation appears at the charge motion through the plane boundary of the separation of two isotropic mediums with the different physical properties, if the charge have the constant velocity, which is less, than the phase velocity of radiation in medium. The radiation is mainly directed along the charge motion at the high charge velocities.

The transient radiation has been the subject of the intensive investigations during the last decades. The many investigations were carried out for the creation of the practical systems, using the transient radiation for the identification of the relativistic particles, which are one of the more important problems in the high energy physics.

The investigation of the transient radiation of the non-invariant sources of the electromagnetic field, in particular, the dipole moment was considered in the ref [2-5]. The question about the transient radiation as invariant so non-invariant sources on the blurred boundary of the separation of the mediums was considered in the ref [4-7]. The present paper, deals to the transient radiation of the magnetic moment in the weakly nonhomogeneous plane-layered medium.

2. EQUATIONS FOR THE HERTIZIAN VECTORS IN THE NONHOMOGENEOUS MEDIUM AND THEIR FOURIER TRANSFORMATIONS

Let's consider the non-magnetic $(\mu = 1)$ non-homogeneous medium, the dielectric constant of which depends on the coordinations: $\varepsilon=\varepsilon(x,y,z)$. In addition, for the magnetic Hertizian vector $\vec{\Pi}_m$ as in the case of the isotropic medium we obtain the following nonhomogeneous wave equation:

$$\Box \vec{\Pi}_m = -4\pi \vec{M} \ , \qquad (1)$$

and for the following more complex equation

$$\Box \vec{\Pi}_e = -4\pi \vec{P} + \varepsilon^{-1}\vec{\nabla}\varepsilon(\vec{\nabla}\vec{\Pi}_e) - \left[\vec{\nabla}\varepsilon, \partial\vec{\Pi}_m / c\partial t\right], \qquad (2)$$

for the electric vector $\vec{\Pi}_e$, in the right part of which the two last members are caused by the medium inhomogeneous respect of the dielectric constant, the change of which on the layer thickness of the medium inhomogeneous is the reason of the creation of the radiation field and change of the eigen field; $\vec{M}$ and $\vec{P}$ are vectors of the magnetic and electric polarization. They are defined by the following expressions:

$$\vec{M} = \vec{m}\delta(\vec{r} - \vec{\upsilon}t) \ , \ \vec{P} = \left[\vec{\beta}\vec{m}\right]\delta(\vec{r} - \vec{\upsilon}t) \, ,$$

where $\Box = \vec{\nabla}^2 - \frac{\varepsilon}{c^2}\cdot\frac{\partial^2}{\partial t^2}$ is D'Alembert's operator in the case of the nonhomogeneous medium, $\vec{m}$ is the magnetic moment and $\left[\vec{\beta}\,\vec{m}\right] = \vec{p}$ is the electric dipole moment, combined with the magnetic moment, moving with the constant velocity.

In the general case the equations (1) and (2) impossible to solve. They are solved exactly or approximately only when the dielectric constant depends on the only one variable. In the present paper the dependence $\varepsilon=\varepsilon(z)$ of the dielectric constant of the medium, called the plane-layered is considered. The solutions of the equations (1) and (2) are obtained by the method of the consequent approximation; in addition, one takes into consideration, that:

$$\vec{\Pi}_m(\vec{r},t) = \vec{\Pi}_m^0(\vec{r},t) + \delta\vec{\Pi}_m(\vec{r},t), \qquad (3)$$

$$\vec{\Pi}_e(\vec{r},t) = \vec{\Pi}_e^0(\vec{r},t) + \delta\vec{\Pi}_e(\vec{r},t), \qquad (4)$$

$$\varepsilon(z) = \varepsilon^o + \delta\varepsilon(z) \, , \qquad (5)$$

where $\delta\vec{\Pi}_m$, $\delta\vec{\Pi}_e$ and $\delta\varepsilon(z)$ are small values of the first order, ε^o is the dielectric constant of the homogeneous medium. The summand $\delta\varepsilon(z)$ in the function (5), caused by the dielectric inhomogeneous, has to change gradually from $-\Delta\varepsilon/2$ to the $+\Delta\varepsilon/2$ on the all inhomogeneous, in addition, $\varepsilon_1=\varepsilon^o-\Delta\varepsilon/2$ and $\varepsilon_2=\varepsilon^o+\Delta\varepsilon/2$. From (1) and (2) with (3-5) we obtain the following equations:

$$\Box_o \vec{\Pi}_m^o(\vec{r},t) = -4\pi\vec{M}(\vec{r},t) \ , \qquad (6)$$

$$\square_o \vec{\Pi}^o_e(\vec{r},t) = -4\pi\vec{P}(\vec{r},t) \ , \qquad (7)$$

$$\square_o \delta\vec{\Pi}_m(\vec{r},t) = \frac{\delta\varepsilon}{c^2}\cdot\frac{\partial^2\vec{\Pi}^o_m(\vec{r},t)}{\partial t^2}, \qquad (8)$$

$$\square_o \delta\vec{\Pi}_e(\vec{r},t) = \frac{\delta\varepsilon}{c^2}\cdot\frac{\partial^2\vec{\Pi}^o_e(\vec{r},t)}{\partial t^2} + \vec{e}_3\frac{1}{\varepsilon^o}\cdot\frac{\partial\delta\varepsilon}{\partial z}\left(\vec{\nabla}\vec{\Pi}^o_e(\vec{r},t)\right) - \frac{\partial\delta\varepsilon}{\partial z}\left[\vec{e}_3,\frac{1}{c}\cdot\frac{\partial\vec{\Pi}^o_m(\vec{r},t)}{\partial t}\right] \qquad (9)$$

where $\square_o = \nabla^2 - \frac{\varepsilon^o}{c^2}\cdot\frac{\partial^2}{\partial t^2}$ is the D'Alembert's operator for the homogeneous nonmagnetic medium.

In considered problem the all values it is need to expand in the Fourier integral on the time and transverse component of the radius vector because of the homogeneous in the time and on the directions, which are perpendicular to the field source velocity [2]:

$$\vec{\Pi}^o_m(\vec{r},t) = \int\vec{\Pi}^o_{m\omega\vec{\chi}}(z)\exp(i\vec{\chi}\vec{r}_\perp - i\omega t)d\omega d\vec{\chi} \qquad (10)$$

and e.t.c. In addition, we obtain the Fourier images of the equations (7-9):

$$L\vec{\Pi}^o_{m\omega\vec{\chi}}(z) = -4\pi\vec{M}_{\omega\vec{\chi}}(z) \ , \qquad (11)$$

$$L\vec{\Pi}^o_{e\omega\vec{\chi}}(z) = -4\pi\vec{P}_{\omega\vec{\chi}}(z), \qquad (12)$$

$$L\delta\vec{\Pi}_{m\omega\vec{\chi}}(z) = -\frac{\omega^2}{c^2}\delta\varepsilon\vec{\Pi}^o_{m\omega\vec{\chi}}(z) \ , \qquad (13)$$

$$L\delta\vec{\Pi}_{e\omega\vec{\chi}}(z) = -\frac{\omega^2}{c^2}\left(\delta\varepsilon - i\frac{c^2}{\omega\upsilon}\cdot\frac{\partial\delta\varepsilon}{\partial z}\right)\vec{\Pi}^o_{e\omega\vec{\chi}}(z) + i\vec{e}_3\frac{1}{\varepsilon^o}\cdot\frac{\partial\delta\varepsilon}{\partial z}\left(\vec{\chi}\vec{\Pi}^o_{e\omega\vec{\chi}}(z)\right) \ , \qquad (14)$$

where $L = \partial^2/\partial z^2 + k_{rz}^2$, $k_{rz} = \frac{\omega}{c}\sqrt{\varepsilon^0 - \chi^2c^2/\omega^2}$ is the longitudinal component of the vector of the radiation field and

$$\vec{M}_{\omega\vec{\chi}}(z) = \frac{\vec{m}}{(2\pi)^3\upsilon}exp(i\omega z/\upsilon) \ , \qquad (15)$$

$$\vec{P}_{\omega\vec{\chi}}(z) = \frac{\left[\vec{\beta}\vec{m}\right]}{(2\pi)^3\upsilon}exp(i\omega z/\upsilon) \qquad (16)$$

the Fourier images of the magnetic and electric polarizations.

3. THE RETARDED SOLUTIONS OF THE EQUATIONS

We know about the solutions of the equations (11) and (12) [3]:

$$\vec{\Pi}^o_{m\omega\vec{\chi}}(z) = -\frac{4\pi\vec{m}c^2}{(2\pi)^3\upsilon\omega^2}\left(\varepsilon^o - c^2/\upsilon^2 - \chi^2c^2/\omega^2\right)^{-1}\exp(i\omega z/\upsilon) \ , \qquad (17)$$

$$\vec{\Pi}^o_{e\omega\vec{\chi}}(z) = -\frac{4\pi c^2\left|\vec{\beta}\vec{m}\right|}{(2\pi)^3\upsilon\omega^2}\left(\varepsilon^o - c^2/\upsilon^2 - \chi^2c^2/\omega^2\right)^{-1}\exp(i\omega z/\upsilon) \ . \qquad (18)$$

the Fourier images of Hertizian vectors $\vec{\Pi}^0_{m\omega\vec{\chi}}$ and $\vec{\Pi}^0_{e\omega\vec{\chi}}$ define the eigen field of the source in the homogeneous medium with the dielectric constant ε^o (the radiation field in the homogeneous medium is supposed to be absent). The main problem is that solving equations (13) and (14) it is necessary to find the additions to the zero solutions (17) and (18), corresponding to the eigen field, and the general solutions of the homogeneous equation, defining the radiation field.

For the solutions of the equations (13) and (14) firstly it is need to expand $\partial\varepsilon(z)$ in the Fourier integral:

$$\delta\varepsilon(z) = \int\delta\varepsilon_\eta\cdot exp(i\eta z)d\eta \ . \qquad (19)$$

By way of the concreate expressions for $\partial\varepsilon(z)$ we can choose the following functions:

$$\delta\varepsilon(z) = \frac{\Delta\varepsilon}{2}th\frac{z}{\Delta z} \ , \qquad (20)$$

$$\delta\varepsilon(z) = \frac{\Delta\varepsilon}{\pi}arctg\frac{z}{\Delta z} \ , \qquad (21)$$

$$\delta\varepsilon(z) = \frac{\Delta\varepsilon}{\sqrt{\pi}}\int_o^z\exp\left[-(x/\Delta z)^2\right]dx \ , \qquad (22)$$

the Fourier images of which are defined by the appropriate expressions:

$$\delta\varepsilon_\eta = \frac{\Delta\varepsilon}{4i}\cdot\frac{\Delta z}{sh(\pi\eta\cdot\Delta z/2)}\ , \qquad (23)$$

$$\delta\varepsilon_\eta = \frac{\Delta\varepsilon}{2\pi i\eta}\cdot\exp\left(-|\eta|\Delta z\right)\ , \qquad (24)$$

$$\delta\varepsilon_\eta = \frac{\Delta\varepsilon}{2\pi i\eta}\cdot exp\left[-(\eta\cdot\Delta z/2)^2\right]\ . \qquad (25)$$

Substituting the solutions (17) and (18) and the equality (19) in the right parts of (13) and (14), we obtain:

$$\delta\vec{\Pi}_{m\omega\vec{\chi}}(z) = \int\vec{G}^{m}_{\omega\vec{\chi}}(\eta)\exp\left[i(\eta+\omega/\upsilon)z\right]d\eta\ , \qquad (26)$$

$$\delta\vec{\Pi}_{e\omega\vec{\chi}}(z) = \int\vec{G}^{e}_{\omega\vec{\chi}}(\eta)\exp\left[i(\eta+\omega/\upsilon)z\right]d\eta\ , \qquad (27)$$

where

$$\vec{G}^{m,e}_{\omega\vec{\chi}}(\eta) = 4\pi\delta\varepsilon_\eta\frac{(\varepsilon^\circ - c^2/\upsilon^2 - \chi^2c^2/\omega^2)^{-1}}{(2\pi)^3\cdot\upsilon}\left\{\begin{matrix}\vec{m}\\ \left[\vec{\beta}\,\vec{m}\right]\left(1+\eta\dfrac{c^2}{\omega\upsilon}\right)-\vec{e}_3\left[\vec{\chi}\,\vec{m}\right]_z\dfrac{c\upsilon\eta}{\varepsilon^\circ\omega^2}\end{matrix}\right\}\ . \qquad (28)$$

The inhomogeneous magnetic and electric polarizations appear in the layer-inhomogeneous medium at the magnetic moment motion. Taking into consideration the expressions (15) and (16), the right parts of the equations (26) and (27) can be expressed trough the magnetic and electric polarizations correspondingly, in addition, the last three play role of the source functions. That's why at the solving it is need to take into consideration, that Green functions in the left part of the equalities have to be retarded, i.e. to describe the retarded fields:

$$\delta\vec{\Pi}_{m\omega\vec{\chi}}(z) = -\int\frac{\vec{G}^{m}_{\omega\vec{\chi}}(\eta)\exp\left[i(\eta+\omega/\upsilon)z\right]}{(\eta-\eta_1)\cdot(\eta-\eta_2)}d\eta\ , \qquad (29)$$

$$\delta\vec{\Pi}_{e\omega\vec{\chi}}(z) = -\int\frac{\vec{G}^{e}_{\omega\vec{\chi}}(\eta)\exp\left[i(\eta+\omega/\upsilon)z\right]}{(\eta-\eta_1)\cdot(\eta-\eta_2)}d\eta\ , \qquad (30)$$

where

$$\eta_{1,2} = -\frac{\omega}{\upsilon}\pm\frac{\omega}{c}\sqrt{\varepsilon^\circ-\chi^2c^2/\omega^2}\ . \qquad (31)$$

In the considered case the Cerenkov radiation is absent as in the homogeneous so in the inhomogeneous parts of all medium, when the condition $\varepsilon^\circ<c^2/\upsilon^2$ is carried out, the values η_1 and η_2 became the indeed in the high frequencies region $\varepsilon^\circ>>\chi^2c^2/\omega^2$ and the expression $(\varepsilon^\circ-c^2/\upsilon^2-\chi^2c^2/\omega^2)<0$. It follows from the expression $\eta_1\eta_2 = -\frac{\omega^2}{c^2}\left(\varepsilon^\circ - c^2/\upsilon^2-\chi^2c^2/\omega^2\right)>0$ that both values are equal to each other on the sign, i.e. if $\eta_2<0$, then $\eta_1<0$. Introducing the designation $\xi=\eta+\omega/\upsilon$, then we obtain

$$\xi_1 = \omega\sqrt{\varepsilon^\circ-\chi^2c^2/\omega^2}/c = \xi_o>0,$$

$$\xi_2 = -\omega\sqrt{\varepsilon^\circ-\chi^2c^2/\omega^2}/c = -\xi_o<0\ .$$

Taking into consideration the introduced designation, the integrals (29) and (30) are written in the form of:

$$\delta\vec{\Pi}_{m\omega\vec{\chi}}(z) = -\int\vec{G}^{m}_{\omega\vec{\chi}}(\xi)(\xi^2-\xi_o^2)^{-1}exp(i\xi z)d\xi\ , \qquad (32)$$

$$\delta\vec{\Pi}_{e\omega\vec{\chi}}(z) = -\int\vec{G}^{e}_{\omega\vec{\chi}}(\xi)(\xi^2-\xi_o^2)^{-1}exp(i\xi z)d\xi\ . \qquad (33)$$

For the diverging waves the ratio of the exponent in the exponential function, being in the integrand expression, must be positive $z>0$. That's why at the forward radiation $(z>0)\xi_1>0$, and at the back radiation $(z<0)\xi_2<0$. It means that if $z>0$, then the forward radiation field is proportional to $exp\left(i\omega z\sqrt{\varepsilon^\circ-\chi^2c^2/\omega^2}/c\right)$, and if $z<0$, then the back radiation field is proportional to $exp\left(-i\omega z\sqrt{\varepsilon^\circ-\chi^2c^2/\omega^2}/c\right)$.

To obtain the retarded solutions of the equations (32) and (33), satisfying the principle of the causality, it is necessary to make the analytic continuation of the integrand function at $z>0$ on the upper complex half-plane, and $z<0$ on the low complex half-plane and instead of the detour of singular points to shift them from the indeed axis. It can be done, if we consider that ε° has the infinitesimal addition. In addition the pole $\xi_1=\xi_o$ changing on $\xi_o+i\omega\delta/c$ passes to the upper half-plane, and the pole $\xi_2=-\xi_o$ changing on $-\xi_o-i\omega\delta/c$, passes to the low half-plane (here δ is the infinitesimal positive number), and the pole $\xi_3=\omega/v$, not having ε°, isn't shift staying on the indeed axis; the corresponding contours for $z>0$ and $z<0$ are given in the picture.

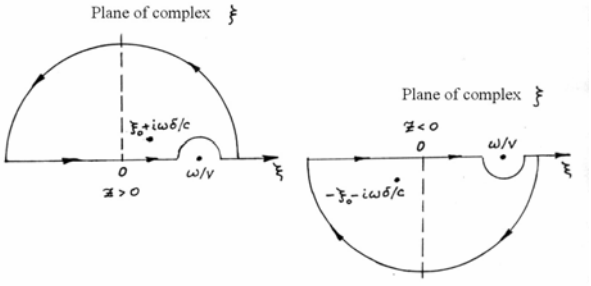

Fig. Circuit of integration in complex plane

The integrand functions (32) and (33) are analytic in the all points of the indeed axis, besides the points ξ_1, ξ_2, ξ_3, being the simple poles, and satisfy $\vec{G}(\xi)\left(\xi^2-\xi_0^2\right)^{-1}\to 0$ and $\xi\to\infty$. As the integrand functions have the finish number of the simple poles on the indeed axis, so integrals are understood by their main values [8,9]. That's why at $z>0$ we have:

$$V.p.\int_{-\infty}^{\infty}\vec{\Phi}(\xi)d\xi=\pi i\,\mathrm{Re}\,s\left[\vec{\Phi}(\xi)\right]_{\xi=\omega/\upsilon}+2\pi i\lim_{\delta\to 0}\mathrm{Re}\,s\left[\vec{\Phi}(\xi)\right]_{\xi=\xi_0+i\omega\delta/c}\quad,\tag{34}$$

$$V.p.\int_{-\infty}^{\infty}\vec{\Phi}(\xi)d\xi=-\pi i\,\mathrm{Re}\,s\left[\vec{\Phi}(\xi)\right]_{\xi=\omega/\upsilon}+2\pi i\lim_{\delta\to 0}\mathrm{Re}\,s\left[\vec{\Phi}(\xi)\right]_{\xi=-\xi_0-i\omega\delta/c}\quad,\tag{35}$$

where

$$\vec{\Phi}(\xi)=\vec{G}^{m,e}_{\omega\vec{\chi}}(\xi)(\xi^2-\xi_0^2)^{-1}\exp(i\xi z)\quad.\tag{36}$$

In the formulas (34) and (35) the first summands define the change of the eigen field, accordingly, on the and against the direction of the source movement correspondingly and second summands define the forward and back radiation field. The such solution corresponds with the diversing wave, distributing in two sides from the boundary of the blurred band.

In the result of the calculation of the residues of the first terms in the formulas (34) and (35) in the pole $\xi=\omega/\upsilon$, not depending on the concreate expressions for $\delta\varepsilon_\xi$, we obtain the similar additions to Hertizian vectors, defining the change of the eigen field:

$$\delta\vec{\Pi}^{s}_{m,e}(\omega,\vec{\chi},z)=\frac{z}{|z|}\cdot\frac{\Delta\varepsilon\cdot c^2}{(2\pi)^2\upsilon\omega^2}\left(\varepsilon^\circ-c^2/\upsilon^2-\chi^2c^2/\omega^2\right)^{-2}\begin{Bmatrix}\vec{m}\\ [\vec{\beta}\vec{m}]\end{Bmatrix}\exp(i\omega z/\upsilon)\quad.\tag{37}$$

The Hertizian vectors describing the radiation field, are found by the calculation of the residues of the last terms in the formulas (34) and (35) in the poles $\xi=\xi_1$ (the radiation forward) and $\xi=\xi_2$ (the radiation back) correspondingly:

$$\delta\vec{\Pi}^{r_{1,2}}_{m,e}(\omega,\vec{\chi},z)=\mp\frac{ic}{2\pi\upsilon\omega}\delta\varepsilon_{\xi_{1,2}}\cdot\frac{\left(\varepsilon^\circ-c^2/\upsilon^2-\chi^2c^2/\omega^2\right)^{-1}}{\sqrt{\varepsilon^\circ-\chi^2c^2/\omega^2}}\exp\left(\pm i\omega z\sqrt{\varepsilon^\circ-\chi^2c^2/\omega^2}/c\right)\times$$

$$\times\begin{Bmatrix}\vec{m}\\ [\vec{\beta}\vec{m}]\left(1-\dfrac{c^2}{\upsilon^2}\pm\dfrac{c}{\upsilon}\sqrt{\varepsilon^\circ-\chi^2c^2/\omega^2}\right)+\vec{e}_3[\vec{\chi}\vec{m}]\dfrac{c}{\varepsilon^\circ\omega}\left(1\mp\dfrac{\upsilon}{c}\sqrt{\varepsilon^\circ-\chi^2c^2/\omega^2}\right)\end{Bmatrix}\quad.\tag{38}$$

In the formulas (37) and (38) and the following ones the index *s* corresponds with the eigen field, and the index *r* corresponds with the radiation field; the upper sign and index *1* corresponds with the forward radiation, and the low sign and index *2* corresponds with the back radiation; $\delta\varepsilon_{\xi_{1,2}}$ are values of the changing of the dielectric constant in the poles $\xi=\xi_1$ and $\xi=\xi_2$.

[1] *V.L. Ginzburg, I.M. Frank.* JETF, t. 16, s. 15, 1946 (in Russian)

[2] *B.L Ginzburg, V. H. Citovich.* Perekhodnoye izlucheniye i perekhodnoye rasseyaniye, M., "Nauka", 1984, (in Russian).

[3] *I.M. Abutalibov, I.G. Jafarov, M.B. Asadova.* J."Bilgi", Fizika, Matematika, Nauka o Zemle № 1, 19, 2000 (in Russian).

[4] *I.M. Abutalibov, I.G. Jafarov, M.B. Asadova.* J."Bilgi", Fizika, Matematika, Nauka o Zemle № 1, 4, 2001 (in Russian).

[5] *I.M. Abutalibov, M.B. Asadova, I.G. Jafarov*. II Respublikanskaya nauchnaya konferenciya "Aktualniye problemi fiziki" Tezisi dokladov, s. 11, Baku, 2001 (in Russian).

[6] *A.C. Amatuni, N.A. Korkhmazyan.* JETF, t. 39, s. 1011, 1960 (in Russian).

[7] *A.A. Galeev*. JETF, t. 46, s. 1335, 1964 (in Russian).

[8] *E.T. Uittekker, J.N. Vatson.* Kurs sovremennogo analiza, ch. I, GIFMA, M., 1963 (in Russian).

[9] *G. Arfken.* Matematicheskiye metodi v fizike, Atomizdat, M., 1970 (in Russian).

İ.M. Abutalıbov, M.B. Əsədova, İ.H. Cəfərov

MÜSTƏVİ TƏBƏQƏLİ MÜHİTDƏ QEYRİ-İNVARİANT MƏNBƏNİN KEÇİD ŞÜALANMASI

Müstəvi təbəqəli qeyri-maqnit mühitdə qeyri-invariant relyativistik elektromaqnit sahə mənbənin, xüsusi halda maqnit dipol momentinin, şüalanmasına baxılıb. Şüalanma sahəsi və məxsusi sahənin dəyişməsini təsvir edən ümumi ifadələr alınmışdır. Maqnit momentinin ultrarelyativistik sürəti üçün alınan düsturların təhlili aparılır.

И.М. Абуталыбов, М.Б. Асадова, И.Г. Джафаров

ПЕРЕХОДНОЕ ИЗЛУЧЕНИЕ НЕИНВАРИАНТНОГО ИСТОЧНИКА В ПЛОСКОСЛОИСТОЙ СРЕДЕ I

Рассматривается процесс переходного излучения неинвариантного релятивистского источника электромагнитного поля, в частности, магнитного дипольного момента в плоскослоистой немагнитной среде. Получены общие выражения, описывающие поле излучения и изменение собственного поля. Проводится анализ полученных формул для ультрарелятивистской скорости магнитного момента.

Received: 25.04.03

LAYERED CHARACTER OF DIELECTRIC FUNCTION DEFINED BY THE METHOD OF EXCITON SPECTROSCOPY IN $TlGaSe_2$ AND $TlInS_2$ CRYSTALS AT PHASE TRANSITIONS

O.Z. ALEKPEROV, V.R. ABDURRAHMANOV
Institute of Physics, Azerbaijan National Academy of Sciences,
Baku. Az - 1143, H. Javid av. 33

It is shown that within the temperature region, corresponding to paraphasia - ferroelectric phase transition, the dielectric constant of layered crystals $TlGaSe_2$ and $TlInS_2$ can be considered as consisting of two slabs with different dielectric constants ϵ_1, ϵ_2 and thickness d_1 and d_2 ($d_1+d_2=c$, c is the lattice vector projection in the direction normal to layer). So, the dielectric anomaly and spontaneous polarization occurring at phase transition takes place only in one of the slabs. This model is confirmed by some experimental results, such as dielectric function anisotropy and spectroscopy of excitons at temperatures corresponding to phase transition.

KEYWORDS: exciton, phase transition, layered crystal, spatial dispersion, dielectric anomaly.

INTRODUCTION

Some layered crystals A^3B^6, A^4B^6 and their ternary compounds exhibit at temperature fall the structural phase transitions (PT) from high symmetric paraphase to lower symmetric ferroelectric phase [1-5]. Such a PT is accompanied by appearing of spontaneous polarization in low symmetric commensurate and incommensurate (IC) phases [6]. Anomalies of physical parameters of a crystal take place near the critical temperatures T_i and T_c. For example, the order of value of the dielectric function ϵ_0 in $TlGaSe_2$ and $TlInS_2$ increases more than two times reaching the value up to 10^3 and more in IC phase. This anomaly is believed due to the appearing of spontaneous polarization in layer plane as a result of small positional shifts of T_l atoms situated inside prisms. This second order PT takes place only in monoclinic modification of these crystals which have numerous polytypes with different lattice parameters $c=c'$, $2c'$, $4c'$, $8c'$ ($c' \approx 15$Å).

Wannier and intermediate type exceptions were observed in these layered crystals [7]. The order of ionization energy and effective Bohr radius are the following

$$\varepsilon_i \sim m^* \cdot Ry \cdot \epsilon_0^{-2}, \qquad r_B^* \sim r_B^* \sim \varepsilon_i^{-1} \epsilon_0^{-1}, \qquad (1)$$

where m^* is electron-hole reduced effective mass, Ry-hydrogen Ridberg. The value of ε_i is ~20meV for Wannier type and about 100meV for intermediate type excitons. It is seen from (1) that excitons should be sensitive to change of ϵ_0. So, they are to be destroyed at such increase of ϵ_0 due to screening of Coulomb interaction between electron and hole. Therefore it is natural to expect disappearance of appropriate lines in excitons spectra at temperatures near $T_{i,c}$. However, some experimental works concerning temperature dependence of band edge excitons line shape, including PT region witnesses the existence of excitons lines at PT temperatures [8,9]. Another surprising fact, to our mind, follows from the dielectric measurements. Being almost isotropic at temperatures far from PT the dielectric function ϵ_0 became strongly anisotropic at PT. So, the dielectric anomaly takes place only for $\epsilon_{\parallel}$ in all directions in layer plane, having remained practically unchanged for $\epsilon_{\perp}$ in direction normal to layers.

In this work the exciton spectroscopy method is applied for more detailed studying of PT in $TlGaSe_2$ and $TlInS_2$. The lines shapes of three excitons at quantum energies E_1=2.13eV, E_2=2.21eV, E_3=2.37eV (hereafter labeled as *A*, *B* and *C* correspondingly) in $TlGaSe_2$ with different Bohr radius are investigated at PT temperatures (107-120K). The comparative analysis of temperature dependences of the excitons lines shapes and dielectric function has been made. Excitons lines shapes were detected with standard methods of photoconductivity (PC) and absorption spectra, using monochromator MDR-23 and spectrometer DFS-24 respectively. PC spectra was registered as a conductivity change

$$\Delta\sigma(\lambda) = e\Delta n\mu_n + e\Delta p\mu_p, \qquad (2)$$

(Δn, Δp- carriers concentrations changes and $\mu_{n,p}$ - their mobilities) of samples under the monochromatic radiation with wavelength λ by cross-modulation method with modulation frequency 12-1200Hz. The PC spectra are normalized to equal number of quantum. For this purpose the thickness h of the samples was chosen more than the value of reciprocal absorption coefficient for the band edge *A*-exciton ($h > \alpha_A^{-1} \approx 3\cdot10^{-3}$cm). For capacitance measurements alternate current bridge E7-12 (at frequency 100Hz) was used.

All the crystals of monoclinic modification of $TlGaSe_2$ and $TlInS_2$ used in this work had been grown by Bridgmen method. Samples were prepared from different ingots with different residual impurity concentrations. *X*-ray investigations show the existence of the different polytypes of monoclinic structure. The value of dielectric constant at IC phase depends on crystal polytype and impurity concentration. In this work we did not identified the residual impurities and polytypes of samples investigated.

EXCITON SPECTROSCOPY RESULTS

For the most of $TlGaSe_2$ investigated samples the behavior of excitons line shape temperature dependence is not adequate to the results of dielectric measurements. Investigating various samples there were obtained three types

of the line shape temperature dependence. For the first type samples *C*-exciton line indicated in fig.1 disappear completely in absorption as well in PC spectra. The absorption coefficient for *A*-exciton line indicated in fig.2 (which is not resolved from B line in absorption spectra at T>80K) decreases about 2 times for these samples in IC region. Also strong decrease of PC signal takes place. At *C*-line the signal lowers up to noise values but for lines *A* and *B* it decreases about two order of magnitude. Any shift of excitons lines to the violet region of spectra as it would be expected from (1) was not observed. In contrast the small shift (~meV) of *A*-line to the red side of spectra occurs [8]. For these samples the capacitance measurements show the drastic anomaly of dielectric function reaching the value of $\in_0 \approx 1100$ for $TlGaSe_2$ and $\in_0 \approx 1800$ for $TlInS_2$.

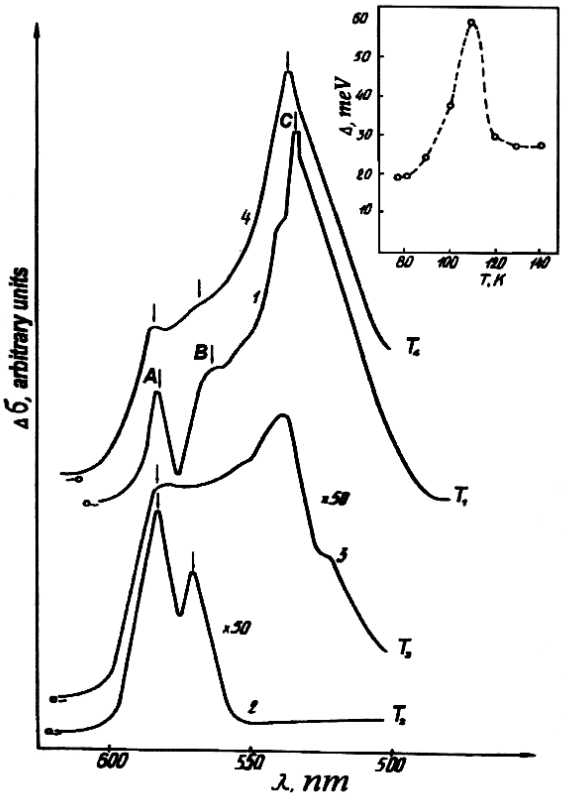

Fig.1. PC distribution against wavelength at different temperatures for first type samples of $TlGaSe_2$. 1-T_1=80K; 2-T_2=115K; 3-T_3=120K; 4-T_4=140K; insert-line width dependence on temperature.

From the fact that the absorption coefficient for *C*-exciton (α_C~10^{-4} cm^{-1}) is more than for *A* one (α_A~$3\cdot10^2 cm^{-1}$) it follows that carriers exited at *C* are much closer to the surface of crystal and participate in surface PC. But despite this, as it is seen from figs.1 and 3 the PC signal at *C*- exciton at low temperature commensurate phase is much more than one for band edge *A*- exciton. From this fact and (2) it can be concluded that the mobility μ of carriers exited at *C*- line is much higher (or effective mass $m^*=e\tau/\mu$ is lower) than that of band edge carriers. Hence it follows from (1) that *C*-exciton has greater r_B^* than that of *A*.

The *C*-line for the second type samples in IC phase is barely seen in PC (fig.3) and absorption spectra. But the decrease of intensity for C- line in IC phase is more than one for *A* and B lines (especially in PC). The intensity of *A*-line also decreases in absorption (about 1.5 times) and in PC (10-20 times) spectra. For these types of samples the dielectric anomaly takes place with moderate values of $\in_0 (T) \sim 200 - 500$.

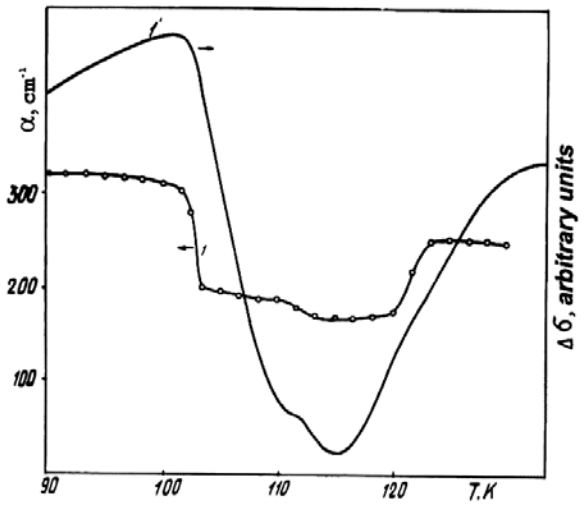

Fig.2. Absorption coefficient and PC dependence on temperature for *A*-exciton.

The rarely found samples of the third type have the usual excitons line shape dependence on temperature -gradual broadening and slight shifting to low energy, without any drastic change in PC and absorption spectra. Behavior of excitons line shape of such sample is in accordance with $\in_0 (T)$, because the capacitance measurements have shown no anomaly of $\in_0 (T)$ (cf. [6]). Probably PT for such samples hardly occurs.

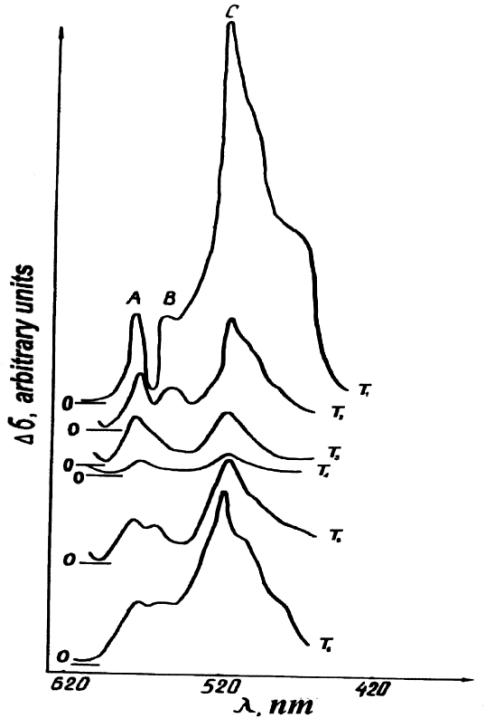

Fig.3. PC distribution against wavelength at different temperature for seconds type samples of $TlGaSe_2$ 1 - T_1=80K; 2 - T_2=105K; 3 - T_3=170K, 4 - T_4=115K; T_5=125K; T_6=140K.

In fact the higher radius *C*-exciton temperature dependence is more or less in accordance with dielectric function measurements, especially for the first type samples. But the situation is different for a smaller radius *A*-exciton, which exists at IC temperatures despite of drastic grow of ϵ_0. This allows one to suppose that in some parts of crystal's space the ϵ_0 remains practically unchanged, despite the dielectric anomaly for whole crystal. The size of these parts must be sufficiently large for a small radius *A*-exciton to be inserted inside it, but small for higher radius *C*-exciton. However, ϵ_0 being derived from measurements of capacitance has a value averaged over a whole unit cell. The unit cell of these crystals contains one or more layered blocks (with thickness 15Å) for different polytypes. [10-11]. The wave functions of conduction and valence bands are practically localized in separate blocks due to the weak Van der Waals interaction between the layers. At the same time the wave functions are free in the plane of a layer. As a result the excitons have a pancake- like shape. In other words, at least in IC region, it is possible to consider crystals as a medium with spatial dispersion in direction normal to layers $\epsilon_0\ (z)$, consisting from two (or more) slabs with thickness d_1 and $d_2 (d_1+d_2=c)$ and dielectric constants ϵ_1 and ϵ_2 respectively. According to this model the dielectric anomaly and spontaneous polarization appearing at IC phase take place only in the planes of Tl atoms. Appearance of the polarization laying in the plane of Tl^+ ions is due to shift of the Tl^+ [12]. The shift is taking place at PT inside prisms, which are included into a layered block. The ion radius of Tl^+ is about 1.3Å *A* layered block includes four Tl planes So, one can estimate the value of $d_2/d_1 \approx 2$.

For the first and second type samples strong broadening of excitons lines takes place at IC phase (inset in fig.1). The line width of *A*-exciton at IC phase is 3-4 and 2-3 times greater than one at low symmetric ($T<T_c$) and high symmetric ($T>T_i$) phase respectively. The given model allows one to consider the exciton line broadening mechanism as inhomogeneous broadening. The broadening arises due to fluctuations of exciton binding energy because of *z*-dependence of $\epsilon_0\ (z)$. The strong decrease of PC in IC phase (fig.2), which has been also observed at PT in $TlInSe_2$ [13], according to (2) is connected with change of μ as a result of carriers scattering mechanism alteration. For $TlInS_2$ crystals the result of excitons line shape investigations at PT temperatures 195-215K is practically the same. The exciton lines do not disappear completely in IC phase if the crystals are not doped specially. However, their intensities are lowered differently depending on ionization energy of excitons.

INTERPERETATION OF DIELECTRIC FUNCTION MEASUREMENTS RESULTS

The above given model of layered dielectric function in unit cell explains well the anisotropy of dielectric function anomaly at PT. To demonstrate this one can compare the effective dielectric constants in directions parallel and normal to layers $\epsilon_{ef}^{//}$ and $\epsilon_{ef}^{\perp}$. For this reason we consider two capacitors of cubic form with edge $d=d_1+d_2=c$ made as indicated in inset of fig.4. It is easy to obtain for $\epsilon_{ef}^{//}$ and $\epsilon_{ef}^{\perp}$ the following expressions:

$$\epsilon_{ef}^{//}=\frac{\epsilon_1 d_1+\epsilon_2 d_2}{d_1+d_2}, \qquad \epsilon_{ef}^{\perp}=\frac{\epsilon_1\cdot\epsilon_2\cdot(d_1+d_2)}{\epsilon_1\cdot d_2+\epsilon_2\cdot d_1},$$

(3) taking in the expression $\epsilon_{ef}=C/(d_1+d_2)$ C respectively as sequentially and parallel joint capacitors with ϵ_1, d_1 and ϵ_2, d_2.

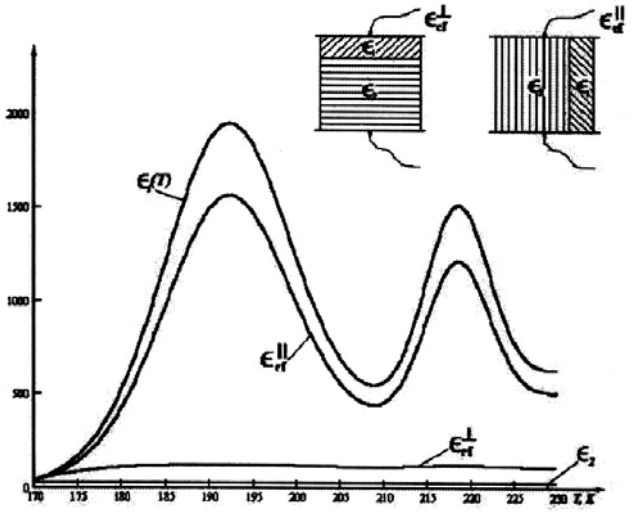

Fig.4. Calculated values of temperature dependence of $\epsilon_{ef}^{//}$ and $\epsilon_{ef}^{\perp}$; $\epsilon_2=\epsilon_0=10$; $d_2/d_1=2$.

The result of calculations of $\epsilon_{ef}^{//}$ and $\epsilon_{ef}^{\perp}$ are shown in fig.4. It is supposed that the dielectric anomaly takes place only for $\epsilon_1\ (T)$ which is represented as a superposition of ϵ_0 and two Gaussians centered at T_i=105K and T_c=115K (for $TlGaSe_2$) with different heights and widths so that $\epsilon_{ef}^{//}$ and $\epsilon_{ef}^{\perp}$ to be corresponded the results obtained from capacitance experiments. Just this kind of results shown in fig.4 is typical for capacitance measurement at PT. For $d_2/d_1=2$ the anomaly takes place only for $\epsilon_{ef}^{//}$ and is not seen for $\epsilon_{ef}^{\perp}$. At strong decrease of d_2/d_1 the week anomaly is seen for $\epsilon_{ef}^{\perp}$ also. Note that two-period nature of interference for some layered crystals is also in accordance with this model [14].

CONCLUSIONS

1. At least at IC phase $TlGaSe_2$ and $TlInS_2$ crystals can be considered as a naturally spatial dispersion mediums with periodic dielectric function $\epsilon(z+c)=\epsilon(z)$ in the direction normal to layers.

2. The same or similar effects should be observed in impurity spectroscopy (especially for shallow impurities). The impurity states disappearing or decreasing their density of states must take place at PT. This would lead to disappearing or decreasing of related line intensity in PC, photoluminicence and absorption spectra. The drastic decrease of donor–acseptor photoluminicence line, which was observed at PT temperatures in $TlGaS_2$ [15] can be explained by this model.

3. The small localization region of excitons in layered crystals makes the excitons spectroscopy diagnostic more informative in PT investigations in comparison with macroscopic parameters measurements, including dielectric constant measurements.

[1] *A.A.Volkov, U.G.Goncharov, G.V.Kozlov and R.M.Sardarly*. Zh. Eksper. Teor.Fiz.,Pisma 39, 1984, 293, (in Russian).

[2] *A.A. Volkov, U.G. Goncharov, G.V. Kozlov, K.R.. Allakhverdiev and R.M. Sardarly*. Fiz.Tverd. Tela, 1984, 26, 1754 (in Russian).

[3] *S.B. Vakhryshev, V.V. Zhdanova, B.E. Kvatkovskiy, N.M.Okuneva, K.R. Allakhverdiev, R.A. Aliev, R.M. Sardarly*. Zh. Eksper. Teor.Fiz., Pisma 39, 1984, 247, (in Russian).

[4] *K.R. Allakhverdiev, A.J. Baranov, T.G. Mamedov, D.A.Sandler, Y.R. Sharifov*. Ferroelectric Letter, 8, 1988, 125, (in Russian).

[5] *K.R. Allakhverdiev , N.D. Akhmedzade, T.G. Mamedov, T.S. Mamedov, M.Y. Seidov*. Fiz.Tverd. Tela, 2000, 26, 76, (in Russian).

[6] *R.M. Sardarly, O.A. Samedov, I.Sh. Sadykhov, E.I.Mardukhaeva and T.A. Gabilov*. Solid State Communications, 1991, 77, 453.

[7] *O.Z. Alekperov, M.O. Godjaev, M.Z.Zarbaliev and R.A.Suleimanov*. Solid State Communications, 1991, 77, 65.

[8] *S.G. Abdullaeva, N.T. Mamedov*. Fiz.Tverd. Tela, 1986, 28, 894, (in Russian).

[9] *G.I. Abutalybov, L.S. Larionkina, N.A. Ragimova*, Fiz.Tverd. Tela, 1989, 31, 312, (in Russian).

[10] *Von Dieter Muller, H. Hahn*, Z. anorg. allg. Chem., 1978, 438, 258.

[11] *S. Kashida, K. Nakamura and S.Katayama*. J.Phys.: Condens. Matter, 1993, 5, 4243.

[12] *H.D. Hochhimer, E.Gmelin, B.Bauhofer*. Ch. von Schnering-Schwarz, H.G. von Schnering, J.Ihringer, and W. Appel, Z.Phys. B-Condensed Matter, 1988, 73, 257.

[13] *O.Z. Alekperov, M. Aljanov, E. Kerimova*. Tr. J. of Physics, 1998, 22, 1053.

[14] *O.Z. Alekperov, D.O. Gamzaev, A.M. Kulibekov and R.A. Suleimanov*. Fiz.Tverd. Tela, 1993, 35,184, (in Russian).

[15] *Kato, M. Nishigaki, N. Mamedov M. Yamazaki, S.Abdullayeva, H. Uchiki and S. Iida*. 13th International Conference on Ternary and Multinary Compaunds, Book of Abstracts, 2002, p.101, Paris.

O.Z. Ələkperov, M.R. Abdurraxmanov

$IGaSe_2$ VƏ $TlInS_2$ KRİSTALLARININ FAZA KEÇİDİNDƏ EKSİTON SPEKTROSKOPİYASI METODU İLƏ TƏYİN EDİLMİŞ DİELEKTRİK FUNKSİYASININ LAYLI XARAKTERİ

Laylı və kristallarındp seqnetoelektrik faza keçidi temperatur oblastında dielektrik sabitinin laylara parallel iki (və çox), dielektrik nüfuzluğu ϵ_1 və ϵ_2 müvafiq olaraq qalınlığı d_1 və d_2 ($d_1+d_2=c$, c - гяфяс векторунун laylara perpendikulyar proyeksiyasıdır) təbəqədən ibarət olduğu göstərilmişdir. Fərz olunur ki, faza keçidi temperaturlarında dielektrik anomaliya və spontan polyarizasiyanın əmələ gəlməsi ancaq təbəqələrin birində (ϵ_1, d_1). Baş verir. Təklif olunan model faza keçidində dielektrik nüfuzluğunun anizotropiyası və bu kristallarda eksitonların spektroskopiyasından alınan eksperimental nəticələrlə uzlaşır.

О.З. Алекперов, В.Р Абдуррахманов

СЛОИСТЫЙ ХАРАКТЕР ДИЭЛЕКТРИЧЕСКОЙ ФУНКЦИИ, ОПРЕДЕЛЕННЫЙ МЕТОДОМ ЭКСИТОННОЙ СПЕКТРОСКОПИИ ПРИ ФАЗОВЫХ ПЕРЕХОДАХ В КРИСТАЛЛАХ $TlGaSe_2$ И $TlInS_2$

Показано, что по крайней мере в области температур, соответствующих сегнетоэлектрическому фазовому переходу (ФП) диэлектрическая постоянная слоистых кристаллов $TlGaSe_2$ и $TlInS_2$ может быть представлена методом двух (или более) пластинок с различными диэлектрическими постоянными ϵ_1, ϵ_2 и толшинами d_1 и d_2 ($d_1+d_2=c$, c- проекция вектора решетки в направлении нормальном к слоям). Предполагается, что диэлектрическая аномалия и появление спонтанной поляризации при ФП происходит только в пределах одной из пластинок. Данная модель подтверждается результатами экспериментов по анизотропному поведению диэлектрических измерений и экситонной спектроскопией указанных кристаллов при ФП.

Received: 25.04.2003

DISTRIBUTION OF THE COMPONENTS IN THE CRYSTAL Si-Ge, WHICH HAS BEEN BROUGHT UP BY THE DOUBLE FEEDING OF THE MELT METHOD

G.KH. AZHDAROV, M.A. AKPEROV, V.V. MIR-BAGIROV
Institute of Physics, Azerbaijan National Academy of Sciences,
Baku. Az - 1143, H. Javid av. 33

A problem of component distribution in Si -Ge crystals grown under the continuous feeding of the melt with Silicon and Germanium rods has been solved in consideration of the Pfann approximation. A composition of the single crystal as a function of the rations of the crystallization and feeding rates of the melt as well as the melt composition is established. A possibility in preparing Si-Ge bulk single crystals with a desired uniform and compositionally graded profiles is shown.

The scientific and practical interest to the semiconductor solid solutions is defined mainly by the possibility of the precision control of their forbidden band width, parameters of the crystal structure and electric properties by the way of the corresponding change of the crystal composition. It is known, that classic semiconductors Si and Ge, being in the base of the modern electronics, dissolve in each other at any ratios as in the liquid, so in the solid states completely [1]. The questions, corresponded with the distribution of components in the volume crystals Si-Ge, which has been brought up from the melt by the different methods, were considered in many refs [2-7]. In ref [2] the good agreement of the experimental and calculation dates are established on the distribution of components in crystal Si-Ge, which have been brought up by Chohral method and feeding of the melt by the second component (Si) method.

In the present paper the problem of the distribution of components in the crystals Si-Ge, which have been brought up by Chohral method at the continuous double feeding of the melt by the composite components (Si and Ge) is solved. The aim of this investigation is the establishment of the operational parameters and conditions for the bringing up of the crystals Si-Ge with the given distribution of the components along the axis of the crystallization, including the homogeneous distribution.

The essence of the method of the double feeding of the melt is as follows: from the moment of beginning of the single crystal growth from corresponding melt the rods from composite components are introduced in it. During of the all cycle of the growth the crystallization velocity and velocity of the feeding of the melt by the first and second components are maintained constant.

The task was solved in the Pfann approximation at the satisfaction of the following standard conditions [2]: the crystallization front is plane; the balance, which is defined by the phase diagram between solid and liquid phases, is on the crystallization front; the diffusion of the atoms Si and Ge is the scornly small; the diffusion velocities of the atoms of the composite components in the melt are high enough and that's why the uniformity of melt composition is provided on the all volume.

We note that all these conditions in the system Si-Ge satisfy practically at the crystal velocity of growth <5mm/h [2,3,7].

Let's introduce the following designations V_m^o and V_m are melt volumes in the tigel at the initial and current moments; V_c is the melt volume crystallized in the unite of time; V_{Ge} and V_{Si} are volumes of the feeding ingots of the Ge and Si, introducing into the melt in the unite of time; C_{2m} and C_{2c} are concentrations of the second component atoms (Ge or Si) in the melt and crystal correspondingly; C is the general quantity of the second component in the melt; $K=C_{2c}/C_{2m}$ is the equilibrium segregation coefficient of the second component; t is time. Taking into consideration the above mentioned designations, we have:

$$C_{2m}=\frac{C}{V_m} \text{ and } \frac{dC_{2m}}{dt}=\frac{\dot{C}V_m-\dot{V}C}{V_m^2}=\frac{\dot{C}-\dot{V}_m C_{2m}}{V_m} \qquad (1)$$

On the task consideration we propose that V_c, V_{Ge} and V_{Si} don't depend on time. In this case the following equation takes place:

$$V_m=V_m^0 -(V_c-V_{Ge}-V_{Si})t \quad , \quad \dot{V}_m=-V_c+(V_{Ge}+V_{Si}),$$
$$\dot{C}=-V_c C_m K+V_2 \qquad (2)$$

Substituting the equation (2) into equation (1) we obtain:

$$\frac{dC_{2m}}{dt}=\frac{-V_c C_{2m}K+V_{Si}+V_c C_{2m}-(V_{Si}+V_{Ge})C_{2m}}{V_m^0-(V_c-V_{Si}-V_{Ge})t} \qquad (3)$$

After the variables' separation in the equation (3) and integration, we have:

$$\frac{V_c K-V_c+V_{Si}+V_{Ge}}{V_c-V_{Si}-V_{Ge}} ln\frac{V_m^0}{V_m^0-(V_c V_{Si}-V_{Ge})t}=ln\frac{V_{Si}-(V_c K-V_c+V_{Si}+V_{Ge})C_{2m}^0}{V_{Si}-(V_c K-V_c+V_{Si}+V_{Ge})C_{2m}} \qquad (4)$$

In the equation (4) the integration constant is defined from the initial condition $C_{2m}=C^0_{2m}$ at $t=0$. Let's introduce the following equations: $\gamma=V_c t/V^0_m$, $\alpha=V_{Si}/V_c$, $\beta=V_{Ge}/V_c$ and with the help of them from the equation (4) after the uncompound transformations, we obtain:

$$C_{2c}=C_{2m}K=\frac{K}{K-1+\alpha+\beta}\left\{\alpha-\left[\alpha-(K-1+\alpha+\beta)C^0_{2m}\right]\times\left[1-(1-\alpha-\beta)\gamma\right]^{\frac{K-1+\alpha+\beta}{1-\alpha-\beta}}\right\} \quad (5)$$

For the special case, when $\alpha+\beta=1$ it is obviously that $V_m=V^0_m$ and $V_m=0$. Then from the equation (1) after the several transformations we obtain:

$$C_{2c}=\alpha-(\alpha-KC^0_{2m})e^{-\gamma K} \quad (6)$$

The formulas (5,6) give the distribution of the second component on the crystal length l (as $\gamma\sim l$) in dependence on the operational parameters α, β and C^0_{2m}.

The one of the widespread variants for the single crystals obtaining of the solid solutions Si-Ge by the feeding of the melt method is the using of the pure main component (Si or Ge) in the capacity of the initial melt [2]. Using of this variant is connected with the difficulty of the obtaining of the seedings with the different concentrations of atoms Si and Ge, corresponding with the initial melt composition. For this variant, when $C^0_{2m}=0$, from the equations (5) and (6) correspondingly we obtain:

$$C_{2c}=\frac{K\alpha}{K-1+\alpha+\beta}\left\{1-\left[1-(1-\alpha-\beta)\gamma\right]^{\frac{K-1+\alpha+\beta}{1-\alpha-\beta}}\right\} \quad (7)$$

$$C_{2c}=\alpha(1-e^{-\gamma K}) \quad (8)$$

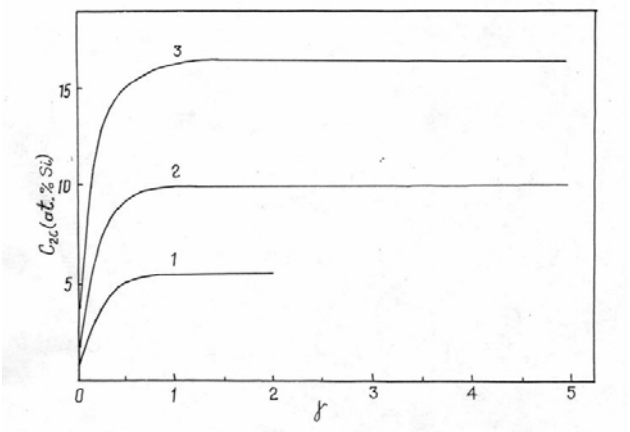

Fig.1. Dependences of concentration of the second component with $K>1$(Si) on γ for crystals Si-Ge, constructed on the base of the expressions (7) (curves 1, 3) and (8) (curve 2).

In the figure 1 for example the dependence curves of the second component-Si in the crystal Ge-Si on γ for the three different values $\alpha+\beta$, which are equal to 0,5, 1 and 2, calculated from the equations (7) and (8) are given. In all cases it is noted that $\alpha:\beta$=1:9, that corresponds with the feeding of the melt by the solid solution with 10 at.%Si. The Si segregation coefficient is equal to equilibrium one, which is defined from the phase diagram (K=5.5 [8]). The initial material of the melt in the tigel is Ge. The analogous calculated curves, for the case when the second component is Ge with K=0,33 [8], are given in the fig. 2. Here the initial material of the melt in the tigel is Si. The curves 2 in the figures correspond with the case, when $\alpha+\beta=1$ and are constructed on the base of the equation (8). If for $\alpha+\beta=1$ the process of the crystal growth can be continued unlimited (curves2 and 3), then for $\alpha+\beta<1$ this process is limited by the melt in tigel (curve1). This corresponds with the expression in the square bracket in the equation (7) is equal to zero. Indeed, if $t=t_{max}$, the term $[1-(1-\alpha-\beta)\gamma]=0$, then $V_m=V^0_m-(V_c-V_{Ge}-V_{Si})t=0$. Practically, of course, the single crystal growth ends earlier, than at $t=t_{max}$. The analysis of the equations (5-8) and given for the example curves' stroke (fig.1) show that at $K>1$ for any remain constant values α, β one can obtain the single crystal with the practically homogeneous composition. In addition, the part of the second component in the homogeneous part of the crystal is defined by the multiplier before the brace in the equation (5) or (7) for the cases, when $\alpha+\beta\neq1$ and is equal α at $\alpha+\beta=1$. The variant, when the second component is Ge with $K<1$ (fig.2), its concentration grows continuously on the crystal length at $\alpha+\beta<1$ (curve 1) and that's why this case can be applied only for the obtaining of the crystals with the variable composition. At $\alpha+\beta=1$ correspondingly with the equations (5-8) and dates of fig.2, in principle the single crystal with the uniform distribution of components can be obtained, but it is no need to apply this method in practically because of the big enough length of the inhomogeneous region (curves 2 and 3). Obviously, that single-minded calculations, carried out for the different values α, β and $\alpha+\beta$, will define the operational parameters for the bringing up of the crystals Si-Ge with the given distribution of components.

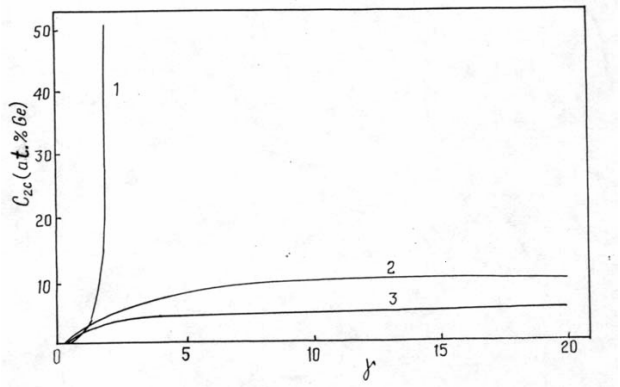

Fig.2. Dependences of concentration of the second component with $K<1$(Ge) on γ for crystals Si-Ge, constructed on the base of the expressions (7) (curves1,3) and (8) (curve 2).

The practical realization of the double feeding of the melt method for the bringing up of the single crystals Si-Ge can be done on the installation, described in the ref [9], which has the automatic system for the supporting of the given diameter

of the growing crystal and the input mechanism of the feeding ingots in the melt. The pulling velocity of the single crystal Si-Ge should be within 1-5mm/h for the carrying out of the criterion of the equilibrium state between crystal and melt [2,3,10].

On the base of the above mentioned we can do the following conclusion. The problem solving of the distribution of components in the crystals SiGe, brought up by the double feeding of the melt method in Pfann approximation, shows the possibility of the obtaining of the single crystals as with variable, so with the homogeneous compositions. The obtained expressions allow to find the optimal conditions of the crystal growth with the given distribution of components.

[1] *V.M. Glazov, V.S. Zemskov* .Fiziko-khimicheskiye osnovi legirovaniya poluprovodnikov. M.: Nauka, 1967, s. 371. (in Russian)

[2] *G.Kh. Azhdarov, T. Kucukomeroglu, A. Varilci, M. Altunbas, A. Kobya, P.G. Azhdarov.* Journal of Crystal Growth, 2001, v. 226, 437.

[3] *K. Nakajima, T. Kusunoki, Y. Azuma, N. Usami, K. Fujima, T. Ujihara, G. Sazaki, T. Shishido.* Journal of Crystal Growth, 2002, v. 240, 373.

[4] *N.A. Agayev, V.V. Mir-Bagirov, G.Kh. Azhdarov.* Izv. AN SSSR, Neorgan. materiali, 1989, t. 25, № 7, 1131 (in Russian).

[5] *G.Kh. Azhdarov, A.A. Musayev, A.S. Ganiyev.* Izv. AN SSSR. Neorgan. materiali. 1980, t. 16, № 7, 1155 (in Russian).

[6] *T.A. Campbell, M. Schweizer, P. Dold, A. Croll, K.W. Benz.* Journal of Crystal Growth, 2001, v. 226, 231.

[7] *P.G. Azhdarov, N.A. Agayev.* Izv. AN SSSR, Neorgan. Materiali, 1999, t. 35, № 8, 903 (in Russian).

[8] *A. Dahlen, Fattah, G. Hanke, Karthaus.* Cryst. Res. Technol., 1994, v. 29, 187.

[9] *N.V. Abrosimov, S.N. Rossolenko, W. Thieme, A. Gerhardt, W. Schroeder.* Journal of Crystal Growth, 1997, v. 174, 182.

[10] *A. Varilci, T. Kucukomeroqlu, G. Azhdarov.* Chinese Journal of Physics, 2003, v. 41, n. 1, 2003.

H.X. Əjdərov, M.Ə. Əkbərov, V.V. Mir-Bağırov

ƏRİNTİNİ İKİQAT QİDALANDIRMA ÜSULU İLƏ ALINAN Si-Ge KRİSTALLARINDA KOMPONENTLƏRİN PAYLANMASI

Silisium və germanium ilə fasiləsiz qidalanan ərintidən yetişdirilən Si-Ge kristallarında komponentlərin paylanma məsələsi Pfann yaxınlaşmasında həll edilib. Yetişdirilən monokristalın tərkibinin ərintinin kristallaşma və qidalanma sürətlərinin münasibətindən və onun başlanğıc konsentrasiyasından asılılıq tənlikləri alınıb. Si-Ge monokristallarında verilmiş dəyişən və bircinsli komponent paylanması əldə etmək imkanı göstərilib.

Г.Х. АЖДАРОВ, М.А. АКПЕРОВ, В.В. МИР-БАГИРОВ

РАСПРЕДЕЛЕНИЕ КОМПОНЕНТОВ В КРИСТАЛЛАХ Si-Ge, ВЫРАЩЕННЫХ МЕТОДОМ ДВОЙНОЙ ПОДПИТКИ РАСПЛАВА

В пфанновском приближении решена задача распределения компонентов в кристаллах Si-Ge, выращенных в условиях непрерывной подпитки расплава кремниевым и германиевым стержнями. Получены уравнения, определяющие композицию растущего монокристалла в зависимости от соотношения скоростей кристаллизации и подпитывания расплава, а также стартового состава расплава. Показана возможность получения монокристаллов Si-Ge с заданными переменными и однородными составами.

Received: 26.03.03

THE ELECTRIC AND THERMOELECTRIC PROPERTIES OF Ag_2Se AT THE LOW TEMPERATURES

F.F. ALIYEV, G.P. PASHAYEV
Institute of Physics, Azerbaijan National Academy of Sciences,
Baku. Az - 1143, H. Javid av. 33

N.A. VERDIEVA
Azerbaijan State Oil Academy, Baku, Azadlig ave.20

In this work the temperature dependences of the conductivity- $\sigma\sigma(T)$, the Hall coefficient-*R(T)*, thermoelectromotive force-α_0 *(T)* of Ag_2Se at low temperatures have been analysed on the one type charge carriers and Kane low dispersion theory basis. It is established at the electron concentration $n \leq 6{,}9 \cdot 10^{18} cm^{-3}$ the carriers have been scattered by the ion impurities and the point defects, but at $n \geq 1{,}2 \cdot 10^{19} cm^{-3}$ its have been scattered on the ion impurities and heat vibrations of lattice. It is shown, that at T<30K the electron-electron interaction has elasnic character.

The set of the refs [1-3] is devoted to the electric and thermal properties of selenide of argentum. The authors [1,2] showed that the electron dispersion law in Ag(2)Se is subject to Kein's model and at T>80K the main scattering mechanism of carriers of current is the scattering on the ionized and acoustic phonons [3]. In the region 80 - 250K the electron and phonon shares of the heat conduction are studied [3] and it is established that the Lorentz number (L) in Ag_2Se is the essential less than Zommerfeld's one (L_0) and the interelectronic interaction becomes inelastic

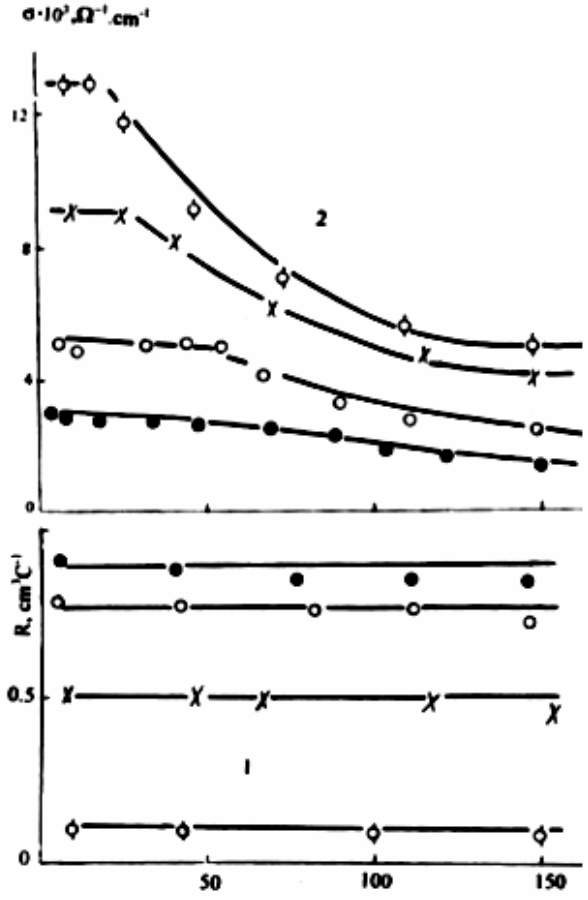

Fig.1.

Inspite of the fact that the given questions aren't studied at the low temperatures, nevertheless they represent the special interest for the studying of an electronic spectrum.

In present paper the temperature dependences of electric conduction $\sigma(T)$, Hall coefficient *R(T)* and thermoelectromotive force $\alpha_0(T)$ at the low temperatures are studied.

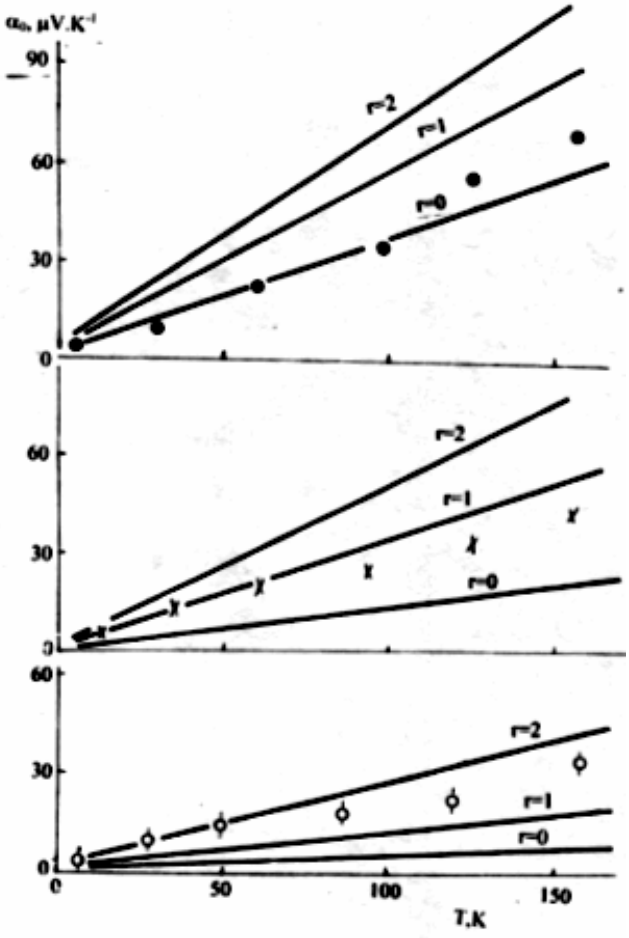

Fig.2.

The samples of Ag_2Se were obtained by the unified technology Ag_2Se [4]: the stoichiometric composition with the excess of Se and Ag up to ~0,2 at.%. The investigations are carried out by the methodics [5]. In fig. 1,2 the *R(T)* (1.1) and $\sigma(T)$ (1.2) are represented and $\alpha_0(T)$ is represented in fig.2. In all samples *R(T)* staies constant, but $\alpha_0(T)$ increases linearly, that is typical for strong degenerate gas. It is visible that at $n \sim 12 \div 20 \cdot 10^{18} cm^{-3}$ σ almost doesn't depend on T up to

T~2K. At T>20K σ increases with the temperature growth. With the electron concentration decrease σ depends on T very weakly up to T~150K. The weak dependence $\sigma(T)$ is caused by the weak temperature dependence of the electron mobility that is confirmed by the constant concentration in the investigated temperature interval. Usually the intensity of scattering on the scattering centers increases with the decrease of the concentration carriers [6].

For the conception of the given question, it is need to calculate the temperature dependence of the mobility of the carrier of charge. The mobility of carriers of current at the strong degeneration and Kein's dispersion law at the scattering on the acoustic phonons *(r=0)* and ions *(r=2)* is expressed by the following formulas [7]:

$$U_{ak} = \left(\frac{\pi}{3}\right)^{1/3} \frac{e\rho U_0^2 \hbar^3 n^{-1/3}}{E_d K_0 T (m*)^2} \frac{1}{f_{ak}} \qquad (1)$$

$$U_i = \frac{3\pi^2 \hbar^3 \chi^2}{2em*} \frac{1}{f_i} \qquad (2)$$

where p is the crystal density, U_0 is the strain lattice potential, E_d is the lattice deformation potential, m* is the effective electron mass on Fermi level, χ is the dielectric constant of the crystal (where p=7,6g/cm^3 [4], U_0=5·10^{5}cm/s, E_d=10eV [7], m*=0.18 m_0 [2], γ=16[7] correspondingly), and f are factors, taking into consideration the influence of unparabolic on the scattering probability, which are calculated by the following formulas [7]:

$$f_{ak}(p/p_0) = \frac{2.3}{12} - \frac{1}{20}\frac{p}{p_0} + \frac{10.3}{12}\left(\frac{p}{p_0}\right)^2$$

$$f_i(p/p_0) = a - \frac{b}{2} + \frac{1}{16}(b+3c) + \left[\frac{b}{2} - \frac{1}{8}(b+3c)\right]\left(\frac{p}{p_0}\right) + \frac{b+3c}{16}\left(\frac{p}{p_0}\right)^2$$

$$a = ln\left(1+\frac{1}{\xi}\right) - \frac{1}{1+\xi}; b = 4 + \frac{4\xi}{1+\xi} - 8\xi ln\left(1+\frac{1}{\xi}\right); c = 2 - 12\xi + \frac{4\xi}{1+\xi} + 12\xi^2 ln\left(1+\frac{1}{\xi}\right)$$

$$p = \left(\frac{m}{m^*} - 1\right); p_0 = \left(\frac{m_0}{m_n} - 1\right); \xi = \frac{e^2 m*}{\pi\hbar^2 \chi (3\pi n)^{1/3}} = \frac{1}{4K_f^2 r_s^2};$$

m_n is the effective electron mass on the conduction band bottom (m_n=0,08[7]), K_f is the quaziimpulse on Fermi level and r is the screening radius, which is defined for the strong degenerative semiconductors as follows [8]:

$$r_s = \left[\frac{\chi\hbar^2}{4m_n e^2}\left(\frac{\pi}{3n}\right)^{1/3}\right]^{1/2} \qquad (3)$$

where n is the concentration of electrons. The results of the calculation $U(T)$ for strong degenerative electron gas expressed by the following formulae with the use (1) and (2)

$$U = \left(\frac{1}{U_{ak}} + \frac{1}{U_i}\right)^{-1} \qquad (4)$$

are given in the fig.3(a.1) for n~7·10^{18}cm^{-3}.

From the fig.3(a.1) it is seen that $U(T)$ up to T<=35K staied constant. The $U(T)$ decreases with the temperature growth higher than 35K and the calculated values of electron mobility less than experimental in the given temperature interval. This can be connected with that in Ag_2Se the value r_s doesn't close to value of lattice constant. The divergence of the calculated and experimental dates needs to take into consideration the new scattering centers inside of U_{ac} in (4).

The authors [9] inform that Ag_2Se is characterized by the Frenkel defect (it is obvious that these defects are point ones), Ag vacancies in the interstices appearing because of the Ag atoms, disposed statistically in sublattice. It is need to take into consideration the contribution of mobility U_d, calculated with the help of the relaxation time at the scattering mechanism on the point defects for the standard band as in [8]

$$\tau_d(T) = \frac{\pi\hbar^4}{(2m_n k_0 T)^{1/2} m_n V_0^2 N_d}\left(\frac{\varepsilon}{k_0 T}\right)^{-1/2} \qquad (5)$$

where V_0 is the constant, characterizing the amplitude of δ-potential, N_d is the concentration of the point defects, which is defined by the following way: in the present time for the compounds $A^{I}_{2-x}B^{VI}$ there are two models of formation of possible Ray's [10] and Vei's [10] defects, in the each of which the dominating types of defects, causing the deflection from the stoichiometry are defined. In the first model it is proposed that creation of the deffect passes in two stages: the neutral vacancy of metal V_a appeares by the jump and then the ionization vacancy appeares and as a result the hole forms. Therefore, the complete? concentration of the defects is defined as $N_d=V_A+V^I_A$, and the concentration of the holes is $p=V^I_A$. In the second model it is possible the introduction

of atoms of metal in the interstices $A_i=A_i^*+n$, where A_i, A_i^* are concentrations of the neutral and ionized donors. The complete concentration of the defects is as follows

$$N_d=V_A+p-A_i-n \qquad (6)$$

where $p-n=V^1_A-A_i^*$, and p, n are defined in compliance with [8]

$$N_d = V_A + V^1_A - A_i - A_i^*$$

or

$$P = \frac{(2m_p k_0 T)^{3/2}}{4\pi^{3/2}h^3} F_{r+1}(\mu_p^*)$$

and

$$n = \frac{(2m_n k_0 T)^{3/2}}{3\pi^2 h^3} I^0_{3/2}(\mu_n^*, \beta) \qquad (7),$$

where m_p is the effective hole mass (m_p=0,54 [12]) $\beta=\varepsilon_g/k_0T$ is the parameter of the parabolitic band, ε_g is the width of the forbidden band (ε_g =0,18eV) [2], $\mu_p^*=\mu_p/k_0T$ and $\mu_n^*=\mu_n^*/k_0T$, μ_p and μ_n are chemicopotentials $F_r(\mu)$ and $I^m_{n,k}$ are the one-parametrical and two-parametrical Fermi integrals.? The chemicopotential μ_n is defined from the following expression [2],

$$\alpha_\infty = -\frac{k_0}{e}\left[\frac{I^1_{3/2,0}(\mu_n^*,\beta)}{I^0_{3/2,0}(\mu_n^*,\beta)} - \mu_n^*\right] \qquad (8)$$

and

$$\mu_p = -\varepsilon_g - \mu_n \quad , \qquad (9)$$

where α is the thermoelectromotive force of the electrons in the strong magnetic fields. Taking into consideration (8) and (9) in (7) one can define p and n, and then calculate N_d. Using the values N_d, V_0 and m_n in (5) the $\tau_d(T)$ is defined. The mobolity $U_d(T)$ is defined as in [7]:

$$U_d(T) = \frac{e\tau_d(T)}{m_n} \qquad (10)$$

Substituting $U_d(T)$ instead of $U_{ac}(T)$ in (4), we obtain:

$$U(T) = \left(\frac{1}{U_i} + \frac{1}{U_d}\right)^{-1} \qquad (11)$$

As it is seen from fig.3a the curve2 is corresponded with experimental one qualitatively. It means that in the rich in Se region, ie. where the argentum vacancies dominate, the scattering on the centres, consisting of the defects of the acceptor type is the dominate scattering mechanism. It can be expected that in this temperature region the ion radius of selen is less than wave length of the acoustic phonon [13]. From this figure it follows that at low temperatures for $n\leq 12{,}35\cdot10^{18}$sm^{-3} U doesn't depend on T that is correspond to the scattering on the ionized impurities. The U decreases proportionally to $T^{-\alpha}$, with the increase of the temperature, that shows on the active role of phonons in the scattering. By dates $U(T)$ the scattering on the acoustic and optical phonons is hardly differed quantitatively. The dominate scattering mechanism is better isolated from concentrational dependence $U(n)$. As it was shown in [14] the $U_{ac}\sim n^{-1}$, $U_{op}\sim n^{1/3}$, $U_i\sim n^{2/3}$. From this it follows that temperaturedependence of the ratio U_i/U_{ak} is defined by the temperature dependence $U_{ak}(U_i/U_{ak}\sim T)$. From the fig.3 it is seen that in dependence $U\sim T^\alpha$ the exponent α=0,6 and is almost doesn't depend on electron concentration ($n\leq 7\cdot10^{18}$sm^3 is exception).It means that in the temperature interval 20-100K the mechanism of electrons scattering has the mixed character. In comparison with the other narrow-band semiconductors the mobility of carriers of current in Ag(2)Se is small. The possible reason of this phenomena is the big effective electron mass [2] in this semiconductor.

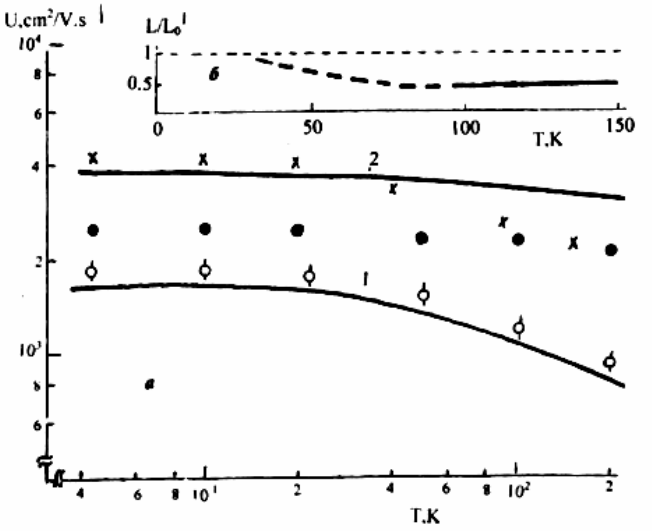

Fig.3.

From the fig.2 it is seen that in the interval 4-150K the animation effect of the electrons by the phonons isn't achieved. Taking into consideration n_0 and $\alpha_0(T)$ the dominated scattering mechanism can be established also. In the case of the one-band model the at the nonquadratic dispersion law and any degree of degeneracy α_0 is defined as:

$$\alpha_0 = -\frac{k_0}{e}\left[\frac{I^1_{r+1,2}(\mu_n^*,\beta)}{I^0_{r+1,2}(\mu_n^*,\beta)} - \mu_n^*\right]. \qquad (12)$$

In the fig.2 the results of $\alpha_0(T)$ calculation on the formulae (12) for the three samples are given. As it is seen the results, obtained about dominated scattering mechanism of current carriers in selenide of argentum agree with the dates [14]. The calculations show that at the different electron concentrations the dominated scattering mechanisms are different. This uncorresponding it is follows that the screening radius changes at the electron concentrations changing. Here it is also important the character of the interelectron interaction at the different scattering mechanisms [15]. In the ref 3 the temperature dependences of the experimental and calculated values L/L_0 for the set of the narrow-band semiconductors [16-18] are given, in particular for the values Ag_2 Te [19], being analog of Ag_2Se. It is also shown that at the decrease of temperature $L\rightarrow L_0$ the

interelectron interaction became elastic at the pure ion scattering realization. The analysis of temperature dependence of the mobility and other kinetic parameters (for example, $\sigma(T)$) show the dominated ion electron scattering at T<30K. Taking into consideration and by analogy to the listed narrow-band semiconductors the temperature dependence L/L_0 can be extrapolated even at the low temperatures (fig.3(б)).

So we can make the following conclusion that the given model with the strong degenerated of one type of current carriers and Kein dispersion law is completely describes electric and thermoelectric properties of Ag_2Se at low temperatures.

[1] *S.A. Aliyev, N.A. Verdiyeva, M.I. Aliyev*. FTP, 1978, 12 (10), 2075 (in Russian).
[2] *S.A. Aliyev, F.F. Aliyev*. Izv. AN SSSR, Neorganich. Mater., 1985, 21 (11), 1869, (in Russian).
[3] *M.G. Ramazanzade, S.A. Aliyev, N.A. Verdiyeva, A.M.Agayev*. Izv. BUZov, Fizika, 1981, №10, 27, (in Russian).
[4] *V.M. Glazov, N.M. Makhmudova*. Izv. AN SSSR, Neorganich. Mater., 1970, 6(8),1409, (in Russian).
[5] *S.A. Aliyev, D.G. Arasli, Z.F. Agayev, Sh.S. Ismailov, E.I. Zulfigarov*. Izv. AN Azerb.SSR, ser. fiz.-tex. I физ-тех. и mat. nauk, 1982, №6,67, (in Russian).
[6] *N. Hieraki, I. Kaznaki, Y. Sataran*. Iap. I. Appl. Phys-pt1, 1999, 38 (10), 5745(1999)
[7] *F.F. Aliyev, E.M. Kerimova, S.A. Aliyev*. FTP, 2002, 36(8),932, (in Russian).
[8] *B.M. Askerov*. Kineticheskiye effekti v poluprovodnikakh. Leningrad, Nauka,1970, (in Russian).
[9] *Andre and C.Simon*.I.Phys.Chem., 1983, 44(2),95.
[10] *H.Ran*.I.Phys.Chem.Sol.1974, 35(11),1553.
[11] *K.Weiss.Ber.Runsenges*. Phys.Chem., 1969, 75, 338.
[12] *P.Yunod.Helv*. Phys.Acta, 1959, 32(6-7),567.
[13] *S.V. Bulyarovskiy, V.I. Fistul*. Termodinamika I kinetika vzaimodeystvuyushshikh defektov v poluprovodnikakh, M., Nauka,1997, (in Russian).
[14] *G.B. Abdullayev, M.I. Aliyev, S.A. Aliyev, D.G. Arasli, N.A. Verdiyeva, R.E. Guseynov*. Preprint IFAN, Az.SSR, Baku, 1974, s.16, (in Russian).
[15] *L.I. Nikiruy, L.Y.Nejilovska, V.M. Klapichka, M.O. Galushshak, V.M.Shkerun*. Ukr. Fiz., 2001, 46(10),1083, (in Russian).
[16] *S.A. Aliyev, L.L. Korenblit, S.S. Shalit*. FTT, 1966, 8(3),705, (in Russian).
[17] *S.S. Shalit, V.M. Mujdaba, A.D. Galeckaya*. FTT, 1968, 10(5), 1277, (in Russian).
[18] *V.M.Mujdaba, V.K. Ogorodnikov,S.A. Aliyev, S.S. Shalit*. FTT, 1969, 11(2),545, (in Russian).
[19] *S.A. Aliyev, F.F. Aliyev, S.G. Abdinova, Z.S. Gasanov, D.M. Ragimova*. Izv. VUZov, Fizika, 1990, №6,41, (in Russian).

F.F. Əliyev, N.A. Verdiyeva, G.P. Paşayev

Ag_2Se KRİSTALININ AŞAĞI TEMPERATURLARDA ELEKTRİK VƏ TERMOELEKTRİK XASSƏLƏRİ

Bir tip keçiricilik üçün Keyn modeli nəzərə alınmaqla dispersiya qanunu əsasında elektrikkeçirmə, Holl effekti və termoelektrik H.Q. tədqiq edilmişdir. Müəyyən olunmuşdur ki, $n \geq 1{,}2\cdot10^{19}sm^{-3}$ elektron konsentrasiyası üçün yükdaşıyıcılar, ion aşqarları və akustik fononlardan, $n \leq 6{,}9\cdot10^{18}sm^{-3}$ üçün isə ion aşqarlarından və nöqtəvi defektlərdən səpilirlər.Göstərilmişdir ki, T<30-də elektronelektron qarşılıqlı təsiri elastiki xarakter daşıyır.

Ф.Ф. Алиев, Н.А. Вердиева, Г.П. Пашаев

ЭЛЕКТРИЧЕСКИЕ И ТЕРМОЭЛЕКТРИЧЕСКИЕ СВОЙСВА Ag_2Se ПРИ НИЗКИХ ТЕМПЕРАТУРАХ

В работе анализированы температурные зависимости электропроводности- $\sigma(T)$, коэффициента Холла-$R(T)$ и термоэдс-$\alpha_0(T)$ в Ag_2Se при низких температурах в рамках теории с одним типом носителей тока и кейновским законом дисперсии, а также с учетом характера межэлектронного взаимодействия. Установлено, что для концентрации $n \leq 6{,}9\cdot10^{18}см^{-3}$ ток носителей рассеивается на ионах примеси и точечных дефектах, а для $n \geq 12\cdot10^{18}см^{-3}$ рассеяние происходит на ионах примесей и тепловых колебаниях решетки.Показано, что при T< 30K межэлектронные взаимодействия носят упругий характер

Received: 24.05.03

THE ANOMALIES OF THE ELECTRIC AND DIELECTRIC PROPERTIES OF THE TIS IN THE PHASE TRANSITIONS AREA

V.P.ALIYEV, S.S.BABAYEV, SH. G. GASIMOV, A.A.ISMAYLOV, T.G.MAMEDOV, MIR-GASAN U. SEIDOV

Institute of Physics, Azerbaijan National Academy of Sciences, Baku. Az - 1143, H. Javid av. 33

In the ref the results of experimental investigations of the electric and dielectric properties of the monoclinic TIS in the temperature interval 260-440K are given. The anomaly at 411K, connecting with the phase transition is registered firstly on the temperature curves of the electric conduction dependence, dielectric constant and tangent of the dielectric loss. The character of the anomaly is typical for the phase transition of II-type. The possible nature of the discovered phase transition is discussed.

I. Introduction

Моносульфид таллия TIS is the semiconductor connection, in respect of the binary connections of A^3B^6 type. By the TIS investigations it is established that this connection can be crystallized in the different crystal structures. The more populated type is the structure type of the chain crystal TIS of the tetragonal modifications with the space group (PG) of the symmetry D_{4h}^{18} (the structure prototype TISe) [1-3]. It was informed comparatively recent [4-8] about possibility of the obtaining of the single crystals TIS with the layer type of the crystal structure as monoclinic, so tetragonal modifications. The monoclinic crystal system of the layer TIS (the structure analog of the layer crystal $TIGaSe_2$) [4-6-8] is described at the room temperature PG C_2^3 (in the literature are also discussed thew variants PG C_s^3 and C_{2h}^3 [5,7]) and characterized by the period of the crystal grid: a=11,01Å, b=11,039Å, c=4+15,039Å and b=100,69°. The tetragonal cell of the layer TIS has the grid parameters at the room temperature: $a=b$=7,803Å and c=29,55Å. According to [7], PG of the layer crystals TIS of the tetragonal modification can be D_4^4 or D_4^8.

The polymorphic transformations of the layer TIS have physical properties. The layer crystals TIS of the monoclinic crystal system are interesting by that at the atmospheric pressure they are endured the successiveness of the structure phase transitions (FP): at T_i=341,1K from the high - temperature paraelectric phase into the incommensurable phase (NS) with the wave vector of the modulation $k_i = \left(\delta;0;\frac{1}{4}\right)$ where δ~0,04 incommensurable parameter; at T_c=318,6K in the unknown, ferroelectric, commensurable phase (S) with the quadrupling of the parameter of the elementar cell along crystal axis $\vec{c}$ [4,6]. The carried investigations in [4] show that lower than T_c dielectric hysteresis loops are observed and vector of the spontaneous polarization is situated in the layer plane. By the dates of the differential thermical analysis (DTA) and measurements of the temperature dependence of the dielectric constant (ε) TIS it is established that [4-6] FP at T_i is FP of II type, and at T_c is FP of I type. The pieces of information about FP realization in the structure of the layer TIS in the system TI-S. The carried investigations have been proved the existence in the structure TIS FP at 353K, in the result of which TIS transfers from the monoclinic phase into tetragonal phase with the totality of the diffraction pictures, which are completely suit to the structure TISe. We mention that in [9] on the TIS diffractograms the appearing of the satellite reflexes, proving the polar C phase existion in the crystal HC.

In the present paper the results of the experimental investigations of the electric and dielectric properties of the monoclynic TIS, obtained with the aim of the later elaboration pecularities of the structure FP in TIS and obtaining of the additional information about this crystal movement in the high-temperature paraelectric phase are informed.

II. The samples and experimental methodics

The investigated samples TIS of the black-grey color had the monoclinic structure, according to carried out x-ray pattern investigations at the room temperature. The especial character of the investigated monoclinic TIS as studied in [4-8,9] is the existing in its composition the superstichiometric sulfur quantity (TIS+4%S). The applicated technology of TIS monoclinic crystal obtaining, and also the dates of X-ray diffraction analysis will be given in [10] more in detail.

For the investigation the several especially picked up samples of the natural spalling of TIS in the form of plane-perallel plates with the mutual perpendicular directions of the edges orientation, cutted out from the growed up ingot are used. All above mentioned measurements correspond to the sample with the line sizes 4+1,8+1,2mm^3.

For the dielectric characteristics TIS measurement in the capacity of the electric contacts the silver paste was used. The electrodes from In were used at the temperature dependence of the electric conduction investigation. Before the electrods drifting the corresponding surfaces of the samples were polished. The samples were in the vacuum inside the thermostated camera with the aim of the averting the possibility of the TIS samples oxidation in time of their measurements. The sample's temperature was controlled by the copper-constantanal thermocouple with precision ±0,1°C. The investigations were carried out in the quazistatistical temperature mode, at this the temperature change velocity was 0,1K+min^{-1}. The dielectric constant (ε) and tangent of

dielectric loss ($tg\delta$) measurememts were on the frequency 9,8Hs with the help of the alternating-current bridge because of the high electric conduction of the TIS samplesin the investigated temperature interval 250-440K. The electric conduction measurements (σ) were carried out on the direct current on the standard methodics.

III. The experimental results and their discussion

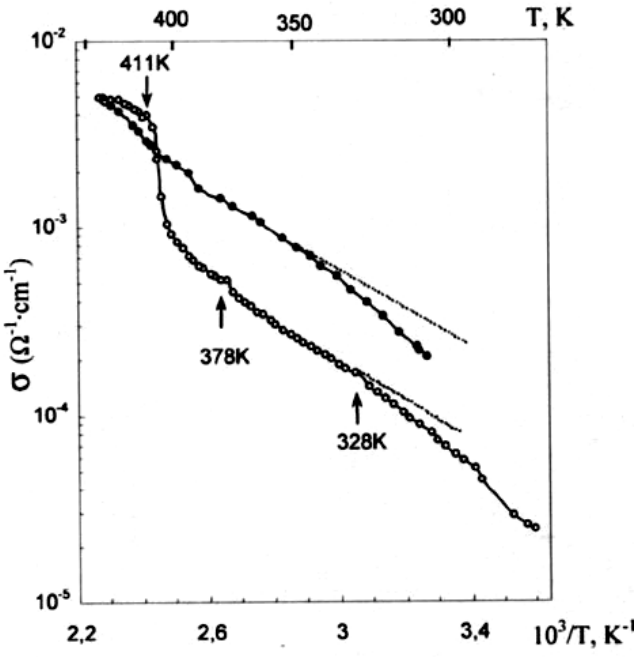

Fig.1. The temperature dependence of TlS electric conduction, measured in the heating (o) and cooling (•) modes of sample

The temperature electric conduction dependences TIS, measured in the mode of the heating and cooling of the sample are given in fig.1. It is need to note, that electrophysical characteristics of TIS, studied on the samples with the mutual perpendicular edge orientation, had practically the similar temperature dependences, but differed by the value strongly. So, for example, the ratio of the electric conduction values of the samples with the mutual perpendicular edge orientation ($3{,}571\cdot10^{-4}\Omega$ cm^{-1} and $5{,}11\cdot10^{-5}\Omega$ cm^{-1}) is ~7 at the room temperature. More over, by the absolute value the electric conduction of the investigated samples at the room temperature exceeds more than one degree the value σ of chained TIS [3] and 3-4 degree the value σ of the layer TIS of monoclinic modification, investigated in [8]. The heating curve σ from the opposite temperature has the line character in the temperature interval 255-401K. The existing of the following anomalies discover the more detailed heating curve analysis $\sigma(1/T)$ (constructed in the logarithmic scale).

1) The change of the slope gradient $\sigma(1/T)$ at T=328K, obtained in the heating mode. The given anomaly is observed on the dependence $\sigma(T)$ and in the cooling mode.

2) The little anomaly in the form of the deflection from the line dependence is observed on the heating and cooling curves $\sigma(T)$ in the neighbourhood T~378K.

3) The strong increase of σ with the temperature growth in the interval 401411K. The relative change σ in the given temperature region is 3,36. The dependence $\sigma(1/T)$ is likely again higher than T=411K. The measurement of σ, carried out in cooling mode of TIS sample after its heating up to 438 showed the abscence of any anomaly in the б movement in the temperature interval 401-411K. The cooling curve $\sigma(1/T)$ has line character in the given temperature region (but no jumped).

The essential pecularity of the growed up TIS samples is the complete reconstruction of their initial electric (and dielectric also) properties after separate thermal maturing of the samples at the temperature 250K during three days are given in the fig.2. As it is seen from the fig. 2 the anomal movement of the electric conduction in the temperature interval 401÷411K doesn't re-create neither at the samples cooling, nor at its heating on the $\sigma(1/T)$ curve. At the same time the pecularities in the movement $\sigma(1/T)$ in the nieghbourhood 328K are clearly followed.

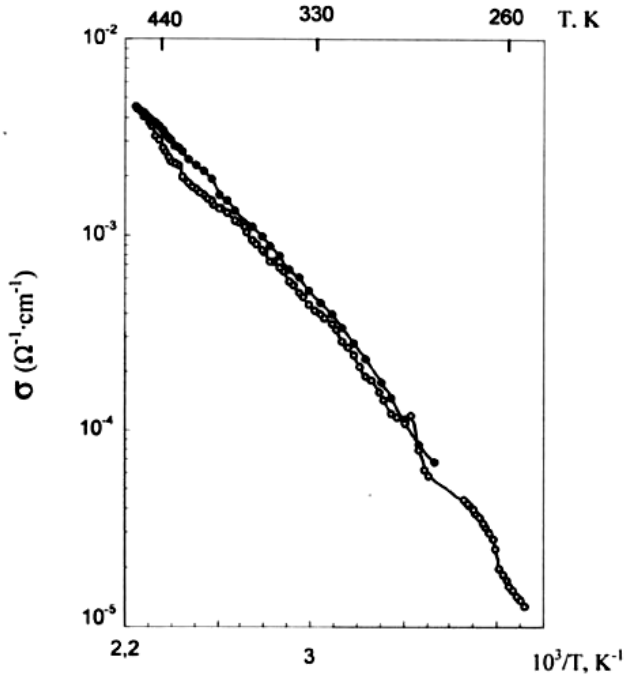

Fig.2. The temperature dependence of TlS electric conduction, measured in the heating (o) and cooling (•) modes after the temperature annealing of sample at 250Kduring of three days

The temperature dependences ε of TIS samples in the temperature interval 270÷425K, obtained in the heating and cooling modes are given the fig. 3. As it is seen from the fig.3, the heating curve $\varepsilon(T)$ is characterised by the anomalies in the nax forms at the temperatures 377,6 K and 411K. The given anomalies don't re-create at the $\varepsilon(T)$ measurements in the cooling mode of the sample. The complete re-creation of these anomalies on the dependence $\varepsilon(T)$ in the heating mode is observed after the ewak thermal maturing of TIS samples at temperature 250K. More over, the little anomaly is observed in the neighbourhood 328K, which also doesn't re-create at $\varepsilon(T)$ of the several TISsamples (see inset to fig.3).

At last, the temperature stroke $tg\delta$ TIS in the hearing and cooling modes of the samples is given in the fig.4. As it is seen from the fig.4 the essential growth tgб TIS takes place at

the heating of the sample in the interval 380-410K. The big electric conduction of TIS samples at temperatures, higher than 410K complicates the $tg\delta$ measurement, that's why we couldn't registrate the max in $tg\delta(T)$ movement in the neighbourhood 411K.

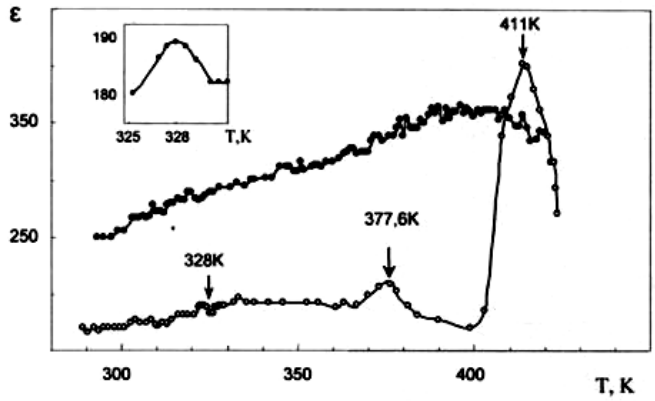

Fig.3. The temperature dependence of TlS dielectric constant, measured in the heating (o) and cooling (•) modes of sample. Insert to fig.3. The anomaly on the curve $\varepsilon(T)$, observed at the investigation of some samples of TlS in the neighbourhood of 328K.

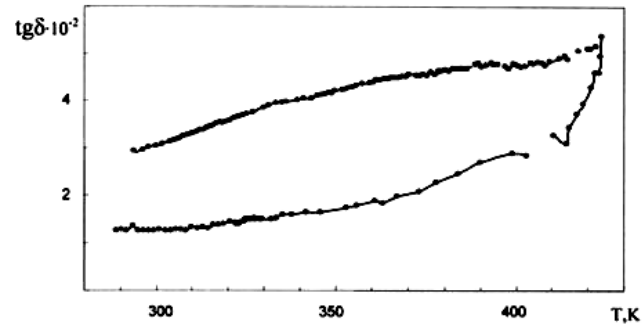

Fig.4. The temperature dependence of $tg\delta$ TlS, measured in heating heating (o) and cooling (•) modes of sample.

Summarizing the above mentioned dates about temperature dependences of electric and dielectric characteristics of the investigated crystal TIS in the temperature interval 250÷440K, we can make the definite conclusions about nature of the discovered anomalies. As it was given in the introduction, the layer TIS crystals of monoclinic modification combine the segnetoelectric and semiconductor properties at the same time [4, 6]. From the other side, according to the thermodynamic theory, the character pecularities on the temperature dependences of the wide of the prohiubited band have to be observed in the segnetoelectric-semiconductors [11] in the structure FP area: the jump at the FP of I type and temperature coefficient change at FP of II type. The registrated the change of the inclination of the curve $\sigma(1/T)$ and the existence of the little anomaly on the curve $\varepsilon(T)$ of the several TIS samples at T=328K could be connected with the discovered [4-6] FP of II type at T_i=341,1K. However, the nonconformity with the temperature of FP of II type, obtained in the given paper with the earlier published dates [4,6] and also the abscence the character anomalies on the dependences $\varepsilon(T)$ and $tg\delta(T)$ are possible connected with that the growed up TIS crystal of the monoclinic modification differs subsantially on its physical properties from layer TIS of the monoclinic crystal system, investigated in [4-6, 8]. It can be proposed that discovered pecularities of the electrophysical properties of the investigated TIS at 328K and in the neighbourhood 378K are connected with the structural FP between different TIS polymorphic transformations. The finding out of the mentioned above anomalies' nature in the temperature movement electric and dielectric properties growed up TIS needs the carrying out the additional structural investigations.

Let's stop on the possible nature of the anomalies at 411K. The combination of the experimental results allows to consider that near T~411K TIS endures FP, having the character traites FP of I type. The phase, appearing at T>411K is metastable. The relaxation time, needed for the complete re-creation of the initial physical properties of the sample is 160-170 hours at the thermal relieving at T=250K. We consider that in TIS in the temperature interval 401÷411K is FP in the state with the superion conductivity. The obvious analogy between pecularities of TIS electric and dielectric properties in the given temperature interval with the properties of the superion semiconductors [12, 13] is the argument in the benefit of this interpretation of the above mentioned experimental results.

As it is known [13-15] the ion currents in the superion semiconductors (solite electrolyties) are caused by the existence of the defects in their structures as vacancies and interstitial atoms (Frenkel and Shottki defects). At the same time the temperature dependence of ion conductivity is subject to thermoactivation law of the аррениусовского type [13-15]:

$$\sigma(T) = \frac{\sigma_0}{T} \cdot exp\left(-\frac{E_\alpha}{kT}\right) \qquad (1)$$

where σ_0 is the frequency factor; E_a is the activation energy, defined by the defect creation energy and ativation energy of its motion; k is Boltzmann constant.

The character pecularity of the heating curve $\sigma(1/T)$ of our samples (as other superion semiconductors) is the existence of three like temperature areas with the different inclination angles.

1) The inclination angle of the like area of the heating curve $\sigma(1/T)$ in the temperature interval 330÷401K is characterized by activation energy E_a=0,224eV. ???

2) The inclination angle of the like area of the heating curve $\sigma(1/T)$ in the temperature interval 401-411K is characterized by E_a=2,66eV. The given temperature area, so-called the intrinsic conductivity area [13], is that type region, where the superion conductivity appears. The ion conductivity on this temperature area is defined by the defects, created in the crystal lattice because of the warmth [13,14]. The activation energy value on this area is more by the value, than in the temperature interval 330÷401K, as Ea is defined by the energies' sum, needed as for the defect creation so for the its motion along the crystal. In many superion conductors this area is finished by FP type order-disorder. The discovered the -------- anomaly on the curve $\varepsilon(T)$ TIS at 411K is connected with the existence of this FP.

3)The inclination angle of the area of the heating curve $\sigma(1/T)$ in the temperature interval 401÷411K corresponds to

the activation energy E_a=0,226 eV. The given temperature area corresponds to conductivity in the strong разупорядочная crystal structure.

We note also, that in [3] the pecularities like above mentioned were discovered in the another temperature region 300÷350K at the investigation of the electric conduction temperature dependence and Hall coefficient of the chain TIS of the tetragonal transformation (structure analog TISe). By the sign of Hall constant in [3] it is established that the main role in the electric conduction of the chain TIS play the positive charge particles (holes according to [3]). Besides by the authors of [3] it is established that in the temperature interval 300÷350K Hall mobility m(n) is subject to law $\mu_H \sim T^{8,33}$, ---------in 215÷300K the temperature dependence $\mu_H \sim T^{6,78}$. In [3] it is noted that such temperature movement of Hall mobility of the chain TIS doesn't correspond to any from the famous carriers' scattering mechanisms in the semiconductors [16].

On our opinion the authors of [3] don't consider the FP possibilities in the state with the superion conductivity, which also takes place in the chain TIS structure of the tetragonal transformation. Using dates about Hall coefficient sign [1,3] it can be proposed that in TIS structure the transition in the state with the superion conductivity is caused by the разупорядочением in таллиевой sublattice because of potential barrier decrease between allowed тфллий cations' positions in the temperature interval 401÷411K.

Nevertheless, the authors of the given paper consider that the above mentioned experimental facts connect with the разупорядочением in the anionic sublattice of the investigated TIS, Because of the existence of the nonctoichiometric quantity of sera anions in TIS lattise, the last, situated in the interstices of the tetragonal elementary all TIS, promotes to the monoclinic distortion of the initial elementary cell. At the achieving of the temperatures, corresponding to the activation energy of the anionic defects is the wide ----- of the anionic sublattice and later the appearing of the pecularities in the temperature movement of TIS electrophysical properties in the temperature interval T>401K.

The authors are thankful to T.S.Mamedov and A.S.Nadjafov for the giving of the samples for the investigations.

[1] *R.S. Itoga, C.R. Kannewure*. J.Phys. Chem. Solids, 1971, v.32, 1099-1110.
[2] *K.R. Allakhverdiev, N.Yu. Safarov, M.A. Nizametdinova, E.A. Vinogradov, N.N. Melnik, A.F. Goncharov*. Solid State Comm., 1982, v.42, №7, 485-488.
[3] *A.T. Nagat* J Phys: Condens. Matter, 1989, v.1, 7921-7924.
[4] *S. Kashida, K. Nakamura, S. Katayama*. Solid State Comm., 1992, v.82, №2, 127-130.
[5] *K. Nakamura, S. Kashida*. Journal of the Phys. Soc. Jpn., 1993, v.62, №9, 3135-3141.
[6] *S. Kashida, K. Nakamura, S. Katayama.* J. Phys. Condens. Matter, 1993, v.5, 4243-4250.
[7] *S. Kashida, K. Nakamura*. J. Sol. St. Chemistry, 1994, v.110, 264-269.
[8] *S. Kashida, T. Saito, M. Mori, Y. Tezuka, S. Shin*. J. Phys: Condens. Matter, 1997, **9,** 10271.
[9] *R.M.Sardarli, A.P.Abdullayev, G.G. Guseynov, A.I. Nadjafov, N.A. Eyubova.* Kristallografiya, 2002, t.45, 4, 606-610 (in Russian)
[10] *A.I.Nadjafov, G.G.Guseinov, M.Yu. Seyidov, T.G. Mammadov, T.S. Mammadov* (to be published)
[11] *V.M. Fridkin: segnetoelektriki* - poluprovodniki. M. Nauka, 1976.
[12] *M. Dammak, H. Khemakhem, T. Mhiri*. Journal Phys. Chem. Solids, 2001, 62**,** 2069-2074.
[13] Light Scattering in Solids III. Recent Results. Ed. by *M.Cordona and G. Guntherodt*, Springer – Verlag, 1982, pp. 311.
[14] *Ch. B. Lushchik, A.Ch. Lushchik*: Decay of electronic excitations with defect formation in solids, Nauka, Moscow, 1989, pp.262.
[15] *A.F. Ioffe*: Fizika poluprovodnikov, Izd., AN SSSR, Moskva, 1957, 491c. (in Russian)
[16] *R.A. Smith*: Semiconductors, Cambridge, 1978, pp. 558.

В.П. Алыев, С.С. Бабаев, Ш.Г. Гасымов, А.А. Исмаилов, Т.Г. Мамедов, Мир-Гасан Ю. Сеидов

АНОМАЛИИ ЭЛЕКТРИЧЕСКИХ И ДИЭЛЕКТРИЧЕСКИХ СВОЙСТВ КРИСТАЛЛОВ TlS В ОБЛАСТИ ФАЗОВЫХ ПЕРЕХОДОВ

В работе представлены результаты экспериментальных исследований электрических и диэлектрических свойств моноклинного TlS в интервале температур 260÷440 К. На кривых температурной зависимости электропроводности, диэлектрической проницаемости и тангенса угла диэлектрических потерь впервые зарегистрирована аномалия при 411К, связываемая с фазовым переходом. Характер аномалии типичен для фазового перехода I- рода. Обсуждается возможная природа обнаруженного фазового перехода.

Ln_2GeS_4 (Ln=La, Ce, Pr, Nd, Sm) TİPLİ BİRLƏŞMƏLƏRİN ELEKTROFİZİKİ XASSƏLƏRİNİN TƏDQİQİ

H.R. QURBANOV, A.Ə. NƏBİYEV
Azərbaycan Dövlət Pedaqoji Universiteti
Bakı, Üz.Hajıbəyov 34.

La_2GeS_4 (La, Ce, Pr, Nd, Sm) tipli birləşmələr alınmış, onların elektrofiziki xassələri: elektrikeçirməsi, termo e.h.q. yükdaşıyıcıların yürüklüyü 300÷1000 K temperatur intervalında tədqiq edilmişdir.

Elektrikkeçirmənin temperaturdan asılılıq qrafikdən məxsusi oblastda qadağan olunmuş zolağın eni hesablanmış və ΔE_t=1,83-2,01eV qiymətlər aldığı müəyyən edilmişdir. Termo e.h.q.temperaturdan asılı olaraq azalır və bütün temperatur intervalında *p*-tip keçiriciliyə malik olduğu göstərilmişdir. $\mu=\sigma P_x$ ifadəsindən yürüklüyün temperaturdan asılılığı öyrənilmiş və səpilmə mexanizmi təyin edilmişdir.

La_2GeS_4, Ce_2GeS_4, Pr_2GeS_4, Nd_2GeS_4 və Sm_2GeS_4 üçlü birləşmələri komponentlərin 1:1-ə nisbətində sintez olunmuşdur. Bu birləşmələr üçün xarakterik xüsusiyyət heksoqonal sinqoniyada kristallaşması və La–dan Sm-a keçdikdə (La→Ce→Pr→Nd→Sm) qəfəs sabitlərin azalmasıdır (a=9,95÷9,80*Å* ; c=6,14÷5,57*Å*). Eyni zamanda mikrobərkliyin qiyməti də həmin birləşmələrdə ardıcıl olaraq artır.

Yuxarıda göstərilən birləşmələrin yarımkeçiricilər olmasını müəyyən etmək məqsədi ilə, onların elektrofiziki xassələri geniş temperatur intervalında tədqiq olunmuşdur. Tədqiq olunmuş birləşmələrin otaq temperaturunda fiziki xassələri cədvəl 1-də verilmişdir.

Cədvəl 1.

Ln_2GeS_4 (Ln=La, Ce, Pr, Nd, Sm) tipli birləşmələrin 300 K-də bəzi fiziki xassələri

Birləşmə	Elektrik keçirmə, σ, om^{-1}, sm^{-1}	Termo-e.h.q. α, MkV/K	Yükdaşıyıcıların yürüklüyü, μ, sm^2/V.san	Yükdaşıyıcıların konsentrasiyası, p, sm^{-3}	Qadağan olunmuş zolağın eni, ΔE_T, eV	Keçiriciliyin tipi n, P
La_2GeS_4	$2,4\cdot10^{-5}$	390	12,4	$8,6.10^{16}$	1,83	P
Ce_2GeS_4	$7,8\cdot10^{-5}$	386	8,42	$9,4.10^{16}$	1,87	P
Pr_2GeS_4	$2,3\cdot10^{-4}$	371	7,44	$4,8.10^{17}$	1,94	P
Nd_2GeS_4	$6,6\cdot10^{-4}$	360	5,70	$6,3.10^{17}$	1,97	P
Sm_2GeS_4	$8,5\cdot10^{-4}$	326	2,62	$7,6.10^{17}$	2,01	P

Cədvəldən göründüyü kimi Ln_2GeS_4 -dən Sm_2GeS_4 -ə keçdikdə (La÷Sm) elektrikkeçirmənin qiyməti artdığı halda, termo e.h.q.-nin qiyməti azalır. Bu zaman yükdaşıyıcıların yürüklüyü təxminən dörd dəfədən çox azalır. Otaq temperaturunda birləşmələrin fiziki parametrlərinin belə dəyişməsi La÷Sm sırasında yükdaşıyıcıların konsentrasiyasının dəyişməsi ilə əlaqələndirilə bilər. Göstərilən halda isə qadağan olunmuş zolağın eni artır. Belə ki, La_2GeS_4 birləşməsi üçün ΔE_T=1,83eV olduğu halda, Sm_2GeS_4 üçün ΔE_T=2,01 eV qiymətini alır.

Qeyd edək ki, tədqiq olunan birləşmələr sırasında əsasən nadir torpaq elementləri (La, Ce, Pr, Nd, Sm) dəyişir. Bu elementlərin ion radiusları ($r_{La}^{+3}=1,061$; $r_{Ce}^{+3}=1,034$; $r_{Pr}^{+3}=1,013$; $r_{Nd}^{+3}=0,995$; $r_{Sm}^{+3}=0,964E$;) La÷Sm sırasında azalır. Eyni zamanda birləşmələrin kristal qəfəsinin sabitləri də azalır. Göstərilən parametrlərin bu cür dəyişməsi tədqiq olunan birləşmələrdə qadağan olunmuş zolağın eninin artmasına səbəb olur. Həmçinin qadağan olunmuş zolağın eninin dəyişməsi birləşmələrdə nadir torpaq elementlərində (La÷Sm) valent elektronlarının lokallaşmasının artması və bununla da keçiricilik zonasında elektronların sayının azalması ilə izah etmək olar.

Fiziki xassələrinin öyrənilməsi gedişində müəyyən olunmuşdur ki, birləşmələrin beşi də 300 K-də *P*-tip keçiriciliyə malikdir.

La_2GeS_4, Ce_2GeS_4, Pr_2GeS_4, Nd_2GeS_4 və Sm_2GeS_4 birləşmələrinin elektrikeçirməsi və termo e.h.q.-si 300÷1000K temperatur intervalında ölçülmüş, alınmış nəticələr isə uyğun olaraq şəkil 1 və 2-də verilmişdir. Elektrikkeçirmənin və termo e.h.q.-nin temperaturun artması ilə dəyişməsi, $lg\sigma \sim f(10^3/T)$ və $\alpha \sim f(10^3/T)$ asılılıq qrafikindən göründüyü kimi yarımkeçiricilər üçün xarakterikdir.

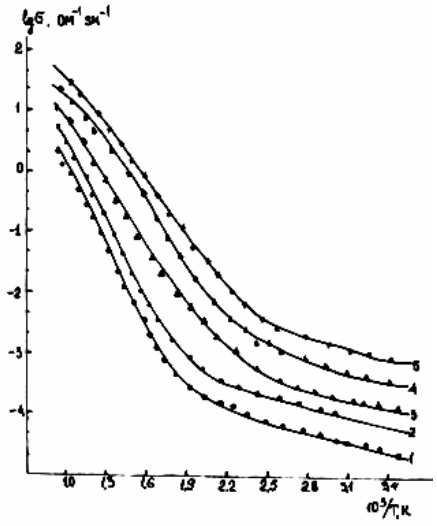

Şəkil 1. Ln_2GeS_4-(Ln=La, Ce, Pr, Nd, Sm) tipli birləşmələrin temperaturdan asılılıq qrafiki: 1-Sm_2GeS_4; 2-Nd_2GeS_4; 3 - Pr_2GeS_4;4 - Ce_2GeS_4, 5- La_2GeS_4.

Tədqiq olunan birləşmələrin 5-də də elektrikkeçirənin qiyməti 300÷1000K temperatur intervalında artır. ~T≤450K temperatur intervalında elektrikkeçirmə nisbətən az dəyişir və bu aşqar keçiricilik oblastına uyğun gəlir. ~T≤500K temperatur intervalında isə elektrikeçirmə temperaturdan asılı olaraq kəskin dəyişir. Bu isə məxsusi keçiricilik oblastına uyğun gəlir.

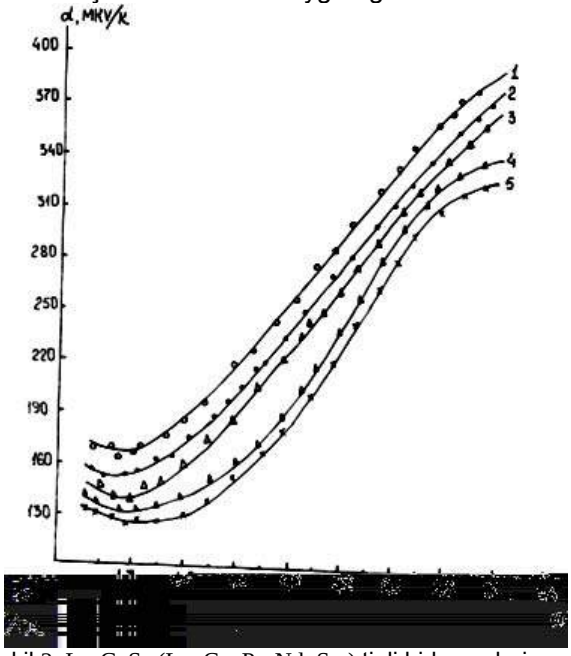

Şəkil 2. Ln_2GeS_4-(La, Ce, Pr, Nd, Sm) tipli birləşmələrin termo e.h.q.-nın mperaturdan asılılıq qrafiki:
1- La_2GeS_4; 2- Ce_2GeS_4; 3 - Pr_2GeS_4;4 - Nd_2GeS_4;
5- Sm_2GeS_4.

Qeyd edək ki, aşqar keçiricilikdən, məxsusi keçiricilik oblastına keçid temperaturu La_2GeS_4-dən Sm_2GeS_4-istiqamətində (La→Ce→Pr→Nd→Sm) aşağı temperaturaya doğru sürüşür (490→460). Aşağı temperatur intervalında (aşqar keçiricilik oblastı) birləşmələrin aktivləşmə enercisinin qiymətləri hesablanmış və ΔE_0=0,22÷0,30eV olduğu müəyyən edilmişdir. Yuxarı temperatur intervalında isə (məxsusi keçiricilik oblastı) birləşmələrin qadağan olunmuş zolağın eni E_T=1,83÷2,01eV qiymətləri almışdır.

Termo e.h.q.-nin qiyməti isə birləşmələrin hamısında temperaturun artması ilə azalır (300÷1000 K temperatur intervalında) Nd_2GeS_4 və Sm_2GeS_4 birləşmələrinin termo e.h.q.-si otaq temperaturuna yaxın temperaturda (~T≤350K) nisbətən az dəyişir.

Tədqiq olunan birləşmələrin hamısında termo e.h.q.-si ~T=750 ÷800 K-dən temperaturun artması ilə kəskin azalır. Temperaturun ~T≥860 K qimətində isə birləşmələrin termo e.h.q.-nin qiymətinin az da olsa artması hiss olunur.

Termo e.h.q.-nin işarəsinin dəyişməsinə görə keçiriciliyin tipi təyin edilmiş və müəyyən olunmuşdur ki, tədqiq olunan temperatur intervalında birləşmələrin hamısı P-tip keçiriciliyə malikdirlər.

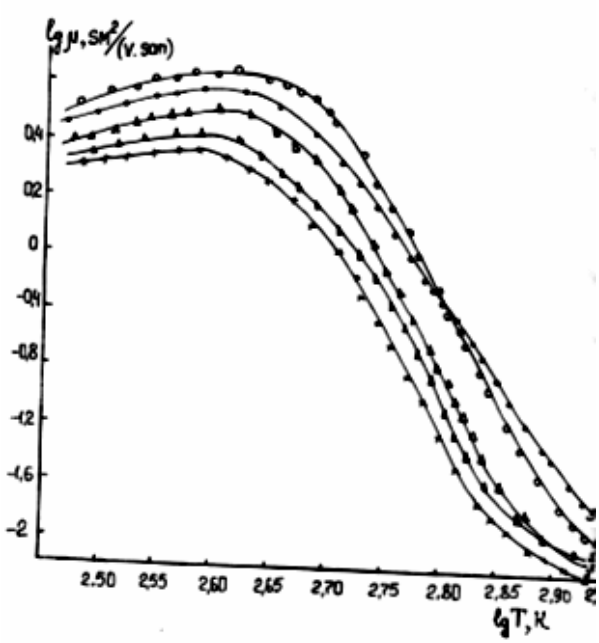

Şəkil 3. Ln_2GeS_4-(Ln=La, Ce, Pr, Nd, Sm) tipli birləşmələrinin yürüklüyünün temperaturdan asılılıq qrafiki:
1- La_2GeS_4; 2- Ce_2GeS_4; 3 - Pr_2GeS_4;4 - Nd_2GeS_4;
5- Sm_2GeS_4.

Yükdaşıyıcıların yürüklüyü ($\mu=\sigma R_x$) və konsentrasiyasını hesablamaq üçün La_2GeS_4, Ce_2GeS_4, Pr_2GeS_4, Nd_2GeS_4 və Sm_2GeS_4 birləşmələrinin Holl effekti ölçülmüşdür (300÷1000K temperatur intervalında). Yükdaşıyıcıların yürüklüyünün temperatur asılılığı (T=300÷1000k temperatur intervalında) şəkil 3-də qrafik olaraq verilmişdir $\ell g\mu \sim f(\ell gT)$. qrafikindən yürüklüyün temperaturdan aslı olaraq dəyişmə dərəcəsini ($\mu \sim T^{\pm K}$) hesablamaq olur. Burada «K» müsbət və mənfi qiymətlər almaqla, μ-nun temperaturdan asılı olaraq dəyişmə dərəcəsini göstərir. Temperaturun ~T≤350K intervalında K≈0,11÷0,18 T≈400÷490K temperatur intervalında isə K≈(0,52÷0,61) qiymətləri almışdır. ~T≥500K temperatur intervalında isə K=-(1,5÷2,1) qiymətlər almışdır. Göründüyü kimi birinci və ikinci temperatur intervalında K-nisbətən kiçik qiymətlər alır və bu baxımdan səpilmə mexanizminin akustik olduğunu demək olar. yuxarı temperatur intervalında isə «K»-nın böyük qiymətlər alması səpilmə mexanizminin həm akustik və həm də optiki olduğunu göstərir.

Elektrikkeçirmə və termo e.h.q-nin temperaturdan asılı olaraq dəyişmə xarakterini, bilavasitə yükdaşıyıcıların yürüklüyünün temperaturdan asılı olaraq dəyişməsi ilə izah oluna bilər. Bu isə yürüklüyün və digər parametrlərin (σ,α) tədqiq olunan kristallarda yükdaşıyıjıların konsentrasiyasının dəyişməsi ilə əlaqələndirilə bilər.

[1] *A.F. İoffe.* Fizika poluprovodnikov. M. L. AN SSSR. 1957.
[2] *İ.M. Carskiy, Q.İ. Novikov*. Fiziçeskie metodı issledovaniə i neorqaniçeskoy ximii. M., Vıs. Şkola, 1988.

H.R. Gurbanov, A.A. Nabiyev

THE INVESTIGATION OF ELECTROPHYSICAL PROPERTIES OF Ln_2GeS_4 (Ln=La, Ce, Pr, Nd, Sm) COMPOUNDS

The compounds of type of Ln_2GeS_4 (Ln=La, Ce, Pr, Nd, Sm) are obtained and at the temperature range of 300-1000 K their electrophysical properties such as electrical conductivity, thermo-e.m.f. and charge carrier mobility are studied.

On temperature dependence of electrical conductivity in intrinsic range of conductivity the band gap energy is determined. It is shown, that at given temperature range with increasing of temperature the thermo-e.m.f decreases and in these compounds appears p-type of conductivity.

On $\mu=\sigma R_x$ relation are determined the temperature dependence of mobility and scattering mechanism.

Г.Р. Гурбанов, Ф.Ф. Набиев

ИССЛЕДОВАНИЕ ЭЛЕКТРОФИЗИЧЕСКИХ СВОЙСТВ СОЕДИНЕНИЙ ТИПА Ln_2GeS_4 (Ln=La, Ce, Pr, Nd, Sm)

Получены соединения типа Ln_2GeS_4 (Ln=La, Ce, Pr, Nd, Sm) и в интервале температур 300÷1000 К, изучены их электрофизические свойства: эелектропроводность, термо –э.д.с. и подвижность носителей заряда.

Из температурной зависимости электропроводности в собственной области определена ширина запрещенной зоны, где ΔE_m=1,83÷2,01эВ.

Показано, что в изученном температурном интервале с ростом температуры термо – э.д.с. уменьшается и данные соединения проявляют р-тип проводимость.

Из соотношения $\mu=\sigma R_x$ определена температурноая зависимость подвижности и определён механизм рассеяния.

Received: 24.05.2003

KİMYƏVİ ÇÖKDÜRMƏ YOLU İLƏ ALINMIŞ YÜKSƏK FOTOKEÇİRİCİLİYƏ MALİK CdS NAZİK TƏBƏQƏLƏRİNİN TƏDQİQİ

Z.Ə. VƏLİYEV
Naxçıvan Dövlət Universiteti

M.H. HÜSEYNƏLİYEV
Azərbaycan MEA-nın Naxçıvan bölməsi

Kimyəvi çökdürmə yolu ilə alınmış CdS nazik təbəqələrində otaq temperaturunda çox yüksək fotokeçiricilik aşkar edilmişdir. $\sigma_{işıq}/\sigma_{qaranl.}$ keçiriciliklərin nisbəti $4\cdot10^{10}$ kimidir. Stasionar hal çox uzun müddət ərzində alınır. $(\alpha h\nu)^2 \sim f(h\nu)$ asılılıqdan təbəqənin qadağan olunmuş zonasının eni müəyyən edilmişdir.

CdS nazik təbəqələrindən fotovoltaik çeviricilər kimi istifadə edilməsi perspektivi onun çox mükəmməl strukturlu təbəqələrinin alınması üçün daha təkmil epitaksial texnologiya üsullarından istifadə etməyi şərtləndirir. Kimyəvi çökdürmə üsulunun sadəliyi və bir çox üstünlükləri [1] ondan geniş miqyasda istifadə etmək üçün stimul yaratmışdır. Xüsusilə bu üsul varizon strukturlar almaq üçün çox əlverişlidir.

CdS nazik təbəqələrinin alınmasında kimyəvi çökdürmə üsulundan istifadə edilmişdir. CdS - nazik təbəqəsi şüşə altlıqlar üzərində alınmışdır. Bunun üçün şüşə altlıq əvvəlcə xrom turşusunda sonra isə destillə suyunda yuyulur. Şüşə altlıq şaquli şəkildə içərisində temperaturu 90-95°S məhlul olan laboratoriya stəkanının daxilinə yerləşdirilir. Məhlul 0,5mol. kadmium asetat və 0,5mol. tiomoçevinadan ibarət olmaqla hazırlanır. Bunlardan əlavə məhlula kompleksəməlgətirən komponent olaraq trietanolamin, adqeziya yaratmaq məqsədi ilə naşatır spirti əlavə edilir. Maqnit qarışdırıcı vasitəsilə məhlul daima qarışdırılır. 15-20 dəqiqədən sonra şüşə altlıq çıxarılır və destillə suyunda yuyulur.

Bu üsulu tətbiq etməklə alınan CdS təbəqəsi kifayət qədər bircins olmaqla yanaşı, onun şüşə ilə adqeziyası da qənaətbəxş olur. CdS-təbəqəsinə In kontaktları vurulmuş və onun fotoelektrik xassələri öyrənilmişdir.

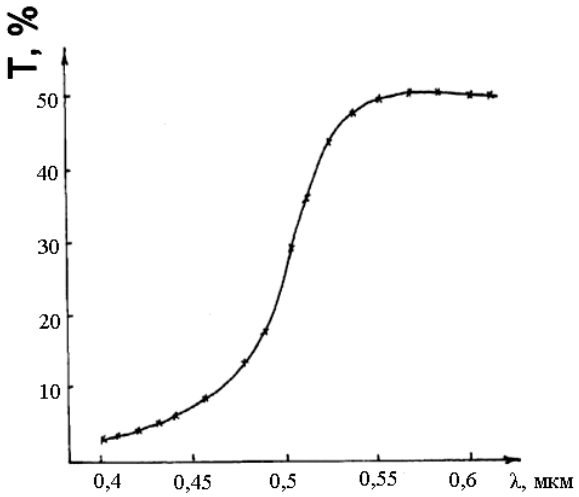

Şəkil 1. Fotokeçiriciliyin zamandan asılılığının kinetikası: 1-təbəqənin üstünə

Otaq temperaturunda çox yüksək fotokeçiricilik müşahidə edilmişdir. Qaranlıqda nümunənin müqaviməti ~10^{15}om olduğu halda 100 vattlıq lampanın işığı altında (~25sm məsafədən) bu müqavimət $2{,}5\cdot10^4$om – a qədər aşağı enmişdir. Yəni işıq-qaranlıq müqavimətinin nisbəti $4\cdot10^{10}$–a bərabər olmuşdur. Şəkil 1-də otaq temperaturunda CdS nazik təbəqəsi üçün fotokeçiriciliyin zamandan asılı qaranlıqdan – işığa (1-əyrisi) və işıqdan – qaranlığa (2-əyrisi) əyriləri göstərilmişdir.

Şəkildən göründüyü kimi işıqdan qaranlığa keçərkən müqavimətin stasionar hala uyğun qiymət alması çox ətalətli prosesdir. 1 əyrisi öz stasionar halını (təbəqənin üstünə işıq salınır) 1 saata aldığı halda (3.10^3 san), 2-əyrisi öz stasionar halını 10 saatdan çox (~ $4\cdot10^4$ san) müddətə alır.

CdS nazik təbəqəsi üçün yüksək fotokeçiricilik haqqında [2] işində məlumat verilmişdir. Bu işdə CdS nazik təbəqəsi piroliz üsulu ilə alınmış və xüsusi olaraq O_2-ilə aşqarlanmışdır. Yalnız bu texnoloji əməliyyatdan sonra CdS nazik təbəqəsində işıq-qaranlıq keçiricilikləri nisbəti ən çox 10^7 - yə bərabər olmuşdur.

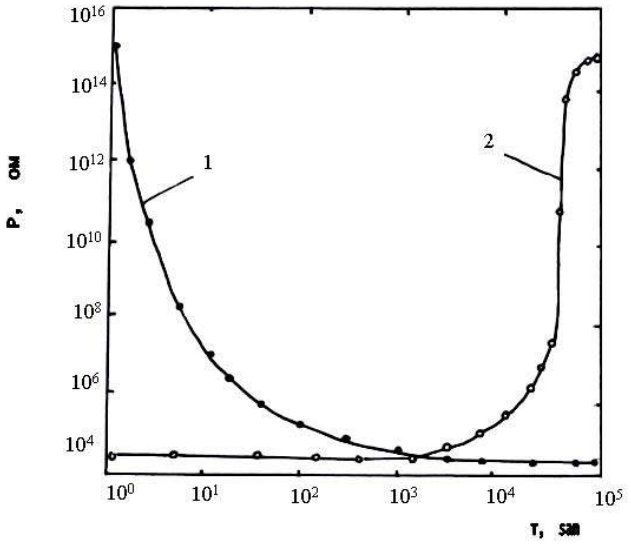

Şəkil 2. CdS nazik təbəqəsinin optik buraxma əyrisi

Kimyəvi çökdürmə yolu ilə aldığımız CdS nazik təbəqəsində isə heç bir aşqar vurulmadan bu nisbət $4\cdot10^{10}$-a qədər qalxmışdır ki, bu da CdS-nazik təbəqələri üçün hələlik ən yüksək nəticədir.

Alınan CdS-nazik təbəqəsinin qadağan zonasının enini müəyyən etmək üçün «SPECORD-40M» spektro-

fotometri vasitəsilə onun optik buraxma əyriləri çəkilmişdir (şəkil 2).

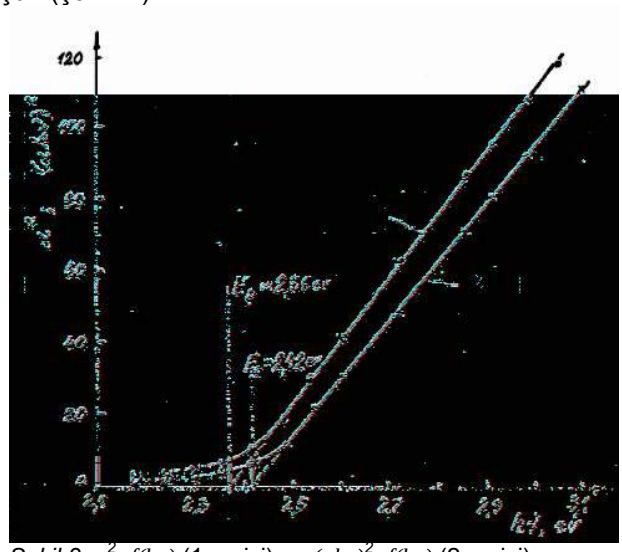

Şəkil 3. $\alpha^2 \sim f(h\nu)$ (1 əyrisi) və $(\alpha h\nu)^2 \sim f(h\nu)$ (2 əyrisi) asılılılqları.

Optik buraxma əyrisinə əsasən $\alpha^2 \sim f(h\nu)$ asılılığı çəkilmiş və bu asılılıqdan düz xətt oblastının ekstropolyası üsulu ilə təbəqənin qadağan zonasının eni müəyyən olunmuşdur: Eg = 2,36 ev (1-əyrisi, şəkil 3). Qeyd etmək lazımdır ki, alınan nazik təbəqələrin qalınlıqlarını ölçmək mümkün olmadığından bu asılılığı əslində sərbəst vahidlərdə α^2 - nın hv-dən asılılığı kimi başa düşmək lazımdır. Bu isə Eg-nın tə'yininə heç bir xələl gətirmir.

Bir çox müəlliflər Eg-nin təyinində $(\alpha h\nu)^2$–nin $h\nu$–dən asılılıq əyrisindən istifadə etməyi üstün bi lirlər. Bu asılılıqdan istifadə etdikdə CdS–nazik təbəqəsi üçün Eg-=2,42 ev (2-əyrisi, şəkil 3) alınmışdır. Bu qiymət [3] işində CdS–in qadağan zonası üçün göstərilən qiymətlə tamamilə eynidir.

CdS nazik təbəqələrində çox yüksək fotokeçiriciliyin müşahidə olunması onu söyləməyə imkan verir ki, kimyəvi çökdürmə üsulundan istifadə etməklə həm də birləşmələrdə bir sıra indikal xassələr müşahidə etmək mümkündür.

[1] *M.H.Hüseynəliyev*. «Müasir riyaziyyat və təbiətşunaslığın problemləri» NDU. Naxçıvan 2001. səh. 89-92.

[2] *D.Richards., A.M. El-Korashi*. «J. Vac. Sci. Technol». A. Vol2. № 2 Apr-June 1984 pp. 332-335.

[3] *G.K.Padam., G.L.Malhotra and S.U.M.Rao*. «J.Appl. Phys» 63 (3) 1988 pp. 770-774.

Z.A.Veliyev, M.H. Huseynaliyev,

THE INVESTIGATION OF THE HIGHLY PHOTO CONDUCTING CHEMICALLY DEPOSITED CdS THIN FILMS

Highly photoconductivity at room temperature is observed in the CdS thin films obtained by the chemically deposition technique.

The ratio of the conductivities $\sigma_{light}/\sigma_{dark}$ is equal to $4 \cdot 10^{10}$. The establishment of the stationary state lasts very long. The energy gap of the film is determined from the dependence $(\alpha h\nu)^2 \sim f(h\nu)$.

З.А. Велиев, М.Г. Гусейналиев

ИССЛЕДОВАНИЕ ТОНКИХ ПЛЁНОК CdS С ВЫСОКОЙ ФОТОПРОВОДИМОСТИ, ПОЛУЧЕННЫХ ХИМИЧЕСКИМ ОСАЖДЕНИЕМ

В тонких плёнках CdS – полученных химическим осаждением обнаружена очень высокая фотопроводимость, при комнатной температуре. Отношение проводимостей $\sigma_{свет}/\sigma_{темн}$ равнялось $4 \cdot 10^{10}$. Установление стационарного состояния длился очень долго. Из зависимости $(\alpha h\nu)^2 \sim f(h\nu)$ определена ширина запрещенной зоны пленки.

Received: 18.06.2003

STATIONARY AXISYMETRIC GRAVITY AS A PRINCIPAL CHIRAL FIELD MODEL

M.A. MUKHTAROV
Institute of Mathematics and Mechanics
370602 Baku, F. Agaev str.9, Azerbaijan

The stationary axisymmetric gravity equations (Ernst equations) are reduced to the principal chiral field problem with moving poles. Applying of the discrete symmetry transformations is discussed.

1. The problem of constructing the exact solutions of nonlinear evolution equations in the explicit form remains important for the present time. The existence of very rich integrable structure of Einstein equations have been conjectured by different authors. But the real discoveries of its integrability properties of stationary axisymmetric version of these equations, known as Ernst equations, and effective procedures for construction of solutions have been started in the papers of Belinskii and Zaharov [1]. In these papers the inverse scattering methods have been developed for vacuum gravitational fields. Among other approaches we have to point out the algebra-geometrical approach of Korotkin, Matveev and Nicolai [2-4]. Ernst equations as almost all so called integrable system can be obtained by symmetry reduction of the four dimensional self-dual Yang Mills (SDYM) equations that plays therefore the central role being the universal integrable system. The problem of integration of SDYM has successfully solved only for the case of SL(2,C) algebra and for instanton number not greater than two. The famous ADHM ansatz [5] gives the qualitative description of instanton solution but not its explicit form. Two effective methods of integration of SDYM for arbitrary semisimple algebra have been proposed in series of papers [6]. Another, the discrete symmetry transformation approach has been suggested [7] that allows to generate new solutions from the old ones. This method has been applied to many cases, for instance, the exact solutions of principal chiral field problem were obtained in [8] for the case of SL(2,C) algebra and in [9] for SL(3,C) and the rest semisimple algebras of the rank greater than two. This method can be effectively applied to the so called principle chiral problem with the moving poles [10].

This work shows how Ernst equations can be reduced to principle chiral problem with the moving poles with future possible application of the discrete symmetry transformation method.

2. The Ernst equation describing stationary axisymmetric metrics in general relativity can be represented in a form [11]:

$$(\rho g_z g^{-1})_{\bar z} + (\rho g_{\bar z} g^{-1})_z = 0 \quad , \tag{1}$$

where g is real and symmetric (2x2) matrix and $\det g = -\rho^2$, subscripts stands for partial derivatives throughout this paper.

Using the known formula from matrix theory

$$\mathrm{sp}(g_t g^{-1}) = \frac{\partial}{\partial t} \ln \det g \tag{2}$$

and taking trace from both sides of (1), we have:

$$(\rho \frac{\partial}{\partial z}(-\rho^2))_{\bar z} + (\rho \frac{\partial}{\partial \bar z}(-\rho^2)_z = 0$$

Finally, we get the D'Alambert equation for ρ

$$\rho_{z,\bar z} = 0$$

and its solution in terms of two arbitrary functions: $\rho = \varphi_1(z) + \varphi_2(\bar z)$.

Due to conformal invariance of the theory we can without loss of generality put $\varphi_1(z) \to z$, $\varphi_2(\bar z) \to \bar z$ and get the expression for ρ as:

$$\rho = z + \bar z \tag{3}$$

Then we can write currents of the corresponding linear system in a form:

$$\begin{aligned} (z + \bar z) g_z g^{-1} &= F_z \\ (z + \bar z) g_{\bar z} g^{-1} &= -F_{\bar z} \end{aligned} \tag{4}$$

If we take the complex conjugate of the first equation of (4) and compare the result with the second one then we come to the conclusion that F is pure imaginary function, i.e.

$$F^* = -F \tag{5}$$

Then using (2) we have

$$\mathrm{sp}F_z = \mathrm{sp}(\rho g_z g^{-1}) = \rho \frac{\partial}{\partial z} \ln \rho^2 = 2$$

Thus we have the second constrained property of F :

$$\begin{aligned} \mathrm{sp}F_z &= 2 \\ \mathrm{sp}F_{\bar z} &= -2 \end{aligned} \tag{6}$$

Let's introduce the element $\bar g = g\sigma$, where σ is a matrix of inner automorhpism having the form:

$$\sigma = \begin{pmatrix} 0 & 1 \\ -1 & 0 \end{pmatrix}$$

One can be convinced by the direct check in the following properties:

$$\begin{aligned} &\mathrm{sp}\bar{g} = 0 \\ &\bar{g}^2 = \rho^2 \mathrm{I} \\ &\bar{g}^{-1} = \rho^{-2}\bar{g} \end{aligned} \tag{7}$$

For the element θ defined as $\theta = F + \bar{g}$ we rewrite relation (4) as

$$\begin{aligned} \theta_z &= \bar{g}_z(\rho^{-1}\bar{g} + \mathrm{I}) \\ \theta_{\bar{z}} &= \bar{g}_{\bar{z}}(-\rho^{-1}\bar{g} + \mathrm{I}) \end{aligned} \tag{8}$$

Note the evident relation coming directly from (7):

$$(\rho^{-1}\bar{g} + \mathrm{I})(-\rho^{-1}\bar{g} + \mathrm{I}) = 0$$

From this relation and (8) it follows that

$$\begin{aligned} &\det\theta_z = \det\theta_{\bar{z}} \text{ or} \\ &\mathrm{rank}\,\theta_z = \mathrm{rank}\,\theta_{\bar{z}} = 1 \end{aligned} \tag{9}$$

By changing variables

$$-\theta/4_{\bar{z}} \to \mathrm{f} \quad , \quad -\bar{z} \to \bar{z} \tag{10}$$

we eventually come to the equation

$$(z - \bar{z})\mathrm{f}_{z,\bar{z}} = [\mathrm{f}_{\bar{z}}, \mathrm{f}_z] \tag{11}$$

with additional relations

$$\mathrm{rankf}_z = \mathrm{rankf}_{\bar{z}} = 1 \tag{11a}$$

$$\begin{aligned} &\mathrm{spf}_z = 1/2 \\ &\mathrm{spf}_{\bar{z}} = -1/2 \end{aligned} \tag{11b}$$

$$\det \mathrm{Re}\,\theta = 1/16 \tag{11c}$$

Equations (11) are equations of principle chiral field problem with moving poles considered in [ ]-[ ] in context of discrete symmetry transformation method. Let's remind that this transformation allows to directly construct new solutions from the known initial ones, i.e. if f is the solution of (11) then $F = D_s(f)$ is again solution of (11). Here D_s stands for discrete symmetry transformation. This transformation has a property

$$\det \mathrm{F}_z = \det \mathrm{f}_z$$

that is conserves a determinant . Comparing with (11c) makes encouraging to construct solutions of Ernst equations in that way and it will be a subject of further investigations.

[1] *V.A.Belinskii and V.A.Zakharov*, Sov. Phys. JETP 48, 1978, 985; 50, 1979, 1

[2] *D. A. Korotkin and V. B. Matveev*, Leningrad Math. J. 1,1990, 379

[3] *D. A. Korotkin*, Class. Quantum Gravity 10, 1993, 2587

[4] *D. A. Korotkin and H.Nicolai*, Nucl. Phys. B 475, 1996, 397

[5] *M.F.Atiyah,N.J.Hitchin,V.G. Drinfeld and Yu.I. Manin*. Phys. Lett. A65, 1978, 2.

[6] *A.N.Leznov and M.A.Mukhtarov.* J.Math. Phys. 28 (11), 1987, 2574; Prepr.IHEP 87-90, 1987; Prepr. ICTP 163, Trieste, Italy,1990; J.Sov. Lazer Research, 13 (4), 1992, 284

[7] *A.N. Leznov*. IHEP preprint-92/87,1990.

[8] *A.N.Leznov,M.A.Mukhtarov and W.J.Zakrzewski.* Tr.J.of Physics 19, 1995, 416

[9] *M.A. Mukhtarov*. Fizika 5, 2002, 38

[10] *M.A. Mukhtarov*. Proc.Ins.Math.Mech., 10(18), 2000, 123

[11] *F. J. Ernst*, Phys. Rev. 168, 1968, 1415

M.A. Muxtarov

STASİONAR AKSİAL SİMMETRİK QRAVİTASİYA ƏSAS KİRAL SAHƏNİN MODELİ KİMİ

Aksional simmetrik qravitasiya tənlikləri (Ernst tənlikləri) hərəkət edən polyuslu əsas kiral sahənin tənliklərinə gətirilmişdir. Diskret simmetrik çevrilmə metodunun tətbiqi müzakirə edilmişdir.

М.А. Мухтаров

СТАЦИОНАРНАЯ АКСИАЛЬНО СИММЕТРИЧНАЯ ГРАВИТАЦИЯ КАК МОДЕЛЬ ГЛАВНОГО КИРАЛЬНОГО ПОЛЯ

Уравнения аксиально симметричной гравитации (уравнения Ернста) сведены к уравнениям главного кирального поля с подвижными полюсами. Обсуждается применение метода преобразований дискретных симметрий .

Received: 10.08.2003

MEASURING METHOD AND ITS GNOSIOLOGICAL ASPECTS IN MODERN PHYSICAL COGNITION

VILAYAT ISMAILOV
Baki State University
Academician Z. Khalilov str, 23, Baku

In the article the experimental method which is one of the empiric methods of the scientific research, its specific features, characteristics, gnosiological opportunities and cognitive functions being applied in the empiric level of knowledge are investigated. It is shown that the main difference of the experimental method from other methods of empiric research is of its synthetic character. Thus during the experiment not only the conditions of the research are changed, but the methods of observation, measuring, comparison of the empiric cognition are in organic way synthesized as well. At the same time in the article the kinds of the natural scientific experiment are discussed too.

It is known that all phenomena of reality which are studied by practical way have objective quantitative and qualitative determination. Qualitative determination of material systems which is increased by apparatus and by organs of sense of the observer is expressed in different numbers (speed, mass, electric charge, energy, pressure, volume etc.). But quantitave peculiarities of process and phenomena are described by figure price determining in measuring operation of physical numbers. Usage of measuring operation first of all is connected with such matter as correctness of realizing of ratio of quantitative and qualitative aspects of the object of cognition [10]. So measuring method is not limited only by marking quantitative description of the object of cognition, it enables to study its qualitative determination as well. And adequate cognition of quantitative aspect of the object is conditioned by cognition of its qualitative aspect in measuring operation.

Taking into consideration of specifity we may define description of measuring in the following way: measuring is an operation of determining figure price of any quality by means of measuring unit or standard. Measuring being based on operating of organs of sense and material – sensual activity of a man is an active cognitive process. Though measuring is based on organs of sense of a man his intellect, knowledge and practice participate in its course as well: the aim and direction of purposeful perception of the object by means of measuring depends on a man‘s knowledge and interest, intellectual experience, outlook, his attitude towards reality directly. Finding out figure price of measurable quantity it is expressed in international system of units by measuring units such as kilogram, newton, coul, veber, mol, candle-power, meter, second etc.

Measuring process is not amorphous, but it has compound structure [7]. First of all measuring is a figure comparison of quantities describing the same quality. For example, while measuring the mass of any thing, in reality we compare two different masses – the mass of the thing and the standard.

Measuring being an empiric investigating method is carried out only within strict conditions and comprise the following elements: 1) object of measuring; 2) measuring unit or object of standard; 3) apparatus being used in measuring process; 4) way of measuring; 5) observer or subject who carries out measuring [1].

Application of measuring method causes some methodological problems among of which the ratio between sensual cognition and abstract thought is of great importance. Measuring unlike observation is connected with logic analysis as well.

Sensual perception goes into measuring as a necessary component. According to sensual perception of readings of apparatus a long of reasonable results are placed between the results of measuring. And that is why sensual perception is the only beginning stage of study of quantity. In such cases independent measuring is applied not only for “net” empiric observation of the phenomena, but it becomes a complicated cognitive operation where intellect is of great importance. Logic intellect is of special great importance in measuring quantities and determining the results of measuring.

Measuring operation in physics is closely connected with the principle of observation. The essence of the principal which appeared in connection with founding theory of relativity and quantum mechanics in physics may be commented so: only those notions and quantities which can be practically tested or measured in the structure of physics may be used; quantities which cannot be measured must be rejected. Let us address to the history of physics. As a result of impossibility of observing of absolute simultaneity on principal A.Einstein came to space – time conception in his theory of relativity. One can tell the same thoughts about Heysenberg’s activity that had abolished difficulties of Bor’s atom model. Heysenberg has created matrix mechanics which explains modern quantum mechanics for the first time.

From the point of view of methodology or general methods which enable to get measuring results, measuring – can be carried out directly and indirectly [12; 13]. Independent measuring, the sought for the result of which is obtained from measuring process directly is based on sensual – visual comparison of measurable quantity with special standard. For example, if we measure the mass, temperature, speed etc. of the thing according to the readings of apparatus – it is a direct measuring. But in indirect measuring the sought for the quantity is taken out mathematically from comparison of other quantities which are obtained by independent way and that is why in indirect measuring a logic comparison of the measurable quantity and standard occurs. For example, determining density of a spheric thing by the formula $\rho = \frac{m}{V}$ is an indirect measuring. Here m - is a mass and V-is a volume of the thing. In this case the mass of the thing is determined by the scales. At first in order to determine the volume of a spheric thing by the formula

$V = \frac{4}{3}\pi r^3$, its radius r is measured by the means of pair of compasses independently. On the basis of this direct measuring the volume of the thing is discovered indirectly. This example proves that the logic analysis of the quantitable descriptions which is obtained in indirect measuring is based on the data of measuring which is implemented on the base of the readings of measuring apparatus. And that's why it is wrong to oppose direct and indirect measurings or isolate one of them metaphysically. Unity of direct and indirect measurings is conditioned by the unity of sensual and logic cognition.

But within this unity both measurings obtain a relative independence. As far as possible each of them is used independently. Indirect measuring is especially extensively used in study of micro-world and society.

At the same time we must underline restriction of direct measuring which is conditioned by the following reasons.

Firstly, the number of measuring standards which are used in direct measuring must be equal common symptoms of measurable thing and other things on the whole. But this is impossible in practice.

Secondly, in direct measuring measurable thing is not associated with standard inside, that is measurable quantity and measuring unit appear as external factors.

Thirdly, in direct measuring it is impossible to determine figure price of quantities which characterize of cosmic objects and micro-objects being beyond our organs of sense.

Measuring method is of great importance in scientific research, especially in study of nature [1]. Measuring, first of all is a way leading towards discovery of laws. Great Russian scientist D.I.Mendeleyev noted more than once that "measuring and weight is everything for study of nature". Measuring is important not only from practical point of view. It is of great importance in formation of scientific theories as well. History of science, especially study of nature is rich with such examples. For example, Tikho Bragen's numerous measurings over the movement of planets enabled I.Kepler to theoretic generalizations in the form of empiric laws; on the base of measuring of atomic weight of chemical elements D.I.Mendeleyev could discover the periodical system of elements; Faradey discovered electrolyze laws according to measuring of number of quantity of material which emanated from electrodes.

In connection with investigating cognitive importance of measuring method such a question comes up: how to explain discovery of objective laws by means of measuring? To our mind the explanation must be in the following way.

In the process of measuring determining quantitative relations of phenomena at the same time we discover their some common relations as well; according to F.Engelse we discover "external determination of things". Every time we measure qualitative determination of things by means of physical quantities (mass, charge, current etc.) which express their important peculiarities. So measuring enables us to study and discover both relations of phenomena – common and important aspects. And it is known that a law is an expression of common and important aspects of relations. This shows evidently that we can define measuring as a true way of discovery of empiric laws [16]. Academician B.M.Kedrov notes that though empiric discoveries don't make revolution in the science, they cause to live latent embrions of future revolution [9].

For example, american scientist A.Maykelson's measuring the speed of light is one of such unical measurings that enriched the history of science. Russian scientist, academician S.L.Vavilov appreciating Maykelson's scientific heroism as "a record of experiment" wrote: "On the base of his experimental discoveries and measurings theory of relativity was founded, wave optics and spectroscopy increased and theoretical astrophysics firmly established" [6].

In modern physical cognition the question of gnosiological basing of the measuring method is in organic way connected with the question of exactness of measuring. Exactness is an important index of qualitative and scientific price of measuring. I.Kepler highly appreciating Tikho Bragen's measurings which are notable for their exactness (the error of them was 8 minutes) wrote: "The eight minutes that is impossible to take no heed will enable us to overturn in astronomy" [17]. I.Kepler had made a mistake: namely Bragen at the expense of combining a very high exactness of his measurings with his extraordinary diligence (he repeated his measurings 70 times) could discover laws of movement of the planets.

And what objective factors is exactness of measuring conditioned by? Exactness of measuring depends on objective and subjective factors and determining their correct ratio. Exactness of measuring requires take into account a number of objective factors which have some influence on measuring process. These factors include qualitative peculiarities of measuring object, conditions under what measuring process is carried out, peculiarities of space and time coordinates of measuring object, its speed of movement and others.

One of the main ways that improves exactness of measuring operation is increasing of quality of operating measuring apparatus based on maintaining principals and making newest measuring apparatus basing on latest achievements of science and engineering. For example, at present changing of frequency is measured by means of Messbauer effect with exactness of 10^{-16} hertz, but time on molecular generators with 10^{-11} second.

Subjective factors that measuring process include are organization of process, choice of measuring way, personal quality of a scientist, his persistency, level of preparation, scientific competence, ability of using of apparatus etc. Though all these subjective factors have an important influence on exactness of results of measuring, in any case not them, but objective factors have decisive role in measuring. That's why in order to get exact and objective result from measuring we must determine correct ratio of factors: not to distort results of measuring by exaggerating the role of subjective factors or reducing importance of objective ones.

The question of role of measuring in modern scientific cognition has been idealized by operationalism which is one of the fields of positivism and pragmatism.

American physicist P.Brijman (1882-1961) came out following thesis in order to ground his position: a) measuring is an absolute arbitrary operation being realized by a subject; b) measuring is the only foundation of scientific cognition [4]. Under these considerations Brijman regarded the object of scientific research as a totality of measuring operations and arbitrary scientific notion as determination of measuring way

of corresponding physical quantity. Thus he was changing the physical world that accepted as a totality of research object into results of measuring operations and the science itself into the system of notions determining by these operations. But by the using of scientific terminology and grounding evristical importance of measuring for scientific research Brijman tried to form operationalism in a scientific shape. But when we consider the contents of primary thesis of operationalism Brijman‘s scientific form of this conception is easily frustrated.

Firstly, one does not need to attribute measuring to absolute arbitrary activity of a subject. No doubt, it is possible to have some freedom in choosing of measuring unit and system of units in measuring operation. But this freedom itself must be founded on objective basis and subordinate to objective requirements. But the trend of operationalism putting aside objectiveness, evaluate relativity of freedom which may be in choosing of scale and system of units as absolute arbitrariness in determining of measuring.

Secondly, though all scientific merits and methodological values which measuring has it is not true to consider it as the only foundation of empiric basis and theoretical contents of scientific cognition. In this context groundless thesis of operationalism are specially shown in Brijman‘s attempt to apply some notions of theory of relativity and quantum mechanics to measuring. In order to prove our thought we remind such a fact that the notions - the curve of “space-time continuum” and “wave function” have been determined not only by the way of measuring. We should remember that the real contents of theoretical notions of physics are not conditioned by concrete measuring operations, but first of all by scientific panorama of the world [15].

Summing up the brief description of measuring method in an article it is necessary the underline that the position of measuring among empiric methods is about like observation and comparison. Measuring is a component of more compound method – experiment as well as observation and comparison.

[1] *E.P. Andreyev.* Questions of philosophy, 1982, №9.
[2] *M. Born.* Achievements of physical sciences, v. LXVI, issue 3. 1958.
[3] *M. Born.* Phusicalische Blatter. 1956, 2, s. 57-58 (in German).
[4] *B.E. Bukhovskiy.* Questions of philosophy, 1958, №2.
[5] *V.V. Bikov.* Methods of science. “Nauka”, M., 1974.
[6] *S.I. Vavilov.* Collection of works. v.3. M., Pub. House “Academy of Sciences of USSR”, 1956.
[7] *Z.M. Goutner.* Philosophical aspects of measuring in modern physics. Pub. House PGU, L., 1978.
[8] *V.A. Kanke.* Principal philosophical directions and conceptions of science. M., “Logos”, 2000, pp. 266-272.
[9] *B.M. Kedrov.* Questions of philosophy, 1966, №12.
[10] *V.A. Masko.* Gnosiological aspects of measuring. Pub. House “Naukova Dumka”, K., 1969.
[11] *O.A. Melnikov.* About the role of measuring in the process of cognition. “Nauka”, 1968.
[12] Methodological problems of measuring theory. “Naukova Dumka”, K., 1966.
[13] *M.E. Omelyanovskiy*. Philosophical aspects of measuring theory. In the book: Materialistic dialectics and methods of natural sciences “Nauka”, M., 1984.
[14] *M.E. Omelyanovskiy.* Development of basis of physics in XX century “Nauka”, M., 1984.
[15] *A.I. Panchenko.* Questions of philosophy, 1982, №3.

V.İ. İsmayılov

MÜASİR FİZİKİ İDRAKDA ÖLÇMƏ METODU VƏ ONUN QNOSEOLOJİ ASPEKTLƏRİ

Məqalədə eksperimental elmi tədqiqatın empirik metodlarından olub, biliyin empirik səviyyəsində tətbiq olunan eksperimental metod, onun səciyyəvi cəhətləri, xarakteristikası, qnoseoloji imkanları və idrak funksiyaları tədqiq olunur. Məqalədə göstərilir ki, eksperimental metodun empirik tədqiqatın digər metodlarından başlıca fərqi onun sintez xarakteri daşımasıdır. Belə ki, eksperimentin gedişində nəinki tədqiqat şəraiti dəyişdirilir, həm də empirik idrakın müşahidə, ölçmə, müqayisə metodları üzvi halda sintez olunur. Məqalədə, habelə təbii elmi eksperimentin növləri də nəzərdən keçirilir.

В.И. Исмайылов

МЕТОД ИЗМЕРЕНИЯ И ЕГО ГНОСЕОЛОГИЧЕСКИЕ АСПЕКТЫ В СОВРЕМЕННОМ ФИЗИЧЕСКОМ ПОЗНАНИИ

V statğe rassmatrivaetsə gksperimentalğnıy metod, kotorıy, əvləəsğ odnim iz gmpiriçeskix metodov nauçnoqo issledovaniə, primenəetsə na gmpiriçeskom urovne znaniə. İssleduetsə eqo osobennosti, xarakteristiki, qnoseoloqiçeskie vozmojnosti i funküii v nauçnom poznanii. Ukazıvaetsə, çto osnovnım otliçiem gtoqo metoda ot druqix metodov gmpiriçeskoqo issledovaniə, əvlətsə eqo sinteziruöhiy xarakter, tak kak narədu s izmeneniem usloviy gksperimenta metodı gmpiriçeskoqo poznaniə, takie kak nablödenie, izmerenie i sravnenie orqaniçeski sinteziruötsə. V statğe tak je rassmatrivaötsə vidı estestvennoqo nauçnoqo gksperimenta.

Received: 10.07.2003

AZƏRBAYCANCA-RUSCA-İNGİLİSCƏ FİZİKİ TERMİNLƏR LÜĞƏTİ

AZERBAIJAN-RUSSIAN-ENGLISH DICTIONARY OF THE PHYSICAL TERMS

АЗЕРБАЙДЖАНО-РУССКО-АНГЛИЙСКИЙ ФИЗИЧЕСКИЙ ТЕРМИНОЛОГИЧЕСКИЙ СЛОВАРЬ

Tərtib edənlər: **AME-nın müxbir üzvü**
A.İ. Muxtarov

SSRİ EA-nın müxbir üzvü,

akademik **H.M. Abdullayev**

Fizika-riyaziyyat elmləri doktoru
T.R. Mehdiyev

Fizika-riyaziyyat elmləri namizədi
E.A. Axundova

N.İ. Acalova

S.İ. Əliyeva

Biz “Fizika” jurnalının birinci nömrəsində başladığımız fizika terminləri lüğətinin nəşrini davam etdiririk. Bu nəşrdə akademik H.M. Abdullayevin nəşr etdirdiyi “Fizika terminləri lüğəti”ndən də istifadə edilmişdir (AREA-nın nəşri, Bakı, 1965-ci il).

Nəşr olunan terminlər haqda öz qeydlərini və terminlərini göndərən şəxslərə redaksiya əvvəlcədən öz təşəkkürünü bildirir.

Müəlliflər və jurnalın redaksiyası

We continue the publication the terminological physical dictionary, which has been began in the journal “Fizika”№1. In the published variant the physical terms, given by academician H.M. Abdullayev are given (“Fizika terminləri lüğəti”, AREA, Bakı, 1965).

The edition of the journal is welcome to all, who will send notes and terms for the publishing dictionary.

Authors and edition of journal “Fizika”

Мы продолжаем публикацию терминологического физического словаря, начатую в первом номере журнала “Fizika”. В публикуемом варианте мы также используем физические термины, предложенные академиком Г.М. Абдуллаевым (“Fizika terminləri lüğəti”, AREA, Bakı, 1965).

Редакция журнала приветствует всех, кто пришлет свои замечания и термины для публикуемого словаря.

Авторы и редакция журнала”Fizika”

Ölçü aparatı	Аппарат измеритель	Measuring apparatus
Kinomatoqraf aparatı	Аппарат кинематографический	Cinema apparatus
Kinoproyeksiya aparatı	Аппарат кинопроекционный	Film projection apparatus
Kompensasiya aparatı	Аппарат компенсационный	Compensated apparatus
Morze aparatı	Аппарат Морзе	Morze's apparatus
Optik aparat	Аппарат оптический	Optical apparatus
Göndərici aparat	Аппарат отправитель	Device-sender
Köçürücü aparat	Аппарат переносный	Portable apparatus
Polyarlaşma aparatı	Аппарат поляризационный	Polarizing apparatus
Qəbuledici aparat	Аппарат приемный	Receiving apparatus
Proyeksiya aparatı	Аппарат проекционный	Projection apparatus
Radio teleqraf aparatı	Аппарат радио телеграфный	Radio-telegraph apparatus
Tənzimedici aparat	Аппарат регулирующий	Regulating apparatus
Rentgen aparatı	Аппарат рентгеновский	X-ray apparatus
Rotasiya aparatı	Аппарат ротационный	Rotation apparatus
Özüyazan aparat	Аппарат самопишущий	Autographic apparatus
Simpleks aparatı	Аппарат симплексный	Simplex apparatus
Eşitmə aparatı	Аппарат слуховой	Hear apparatus
İstilik aparatı	Аппарат тепловой	Thermal apparatus
Cərəyanı kəsən aparat	Аппарат отключения тока	Off-state current apparatus
Dəqiq aparat	Аппарат точный	Preccise apparatus
Cızan aparat	Аппарат чертящий	Drawn apparatus
Yuz aparatı	Аппарат Юза	Yuz's apparatus
Aproksimatik törəmə	Аппроксимативная производная	Approximate derivative
Apriori ehtimal	Априорная вероятность	Apriori probability
Aproton məhlul	Апротонный растворитель	Aprotic solvent
Apsid	Апсида	Apse
Apsid xətti	Апсидная линия	Line of apsides
Araqo-Frenel təcrübəsi	Араго-Френеля опыт	Arago-Frenel experiment
Araqo hadisəsi	Араго явление	Arago effect
Argentometriya	Аргентометрия	Argentometry
Arqon	Аргон	Argon
Arqon lampası	Аргоновая лампа	Argon glow lamp
Arqon ion lazeri	Аргоновый ионный лазер	Argon-ion laser
Arqon lazeri	Аргоновый лазер	Argon laser
Arqon borucuğu	Аргонная трубка	Argon tube
Kompleks ədədin arqumenti	Аргумент комплексного числа	Argument
Perimərkəzin arqumenti	Аргумент перицентра	Argument of perihelion
En dairəsinin arqumenti	Аргумент широты	Argument of latitude
Ardometr	Ардометр	Ardometer
Areometr	Ареометр	Areometer
Faiz areometri	Areометр процентный	Percentage areometer
Areopiknometr	Areопикнометр	Areopycnometer
Arid zonası	Аридная зона	Arid zone
Arifmetikləşmə	Арифметизация	Arithmetization
Arifmetika	Арифметика	Arithmetic
Arifmetik komanda	Арифметическая команда	Arithmetic instruction
Üzən (gəzən) vergül ilə arifmetik əməliyyat	Арифметическая операция с плавающей запятой	Floating-point arithmetic
Fiksə olunmuş vergül ilə arifmetik əməliyyat	Арифметическая операция с фиксированной запятой	Fixed-point arithmetic
Arifmetik alt qrup	Арифметическая подгруппа	Arithmetic subgroup
Arifmetik proqres	Арифметическая прогрессия	Arithmetical progression
Yüksək tərtibli arifmetik proqres	Арифметическая прогрессия высшего порядка	Arithmetic progression of higher order
Arifmetik cəm	Арифметическая сумма	Arithmetic sum
Arifmetik blok	Арифметический блок	Arithmetic unit
Arifmetik operator	Арифметический оператор	Arithmetic operator
Arifmetik sıra	Арифметический ряд	Arithmetic series
Arifmetik dəyişmə	Арифметический сдвиг	Arithmetic shift
Arifmetik üçbucaq	Арифметический треугольник	Arithmetic triangle
Arifmetik ifadə	Арифметическое выражение	Arithmetic expression
Arifmetik əməliyyat	Арифметическое действие	Arithmetic operation

Arifmetik orta	Арифметическое среднее	Arithmetic mean
Arifmetik quruluş	Арифметическое устройство	Arithmetic device
Arifmometr	Арифмометр	1) Adding machine 2) Arithmometer 3) Calculator 4) Desk calculating machine
Arkkosinus	Арккосинус	Arc cosine
Arkkotangens	Арккотангенс	Arc cotangent
Arksinus	Арксинус	Arc sine
Arktangens	Арктангенс	Arc tangent
Arktika cəbhəsi	Арктический фронт	Arctic front
Armatura	Арматура	1) Accessories 2) Armature
Armilyar dairə (mühit)	Армиллярная сфера	Armillary sphere
Armko-dəmir	Армко-железо	Armco-iron
Aromatik birləşmələr	Ароматические соединения	Aromatic compound
Arrenius nəzəriyyəsi	Аррениуса теория	Arrhenius's theory
Arretir	Арретир	1) Arrester 2) Arresting lever 3) Caging device 4) Catch 5) Stop
Arretirləmək	Арретировать	1) Cage 2) Rate-cage
Artikullaşdırma qabiliyyəti	Артикулирующая способность	Articulating ability
Artikulyasiya	Артикуляция	Articulation
Arximed qanunu	Архимеда закон	Archimedes' principle
Arximed qüvvəsi	Архимедова сила	Buoyancy
Arximed vinti	Архимедов винт	Archimedes screw
Asbest	Асбест	Asbestos
Asimmetrik molekul	Ассимметрическая молекула	Asymmetrical molecule
Asimmetrik atom	Асимметрический атом	Asymmetrical atom
Asimmetrik təhlil	Асимметрический анализ	Asymmetrical analysis
Asimmetrik sintez	Асимметрический синтез	Asymmetric synthesis
Asimmetrik dalğa	Асимметричная волна	Asymmetrical wave
Asimmetrik əyri	Асимметричная кривая	Asymmetrical curve
Asimmetrik paylanma	Асимметричное распределение	Asymmetric distribution
Asimmetrik rəqslər	Асимметричные колебания	Asymmetric vibration
Asimmetrik fırfıra	Асимметричный волчок	Asymmetrical top
Asimmetrik rotator	Асимметричный ротатор	Asymmetric rotator
Asimmetriya	Асимметрия	Asymmetry
Şərq-Qərb asimmetriyası	Асимметрия восточно-западная	East-West asymmetry
Şimal-Cənub asimmetriyası	Асимметрия северо-южная	North-South asymmetry
Asimptota	Асимптота	Asymptote
Asimptotik yığılma (sıranın)	Асимптотическая сходимость	Asymptotic convergence
Asimptotik konus	Асимптотический конус	Asymptotic cone
Asimptotik yol	Асимптотический путь	Asymptotic path
Asimptotik sıra	Асимптотический ряд	Asymptotic series
Asimptotik dayanıqlı	Асимптотически устойчивый	Asymptotically stable
Asimptotik ifadə	Асимптотическое выражение	Asymptotic expression
Asimptotik qiymət	Асимптотическое значение	Asymptotic value
Asimptotik istiqamət	Асимптотическое направление	Asymptotic direction
Asimptotik sıraya ayırma	Асимптотическое разложение	Asymptotic expansion
Asimptotik həll	Асимптотическое решение	Asymptotic solution
Asinxron hesablama maşını	Асинхронная вычислительная машина	Asynchronous computer
Asinxron maşın	Асинхронная машина	Asynchronous machine
1) Asinxron işləmə 2) Təkmilləşdirmə	Асинхронная обработка	Asynchronous processing
Asinxron əməliyyat	Асинхронная операция	Asynchronous operation
Asinxron ötürmə	Асинхронная передача	Asynchronous transmission
Asinxron iş	Асинхронная работа	Asynchronous working
Asinxron sistem	Асинхронная система	Asynchronous system
Asinxron generator	Асинхронный генератор	Asynchronous generator

Asinxron mühərrik	Асинхронный двигатель	Asynchronous motor
Asinxron iş qaydası	Асинхронный режим	Asynchronous mode
Aspirator	Аспиратор	Aspirator
Su aspiratoru	Аспиратор водный	Aque aspirator
Qoşa aspirator	Аспиратор двойной	Double aspirator
Aspirasion psixrometr	Аспирационный психрометр	Aspiration psychrometer
Aspirasion termometr	Аспирационный термометр	Aspiration thermometer
Assembler	Ассемблер	Assembler
Assimilyasiya	Ассимиляция	Assimilation
Assosiativ yaddaş	Ассоциативная память	Associative memory
Assosiativ qeyd dəftəri	Ассоциативный регистр	Associative register
Assosiasiya	Ассоциация	Association
İonların assosiasiyası	Ассоциация ионов	Association of ions
Molekulların assosiasiyası	Ассоциация молекул	Molecular association
Assosiasiya olunmuş maye	Ассоциированная жидкость	Asssociated liquid
Assosiasiya olunmuş molekul	Ассоциированная молекула	Asssociated molecule
Maqnit astaziyalaması	Астазирование магнитное	Magnetic astatizing
Astaziyalama	Астазировать	Astatize
Astaziya	Астазия	Astasia
Astatin	Астатин	Astatine
Astatik maqara	Астатическая катушка	Astatic coil
Astatik maqnitlər sistemi	Астатическая система магнитов	Astatic system of magnets
Astatik	Астатический	Astatic
Astatik qalvanometr	Астатический гальванометр	Astatic galvanometer
Astatik maqnitölçən	Астатический магнитометр	Astatic magnetometer
Astatik tarazlıq	Астатическое равновесие	1) Astatic balance 2) Astatic equilibrium
Astatik tənzimləmə	Астатическое регулирование	Astatic control
Astenosfera	Астеносфера	Asthenosphere
Asterizm	Астеризм	Asterism
Asteroid	Астероид	Planetoid
Asiqmatizm	Астигматизм	Astigmatism
Dəstə asiqmatizmi	Астигматизм пучка	Astigmatism of pencil
Asiqmatik fərq	Астигматическая разность	Astigmation difference
Şüaların asiqmatik dəstəsi	Астигматический пучок лучей	Astigmatic pencil of rays
Astrometriya	Астрометрия	Astrometry
Astroqraf	Астрограф	Astrophotometry
Astroid	Астроида	Astroid
Astrologiya	Астрология	Astrology
Astrolyabiya	Астролябия	Astrolabe
Prizma ilə astrolyabiya	Астролябия с призмой	Astrolabe with prism
Astrometriya	Астрометрия	Astrometry
Astronomik uzunluq dairəsi	Астрономическая долгота	Astronomical longitude
Astronomik vahid	Астрономическая единица	Astronomical unit
Astronomik qüvvə vahidi	Астрономическая единица силы	Astronomical unit of force
Astronomik observatoriya	Астрономическая обсерватория	Astronomical observatory
Astronomik refraksiya	Астрономическая рефракция	Astronomical refraction
Astronomik en dairəsi	Астрономическая широта	Astronomical latitude
Astronomik sabitlər	Астрономические постоянные	Astronomical constants
Astronomik alaqaranlıqlar	Астрономические сумерки	Astronomical twilight
Astronomik saat	Астрономические часы	Astronomical clock
Astronomik iqlim	Астрономический климат	Astronomical climate
Astronomik kompas	Астрономический компас	Astronomical compass
Astronomik işarə, əlamət	Астрономический символ	Astronomical sign
Astronomik teleskop	Астрономический телескоп	Astronomical telescope
Astronomik üçbucaq	Астрономический треугольник	Astronomical triangle
Astronomik vaxt	Астрономическое время	Astronomical time
Astronomiya	Астрономия	Astronomy
Astrospektroskopiya	Астроспектроскопия	Astronomical triangle
Astrofizika	Астрофизика	Astrophysics
Astrofiziki observatoriya	Астрофизическая обсерватория	Astrophysical observatory
Astrofotoqrafiya	Астрофотография	Astrophotography
Astrofotometriya	Астрофотометрия	Celestial photometry

Asferik linza	Асферическая линза	Aspherical lens
Asferik səth	Асферическая поверхность	Aspherical surface
Ataksit	Атаксит	Ataxite
Ataktik polimer	Атактический полимер	Atactic polymer
Atermik məhlul	Атермический раствор	1) Athermal solution 2) Athermic solution
Atvud maşını	Атвуда машина	Atwood's machine
Spektral xətlərin atlası	Атлас спектральных линий	1) Spectral atlas 2) Spectral map
Atmoliz	Атмолиз	Atmolysis
Atmosfer	Атмосфера	Atmosphere
Ulduz atmosferi	Атмосфера звезды	Stellar atmosphere
Yerin atmosferi	Атмосфера Земли	Earth atmosphere
Bircins atmosfer	Атмосфера однородная	Homogeneous atmosphere
Tarazlıq (müvazinət) atmosferi	Атмосфера равновесия	Atmosphere of equilibrium
Günəş atmosferi	Атмосфера Солнца	Solar atmosphere
Texniki atmosfer	Атмосфера техническая	Technical atmosphere
Fiziki atmosfer	Атмосфера физическая	Physical atmosphere
Atmosferlər	Атмосферики	Atmospherics
Atmosfer akustikası	Атмосферная акустика	1) Atmospheric acoustics 2) Meteorogical acoustics
Atmosfer diffuziyası	Атмосферная диффузия	Atmospheric diffusion
Atmosfer korroziyası	Атмосферная коррозия	Atmospheric corrosion
Atmosfer optikası	Атмосферная оптика	1) Atmospheric optics 2) Meteorogical optics
Atmosfer refraksiyası	Атмосферная рефракция	Atmosphere refractions
Atmosfer turbiletliyi	Атмосферная турбулентность	Atmospheric turbulence
Atmosfer qatlarının dövr etməsi	Атмосферная циркуляция	Atmospheric circulation
Atmosferin həyəcanlanması	Атмосферное возмущение	Atmospheric disturbance
Atmosfer təzyiqi	Атмосферное давление	Atmospheric pressure, barometric pressure
Atmosferin şüalanması	Атмосферное излучение	Atmospheric radiation
Atmosferin şüa udması	Атмосферное поглощение	Atmospheric absorption
Atmosferin işıqlanması	Атмосферное свечение	Airglow
Atmosfer elektriki	Атмосферное электричество	Atmospheric electricity
Atmosfer dalğaları	Атмосферные волны	Atmospheric waves
Atmosfer ionları	Атмосферные ионы	Atmospheric ions
Atmosfer rəqsləri	Атмосферные колебания	Atmospheric oscillation
Atmosfer çöküntüləri	Атмосферные осадки	Precipitation
Atmosfer maneələri	Атмосферные помехи	Atmospheric disturbance
Atmosfer qabarmaları	Атмосферные приливы	Atmospheric tides
Atmosfer aşqarları	Атмосферные примеси	Atmospheric impurities
Atmosfer şəraiti	Атмосферные условия	Atmospheric conditions
Atmosfer hadisələri	Атмосферные явления	Atmospheric phenomena
Atmosfer güclü yağışı	Атмосферный ливень	Air shower
Atmosfer ozonu	Атмосферный озон	Atmospheric ozon
Atmosfer boşalması	Атмосферный разряд	Atmospheric discharge
Atmosfer sütunu	Атмосферный столб	Air column
Atmosfer səs-küyü	Атмосферный шум	Atmospheric noic
Atmosfer elementi	Атмосферный элемент	Atmophile element
Kottrell atmosferləri	Атмосферы Коттрелла	Cottrell atmospheres
Atom	Атом	Atom
Atomar hidrogen	Атомарный водород	Atomic hydrogen
Burulğanlı atom	Атом вихревой	Eddy atom
Tətbiq edilən atom	Атом внедрения	Interstitial atom
Hidrogenə bənzər atom	Атом водородоподобный	Hydrogen-like atom
Həyəcanlanmış atom	Атом возбужденный	Exited atom
Diamaqnit atom	Атом диамагнитный	Diamagnetic atom
Əvəzedici atom	Атом замещения	1) Atom of substitution 2) Atom of replacement
İonlaşmış atom	Атом ионизированный	Ionization atom
Neytral atom	Атом нейтральный	Neutral atom
Paramaqnit atom	Атом парамагнитный	Paramagnetic atom

Radioaktiv atom	Атом радиоактивный	Radioactive atom
Atomizm	Атомизм	Atomism
Atomistika	Атомистика	Atomistics
Atomistik quruluş	Атомистическое строение	Atomic structure
Atom batareyası	Атомная батарея	Atomic battery
Atom bombası	Атомная бомба	Atomic bomb
Atom dispersiyası	Атомная дисперсия	Atomic dispersion
Atom hissəsi	Атомная доля	Atomic fraction
Atom vahidi	Атомная единица	Atomic unit
Kütlənin atom vahidi	Атомная единица массы	Atomic mass unit
Atom maqnit nüfuzluğu	Атомная магнитная восприимчивость	Atomic magnetic susceptibility
Atom kütləsi	Атомная масса	Atomic weight
Fiziki şkalada atom kütləsi	Атомная масса по физической шкале	Physical atomic weight
Kimyəvi şkalada atom kütləsi	Атомная масса по химической шкале	Chemical atomic weight
Tezliyin atom kütləsi	Атомная масса частоты	Atomic mass frequency
Atom modeli	Атомная модель	Atomic model
Atom orbiti	Атомная орбита	Atomic orbit
Atom orbitalı	Атомная орбиталь	Atomic orbital
Atom müstəvisi	Атомная плоскость	Atomic plane
Atom polyarizasiyası	Атомная поляризация	Atomic polarization
Atom refraksiyası	Атомная рефракция	Atomic refraction
Atom qəfəsi	Атомная решетка	Atomic lattice
Atom spektral xətti	Атомная спектральная линия	Atomic spectral line
Atom nəzəriyyəsi	Атомная теория	Atomic theory
Atom istilik tutumu	Атомная теплоемкость	Atomic heat
Sabit təzyiqdə atom istilik tutumu	Атомная теплоемкость при постоянном давлении	Atomic heat at constant pressure
Sabit həcmdə atom istilik tutumu	Атомная теплоемкость при постоянном объеме	Atomic heat at constant volume
Atom tormozlama qabiliyyəti	Атомная тормозная способность	Atomic stopping power
Atom fizikası	Атомная физика	Atomic physics
Atom energetikası	Атомная энергетика	Atomic power engineering
Atom enerjisi	Атомная энергия	Atomic energy
Atom-absorbsiya spektrofotometriyası	Атомно-абсорбционная спектрофотометрия	Atomic absorption spectrophotometry
Atom-absorbsiya spektral analiz	Атомно-абсорбционный спектральный анализ	Atomic absorption spectral analysis
Atom-absorbsiya spektrofotometr	Атомно-абсорбционный спектрофотометр	Atomic absorption spectrophotometer
Atom fırlanması	Атомное вращение	Atomic rotation
Atom vaxtı	Атомное время	Atomic time
Atom kəsiyi	Атомное сечение	Atomic cross-section
Atomun halı	Атомное состояние	Atomic state
Atom nüvəsi	Атомное ядро	Atomic nucleus
Atom polyarlaşma əmsalı	Атомной коэффициент поляризации	Atomic polarization coefficient
Atom polyarlaşma tenzoru	Атомной тензор поляризации	Atomic polarization tensor
Atom modelləri	Атомные модели	Atomic models
Atom saatı	Атомные часы	Atomic clock
Atom çəkisi	Атомный вес	Atomic weight
Atom generatoru	Атомный генератор	Atomic generator
Atom mühərriki	Атомный двигатель	Atomic energy engine
Atom dipolu	Атомный диполь	Atomic dipole
Atom yükü	Атомный заряд	Atomic charge
Atom udulma əmsalı	Атомный коэффициент поглощения	Atomic absorption coefficient
Atom kristalı	Атомный кристалл	Atomic crystal
Atom şüası	Атомный луч	Atomic ray
Atom nömrəsi	Атомный номер	Atomic number
Atom həcmi	Атомный объем	Atomic volume
Atom qalığı	Атомный остаток	Atomic remainder
Atom faizi	Атомный процент	Atomic percent
Atom dəstəsi	Атомный пучок	Atomic beam
Atom radiusu	Атомный радиус	Atomic radius
Atom reaktoru	Атомный реактор	Atomic reactor

Atom təbəqəsi	Атомный слой	Atomic layer
Atom spektri	Атомный спектр	Atomic spectrum
Atom faktoru	Атомный фактор	Atomic factor
Səpilmənin atom faktoru	Атомный фактор рассеяния	Atomic scattering factor
İtələmə atomu	Атом отдачи	Recoil atom
Qəfəs atomu	Атом решетки	Lattice atom
Attenyuator	Аттенюатор	Attenuator
Audioqram	Аудиограмма	Audiogram
Audimetr	Аудиометр	Audiometer
Auksoxrom	Ауксохром	Auxochrome
Austenizləmə	Аустенизация	Austenitizing
Austenit	Аустенит	Austenite
Austenit quruluşu	Аустенитная структура	Austenitic structure
Austenit toxumu	Аустенитное зерно	Austenitic grain
Austin düsturu	Аустина формула	Austina formula
Autooksidləşdirmə	Аутооксидация	Autoxidation
Afeliy	Афелий	Aphelion
Afokal sistem	Афокальная система	Afocal system
Afin cəbri qrupu	Аффинная алгебраическая группа	Affine algebraic group
Afin həndəsəsi	Аффинная геометрия	Affine geometry
Afin differensial həndəsəsi	Аффинная дифференциальная геометрия	Affine differential geometry
Afin əyriliyi	Аффинная кривизна	Affine curvature
Afin rabitəliyi	Аффинная связность	Affine connection
Afin inikası (əks etməsi)	Аффинное отображение	Affine mapping
Afin çevrilməsi	Аффинное преобразование	Affine transformation
Afin fəzası	Аффинное пространство	Affine space
Afin-konqruent	Аффинно-конгруэнтный	Affinely congruent
Afin koordinatları	Аффинные координаты	Affine coordinates
Afinor	Аффинор	Affinor
Axromaziya	Ахромазия	Achromasia
Axromat	Ахромат	Achromat
Axromatizm	Ахроматизм	Achromatism
Axromatik linza	Ахроматическая линза	Achromatic lens
Axromatik prizma	Ахроматическая призма	Achromatic prism
Axromatik rəng	Ахроматический цвет	Achromatic color
Asetilen-oksigen alovu	Ацетилено-кислородное пламя	Oxyacetylene flame
Aseton	Ацетон	Acetone
Asidimetriya	Ацидиметрия	Acidimetry
Asiklik	Ациклический	Acyclic
Asiklik birləşmə	Ациклическое соединение	Acyclic compound
Aerasiya	Аэрация	1) Aeration 2) Aerification
Aerogel	Аэрогель	Aerogel
Aeroqrafiya	Аэрография	Aerography
Aeroqram	Аэрограмма	Aerogram
Aeroqraf	Аэрограф	Aerograph
Aerodinamika	Аэродинамика	Aerodynamics
Seyrəldilmiş qazların aerodinamikası	Аэродинамика разряженных газов	Rarefied gas dynamics
Səs sürətindən böyük sürətlərin aerodinamikası	Аэродинамика сверхзвуковых скоростей	Supersonic aerodynamics
Aerodinamik interferensiya	Аэродинамическая интерференция	Aerodynamic interference
Aerodinamik burma	Аэродинамическая крутка	Aerodynamic twist
Aerodinamik qüvvə	Аэродинамическая сила	Aerodynamic force
Aerodinamik boru	Аэродинамическая труба	Wind tunnel
Böyük sürətli aerodinamik boru	Аэродинамическая труба больших скоростей	High speed wind tunnel
Qapalı növlü aerodinamik boru	Аэродинамическая труба замкнутого типа	Closed-circuit wind tunnel
Qısa müddətli işləyən aerodinamik boru	Аэродинамическая труба кратковременного действия	Intermittent wind tunnel
Kiçik sıxlıqlı aerodinamik boru	Аэродинамическая труба малой плот-	Low-density wind tunnel

	ности	
Kiçik sürətlərə hesablanmış aerodinamik boru	Аэродинамическая труба малых скоростей	Low-speed wind tunnel
dəyişən sıxlıqlı aerodinamik boru	Аэродинамическая труба переменной плотности	Variable-density wind tunnel
Açıq növlü aerodinamik boru	Аэродинамическая труба разомкнутого типа	Open-circuit wind tunnel
Qapalı işçi hissəli aerodinamik boru	Аэродинамическая труба с закрытой рабочей частью	Closed-jet wind tunnel
Açıq işçi hissəli aerodinamik boru	Аэродинамическая труба с открытой рабочей частью	Open-jet wind tunnel
Aerodinamik xarakteristika	Аэродинамическая характеристика	Aerodynamic characteristics
Aerodinamik tərəzi	Аэродинамические весы	Aerodynamic balance
Aerodinamik qızma	Аэродинамический нагрев	Aerodynamic hearting
Aerodinamik iz	Аэродинамический след	Aerodynamic wake
Aerodinamik fokus	Аэродинамический фокус	Aerodynamic center
Aerodinamik keyfiyyət	Аэродинамическое качество	Lift-drag ratio
Aerodinamik müqavimət	Аэродинамическое сопротивление	Aerodynamic resistance
Aerozol	Аэрозоль	Aerosol
Aerolit	Аэролит	Aerolite
Aerologik xəritə	Аэрологическая карта	Upper-air chart
Aerologik observatoriya	Аэрологическая обсерватория	Aerological observatory
Aerologik analiz (təhlil)	Аэрологический анализ	Upper-air analysis
Aerologiya	Аэрология	Aerology
Aeromaqnitometr	Аэромагнитометр	Airborne magnetometer
Aeromexanika	Аэромеханика	Aeromechanics
Aeronavt	Аэронавт	Aeronaut
Aeronavtika	Аэронавтика	Aeronautics
Aeronomiya	Аэрономия	Aeronomy
Aeroplan, təyyarə	Аэроплан	Airplane
Aeroşəkil	Аэроснимок	Aerial photography
Aerostat	Аэростат	Ballon
Aerostatika	Аэростатика	Aerostatics
Aerostatik qüvvə	Аэростатическая сила	Aerostatic force
Aeromühit	Аэросфера	Aerosphere
Aerotermoelastiklik	Аэротермоупругость	Aerothermoelasticity
Aerofotoqrametriya	Аэрофотограметрия	Aerophotogrametry
Aeroelastiklik	Аэроупругость	Aeroelasticity

Measuring apparatus	Ölçü aparatı	Аппарат измеритель
Cinema apparatus	Kinomatoqraf aparatı	Аппарат кинематографический
Film projection apparatus	Kinoproyeksiya aparatı	Аппарат кинопроекционный
Compensated apparatus	Kompensasiya aparatı	Аппарат компенсационный
Morze's apparatus	Morze aparatı	Аппарат Морзе
Optical apparatus	Optik aparat	Аппарат оптический
Device-sender	Göndərici aparat	Аппарат отправитель
Portable apparatus	Köçürücü aparat	Аппарат переносный
Polarizing apparatus	Polyarlaşma aparatı	Аппарат поляризационный
Receiving apparatus	Qəbuledici aparat	Аппарат приемный
Projection apparatus	Proyeksiya aparatı	Аппарат проекционный
Radio-telegraph apparatus	Radio teleqraf aparatı	Аппарат радио телеграфный
Regulating apparatus	Tənzimedici aparat	Аппарат регулирующий
X-ray apparatus	Rentgen aparatı	Аппарат рентгеновский
Rotation apparatus	Rotasiya aparatı	Аппарат ротационный
Autographic apparatus	Özüyazan aparat	Аппарат самопишущий
Simplex apparatus	Simpleks aparatı	Аппарат симплексный
Hear apparatus	Eşitmə aparatı	Аппарат слуховой
Thermal apparatus	İstilik aparatı	Аппарат тепловой
Off-state current apparatus	Cərəyanı kəsən aparat	Аппарат отключения тока
Preccise apparatus	Dəqiq aparat	Аппарат точный
Drawn apparatus	Cızan aparat	Аппарат чертящий
Yuz's apparatus	Yuz aparatı	Аппарат Юза
Approximate derivative	Aproksimatik törəmə	Аппроксимативная производная
Apriori probability	Apriori ehtimal	Априорная вероятность
Aprotic solvent	Aproton məhlul	Апротонный растворитель
Apse	Apsid	Апсида
Line of apsides	Apsid xətti	Апсидная линия
Arago-Frenel experiment	Araqo-Frenel təcrübəsi	Араго-Френеля опыт
Arago effect	Araqo hadisəsi	Араго явление
Argentometry	Argentometriya	Аргентометрия
Argon	Arqon	Аргон
Argon glow lamp	Arqon lampası	Аргоновая лампа
Argon-ion laser	Arqon ion lazeri	Аргоновый ионный лазер
Argon laser	Arqon lazeri	Аргоновый лазер
Argon tube	Arqon borucuğu	Аргонная трубка
Argument	Kompleks ədədin arqumenti	Аргумент комплексного числа
Argument of perihelion	Perimərkəzin arqumenti	Аргумент перицентра
Argument of latitude	En dairəsinin arqumenti	Аргумент широты
Ardometer	Ardometr	Ардометр
Areometer	Areometr	Ареометр
Percentage areometer	Faiz areometri	Ареометр процентный
Areopycnometer	Areopiknometr	Ареопикнометр
Arid zone	Arid zonası	Аридная зона
Arithmetization	Arifmetikləşmə	Арифметизация
Arithmetic	Arifmetika	Арифметика
Arithmetic instruction	Arifmetik komanda	Арифметическая команда
Floating-point arithmetic	Üzən (gəzən) vergül ilə arifmetik əməliyyat	Арифметическая операция с плавающей запятой
Fixed-point arithmetic	Fiksə olunmuş vergül ilə arifmetik əməliyyat	Арифметическая операция с фиксированной запятой
Arithmetic subgroup	Arifmetik alt qrup	Арифметическая подгруппа
Arithmetical progression	Arifmetik proqres	Арифметическая прогрессия
Arithmetic progression of higher order	Yüksək tərtibli arifmetik proqres	Арифметическая прогрессия высшего порядка
Arithmetic sum	Arifmetik cəm	Арифметическая сумма
Arithmetic unit	Arifmetik blok	Арифметический блок
Arithmetic operator	Arifmetik operator	Арифметический оператор
Arithmetic series	Arifmetik sıra	Арифметический ряд
Arithmetic shift	Arifmetik dəyişmə	Арифметический сдвиг
Arithmetic triangle	Arifmetik üçbucaq	Арифметический треугольник
Arithmetic expression	Arifmetik ifadə	Арифметическое выражение
Arithmetic operation	Arifmetik əməliyyat	Арифметическое действие

Arithmetic mean	Arifmetik orta	Арифметическое среднее
Arithmetic device	Arifmetik quruluş	Арифметическое устройство
1) Adding machine 2) Arithmometer 3) Calculator 4) Desk calculating machine	Arifmometr	Арифмометр
Arc cosine	Arkkosinus	Арккосинус
Arc cotangent	Arkkotangens	Арккотангенс
Arc sine	Arksinus	Арксинус
Arc tangent	Arktangens	Арктангенс
Arctic front	Arktika cəbhəsi	Арктический фронт
1) Accessories 2) Armature	Armatura	Арматура
Armillary sphere	Armilyar dairə (mühit)	Армиллярная сфера
Armco-iron	Armko-dəmir	Армко-железо
Aromatic compound	Aromatik birləşmələr	Ароматические соединения
Arrhenius's theory	Arrenius nəzəriyyəsi	Аррениуса теория
1) Arrester 2) Arresting lever 3) Caging device 4) Catch 5) Stop	Arretir	Арретир
1) Cage 2) Rate-cage	Arretirləmək	Арретировать
Articulating ability	Artikullaşdırma qabiliyyəti	Артикулирующая способность
Articulation	Artikulyasiya	Артикуляция
Archimedes' principle	Arximed qanunu	Архимеда закон
Buoyancy	Arximed qüvvəsi	Архимедова сила
Archimedes screw	Arximed vinti	Архимедов винт
Asbestos	Asbest	Асбест
Asymmetrical molecule	Asimmetrik molekul	Ассимметрическая молекула
Asymmetrical atom	Asimmetrik atom	Асимметрический атом
Asymmetrical analysis	Asimmetrik təhlil	Асимметрический анализ
Asymmetric synthesis	Asimmetrik sintez	Асимметрический синтез
Asymmetrical wave	Asimmetrik dalğa	Асимметричная волна
Asymmetrical curve	Asimmetrik əyri	Асимметричная кривая
Asymmetric distribution	Asimmetrik paylanma	Асимметричное распределение
Asymmetric vibration	Asimmetrik rəqslər	Асимметричные колебания
Asymmetrical top	Asimmetrik fırfıra	Асимметричный волчок
Asymmetric rotator	Asimmetrik rotator	Асимметричный ротатор
Asymmetry	Asimmetriya	Асимметрия
East-West asymmetry	Şərq-Qərb asimmetriyası	Асимметрия восточно-западная
North-South asymmetry	Şimal-Cənub asimmetriyası	Асимметрия северо-южная
Asymptote	Asimptota	Асимптота
Asymptotic convergence	Asimptotik yığılma (sıranın)	Асимптотическая сходимость
Asymptotic cone	Asimptotik konus	Асимптотический конус
Asymptotic path	Asimptotik yol	Асимптотический путь
Asymptotic series	Asimptotik sıra	Асимптотический ряд
Asymptotically stable	Asimptotik dayanıqlı	Асимптотически устойчивый
Asymptotic expression	Asimptotik ifadə	Асимптотическое выражение
Asymptotic value	Asimptotik qiymət	Асимптотическое значение
Asymptotic direction	Asimptotik istiqamət	Асимптотическое направление
Asymptotic expansion	Asimptotik sıraya ayırma	Асимптотическое разложение
Asymptotic solution	Asimptotik həll	Асимптотическое решение
Asynchronous computer	Asinxron hesablama maşını	Асинхронная вычислительная машина
Asynchronous machine	Asinxron maşın	Асинхронная машина
Asynchronous processing	1) Asinxron işləmə 2) Təkmilləşdirmə	Асинхронная обработка
Asynchronous operation	Asinxron əməliyyat	Асинхронная операция
Asynchronous transmission	Asinxron ötürmə	Асинхронная передача
Asynchronous working	Asinxron iş	Асинхронная работа
Asynchronous system	Asinxron sistem	Асинхронная система
Asynchronous generator	Asinxron generator	Асинхронный генератор

Asynchronous motor	Asinxron mühərrik	Асинхронный двигатель
Asynchronous mode	Asinxron iş qaydası	Асинхронный режим
Aspirator	Aspirator	Аспиратор
Aque aspirator	Su aspiratoru	Аспиратор водный
Double aspirator	Qoşa aspirator	Аспиратор двойной
Aspiration psychrometer	Aspirasion psixrometr	Аспирационный психрометр
Aspiration thermometer	Aspirasion termometr	Аспирационный термометр
Assembler	Assembler	Ассемблер
Assimilation	Assimilyasiya	Ассимиляция
Associative memory	Assosiativ yaddaş	Ассоциативная память
Associative register	Assosiativ qeyd dəftəri	Ассоциативный регистр
Association	Assosiasiya	Ассоциация
Association of ions	İonların assosiasiyası	Ассоциация ионов
Molecular association	Molekulların assosiasiyası	Ассоциация молекул
Asssociated liquid	Assosiasiya olunmuş maye	Ассоциированная жидкость
Asssociated molecule	Assosiasiya olunmuş molekul	Ассоциированная молекула
Magnetic astatizing	Maqnit astaziyalaması	Астазирование магнитное
Astatize	Astaziyalama	Астазировать
Astasia	Astaziya	Астазия
Astatine	Astatin	Астатин
Astatic coil	Astatik maqara	Астатическая катушка
Astatic system of magnets	Astatik maqnitlər sistemi	Астатическая система магнитов
Astatic	Astatik	Астатический
Astatic galvanometer	Astatik qalvanometr	Астатический гальванометр
Astatic magnetometer	Astatik maqnitölçən	Астатический магнитометр
1) Astatic balance 2) Astatic equilibrium	Astatik tarazlıq	Астатическое равновесие
Astatic control	Astatik tənzimləmə	Астатическое регулирование
Asthenosphere	Astenosfera	Астеносфера
Asterism	Asterizm	Астеризм
Planetoid	Asteroid	Астероид
Astigmatism	Asiqmatizm	Астигматизм
Astigmatism of pencil	Dəstə asiqmatizmi	Астигматизм пучка
Astigmation difference	Asiqmatik fərq	Астигматическая разность
Astigmatic pencil of rays	Şüaların asiqmatik dəstəsi	Астигматический пучок лучей
Astrometry	Astrometriya	Астрометрия
Astrophotometry	Astroqraf	Астрограф
Astroid	Astroid	Астроида
Astrology	Astrologiya	Астрология
Astrolabe	Astrolyabiya	Астролябия
Astrolabe with prism	Prizma ilə astrolyabiya	Астролябия с призмой
Astrometry	Astrometriya	Астрометрия
Astronomical longitude	Astronomik uzunluq dairəsi	Астрономическая долгота
Astronomical unit	Astronomik vahid	Астрономическая единица
Astronomical unit of force	Astronomik qüvvə vahidi	Астрономическая единица силы
Astronomical observatory	Astronomik observatoriya	Астрономическая обсерватория
Astronomical refraction	Astronomik refraksiya	Астрономическая рефракция
Astronomical latitude	Astronomik en dairəsi	Астрономическая широта
Astronomical constants	Astronomik sabitlər	Астрономические постоянные
Astronomical twilight	Astronomik alaqaranlıqlar	Астрономические сумерки
Astronomical clock	Astronomik saat	Астрономические часы
Astronomical climate	Astronomik iqlim	Астрономический климат
Astronomical compass	Astronomik kompas	Астрономический компас
Astronomical sign	Astronomik işarə, əlamət	Астрономический символ
Astronomical telescope	Astronomik teleskop	Астрономический телескоп
Astronomical triangle	Astronomik üçbucaq	Астрономический треугольник
Astronomical time	Astronomik vaxt	Астрономическое время
Astronomy	Astronomiya	Астрономия
Astronomical triangle	Astrospektroskopiya	Астроспектроскопия
Astrophysics	Astrofizika	Астрофизика
Astrophysical observatory	Astrofiziki observatoriya	Астрофизическая обсерватория
Astrophotography	Astrofotoqrafiya	Астрофотография
Celestial photometry	Astrofotometriya	Астрофотометрия

Aspherical lens	Asferik linza	Асферическая линза
Aspherical surface	Asferik səth	Асферическая поверхность
Ataxite	Ataksit	Атаксит
Atactic polymer	Ataktik polimer	Атактический полимер
1) Athermal solution 2) Athermic solution	Atermik məhlul	Атермический раствор
Atwood's machine	Atvud maşını	Атвуда машина
1) Spectral atlas 2) Spectral map	Spektral xətlərin atlası	Атлас спектральных линий
Atmolysis	Atmoliz	Атмолиз
Atmosphere	Atmosfer	Атмосфера
Stellar atmosphere	Ulduz atmosferi	Атмосфера звезды
Earth atmosphere	Yerin atmosferi	Атмосфера Земли
Homogeneous atmosphere	Bircins atmosfer	Атмосфера однородная
Atmosphere of equilibrium	Tarazlıq (müvazinət) atmosferi	Атмосфера равновесия
Solar atmosphere	Günəş atmosferi	Атмосфера Солнца
Technical atmosphere	Texniki atmosfer	Атмосфера техническая
Physical atmosphere	Fiziki atmosfer	Атмосфера физическая
Atmospherics	Atmosferlər	Атмосферики
1) Atmospheric acoustics 2) Meteorogical acoustics	Atmosfer akustikası	Атмосферная акустика
Atmospheric diffusion	Atmosfer diffuziyası	Атмосферная диффузия
Atmospheric corrosion	Atmosfer korroziyası	Атмосферная коррозия
1) Atmospheric optics 2) Meteorogical optics	Atmosfer optikası	Атмосферная оптика
Atmosphere refractions	Atmosfer refraksiyası	Атмосферная рефракция
Atmospheric turbulence	Atmosfer turbiletliyi	Атмосферная турбулентность
Atmospheric circulation	Atmosfer qatlarının dövr etməsi	Атмосферная циркуляция
Atmospheric disturbance	Atmosferin həyəcanlanması	Атмосферное возмущение
Atmospheric pressure, barometric pressure	Atmosfer təzyiqi	Атмосферное давление
Atmospheric radiation	Atmosferin şüalanması	Атмосферное излучение
Atmospheric absorption	Atmosferin şüa udması	Атмосферное поглощение
Airglow	Atmosferin işıqlanması	Атмосферное свечение
Atmospheric electricity	Atmosfer elektriki	Атмосферное электричество
Atmospheric waves	Atmosfer dalğaları	Атмосферные волны
Atmospheric ions	Atmosfer ionları	Атмосферные ионы
Atmospheric oscillation	Atmosfer rəqsləri	Атмосферные колебания
Precipitation	Atmosfer çöküntüləri	Атмосферные осадки
Atmospheric disturbance	Atmosfer maneələri	Атмосферные помехи
Atmospheric tides	Atmosfer qabarmaları	Атмосферные приливы
Atmospheric impurities	Atmosfer aşqarları	Атмосферные примеси
Atmospheric conditions	Atmosfer şəraiti	Атмосферные условия
Atmospheric phenomena	Atmosfer hadisələri	Атмосферные явления
Air shower	Atmosfer güclü yağışı	Атмосферный ливень
Atmospheric ozon	Atmosfer ozonu	Атмосферный озон
Atmospheric discharge	Atmosfer boşalması	Атмосферный разряд
Air column	Atmosfer sütunu	Атмосферный столб
Atmospheric noic	Atmosfer səs-küyü	Атмосферный шум
Atmophile element	Atmosfer elementi	Атмосферный элемент
Cottrell atmospheres	Kottrell atmosferləri	Атмосферы Коттрелла
Atom	Atom	Атом
Atomic hydrogen	Atomar hidrogen	Атомарный водород
Eddy atom	Burulğanlı atom	Атом вихревой
Interstitial atom	Tətbiq edilən atom	Атом внедрения
Hydrogen-like atom	Hidrogenə bənzər atom	Атом водородоподобный
Exited atom	Həyəcanlanmış atom	Атом возбужденный
Diamagnetic atom	Diamaqnit atom	Атом диамагнитный
1) Atom of substitution 2) Atom of replacement	Əvəzedici atom	Атом замещения
Ionization atom	İonlaşmış atom	Атом ионизированный
Neutral atom	Neytral atom	Атом нейтральный
Paramagnetic atom	Paramaqnit atom	Атом парамагнитный

Radioactive atom	Radioaktiv atom	Атом радиоактивный
Atomism	Atomizm	Атомизм
Atomistics	Atomistika	Атомистика
Atomic structure	Atomistik quruluş	Атомистическое строение
Atomic battery	Atom batareyası	Атомная батарея
Atomic bomb	Atom bombası	Атомная бомба
Atomic dispersion	Atom dispersiyası	Атомная дисперсия
Atomic fraction	Atom hissəsi	Атомная доля
Atomic unit	Atom vahidi	Атомная единица
Atomic mass unit	Kütlənin atom vahidi	Атомная единица массы
Atomic magnetic susceptibility	Atom maqnit nüfuzluğu	Атомная магнитная восприимчивость
Atomic weight	Atom kütləsi	Атомная масса
Physical atomic weight	Fiziki şkalada atom kütləsi	Атомная масса по физической шкале
Chemical atomic weight	Kimyəvi şkalada atom kütləsi	Атомная масса по химической шкале
Atomic mass frequency	Tezliyin atom kütləsi	Атомная масса частоты
Atomic model	Atom modeli	Атомная модель
Atomic orbit	Atom orbiti	Атомная орбита
Atomic orbital	Atom orbitalı	Атомная орбиталь
Atomic plane	Atom müstəvisi	Атомная плоскость
Atomic polarization	Atom polyarizasiyası	Атомная поляризация
Atomic refraction	Atom refraksiyası	Атомная рефракция
Atomic lattice	Atom qəfəsi	Атомная решетка
Atomic spectral line	Atom spektral xətti	Атомная спектральная линия
Atomic theory	Atom nəzəriyyəsi	Атомная теория
Atomic heat	Atom istilik tutumu	Атомная теплоемкость
Atomic heat at constant pressure	Sabit təzyiqdə atom istilik tutumu	Атомная теплоемкость при постоянном давлении
Atomic heat at constant volume	Sabit həcmdə atom istilik tutumu	Атомная теплоемкость при постоянном объеме
Atomic stopping power	Atom tormozlama qabiliyyəti	Атомная тормозная способность
Atomic physics	Atom fizikası	Атомная физика
Atomic power engineering	Atom energetikası	Атомная энергетика
Atomic energy	Atom enerjisi	Атомная энергия
Atomic absorption spectrophotometry	Atom-absorbsiya spektrofotometriyası	Атомно-абсорбционная спектрофотометрия
Atomic absorption spectral analysis	Atom-absorbsiya spektral analiz	Атомно-абсорбционный спектральный анализ
Atomic absorption spectrophotometer	Atom-absorbsiya spektrofotometr	Атомно-абсорбционный спектрофотометр
Atomic rotation	Atom fırlanması	Атомное вращение
Atomic time	Atom vaxtı	Атомное время
Atomic cross-section	Atom kəsiyi	Атомное сечение
Atomic state	Atomun halı	Атомное состояние
Atomic nucleus	Atom nüvəsi	Атомное ядро
Atomic polarization coefficient	Atom polyarlaşma əmsalı	Атомной коэффициент поляризации
Atomic polarization tensor	Atom polyarlaşma tenzoru	Атомной тензор поляризации
Atomic models	Atom modelləri	Атомные модели
Atomic clock	Atom saatı	Атомные часы
Atomic weight	Atom çəkisi	Атомный вес
Atomic generator	Atom generatoru	Атомный генератор
Atomic energy engine	Atom mühərriki	Атомный двигатель
Atomic dipole	Atom dipolu	Атомный диполь
Atomic charge	Atom yükü	Атомный заряд
Atomic absorption coefficient	Atom udulma əmsalı	Атомный коэффициент поглощения
Atomic crystal	Atom kristalı	Атомный кристалл
Atomic ray	Atom şüası	Атомный луч
Atomic number	Atom nömrəsi	Атомный номер
Atomic volume	Atom həcmi	Атомный объем
Atomic remainder	Atom qalığı	Атомный остаток
Atomic percent	Atom faizi	Атомный процент
Atomic beam	Atom dəstəsi	Атомный пучок
Atomic radius	Atom radiusu	Атомный радиус
Atomic reactor	Atom reaktoru	Атомный реактор

Atomic layer	Atom təbəqəsi	Атомный слой
Atomic spectrum	Atom spektri	Атомный спектр
Atomic factor	Atom faktoru	Атомный фактор
Atomic scattering factor	Səpilmənin atom faktoru	Атомный фактор рассеяния
Recoil atom	İtələmə atomu	Атом отдачи
Lattice atom	Qəfəs atomu	Атом решетки
Attenuator	Attenyuator	Аттенюатор
Audiogram	Audioqram	Аудиограмма
Audiometer	Audimetr	Аудиометр
Auxochrome	Auksoxrom	Ауксохром
Austenitizing	Austenizləmə	Аустенизация
Austenite	Austenit	Аустенит
Austenitic structure	Austenit quruluşu	Аустенитная структура
Austenitic grain	Austenit toxumu	Аустенитное зерно
Austina formula	Austin düsturu	Аустина формула
Autoxidation	Autooksidləşdirmə	Аутооксидация
Aphelion	Afeliy	Афелий
Afocal system	Afokal sistem	Афокальная система
Affine algebraic group	Afin cəbri qrupu	Аффинная алгебраическая группа
Affine geometry	Afin həndəsəsi	Аффинная геометрия
Affine differential geometry	Afin differensial həndəsəsi	Аффинная дифференциальная геометрия
Affine curvature	Afin əyriliyi	Аффинная кривизна
Affine connection	Afin rabitəliyi	Аффинная связность
Affine mapping	Afin inikası (əks etməsi)	Аффинное отображение
Affine transformation	Afin çevrilməsi	Аффинное преобразование
Affine space	Afin fəzası	Аффинное пространство
Affinely congruent	Afin-konqruent	Аффинно-конгруэнтный
Affine coordinates	Afin koordinatları	Аффинные координаты
Affinor	Afinor	Аффинор
Achromasia	Axromaziya	Ахромазия
Achromat	Axromat	Ахромат
Achromatism	Axromatizm	Ахроматизм
Achromatic lens	Axromatik linza	Ахроматическая линза
Achromatic prism	Axromatik prizma	Ахроматическая призма
Achromatic color	Axromatik rəng	Ахроматический цвет
Oxyacetylene flame	Asetilen-oksigen alovu	Ацетилено-кислородное пламя
Acetone	Aseton	Ацетон
Acidimetry	Asidimetriya	Ацидиметрия
Acyclic	Asiklik	Ациклический
Acyclic compound	Asiklik birləşmə	Ациклическое соединение
1) Aeration 2) Aerification	Aerasiya	Аэрация
Aerogel	Aerogel	Аэрогель
Aerography	Aeroqrafiya	Аэрография
Aerogram	Aeroqram	Аэрограмма
Aerograph	Aeroqraf	Аэрограф
Aerodynamics	Aerodinamika	Аэродинамика
Rarefied gas dynamics	Seyrəldilmiş qazların aerodinamikası	Аэродинамика разряженных газов
Supersonic aerodynamics	Səs sürətindən böyük sürətlərin aerodinamikası	Аэродинамика сверхзвуковых скоростей
Aerodynamic interference	Aerodinamik interferensiya	Аэродинамическая интерференция
Aerodynamic twist	Aerodinamik burma	Аэродинамическая крутка
Aerodynamic force	Aerodinamik qüvvə	Аэродинамическая сила
Wind tunnel	Aerodinamik boru	Аэродинамическая труба
High speed wind tunnel	Böyük sürətli aerodinamik boru	Аэродинамическая труба больших скоростей
Closed-circuit wind tunnel	Qapalı növlü aerodinamik boru	Аэродинамическая труба замкнутого типа
Intermittent wind tunnel	Qısa müddətli işləyən aerodinamik boru	Аэродинамическая труба кратковременного действия
Low-density wind tunnel	Kiçik sıxlıqlı aerodinamik boru	Аэродинамическая труба малой плот-

		ности
Low-speed wind tunnel	Kiçik sürətlərə hesablanmış aerodinamik boru	Аэродинамическая труба малых скоростей
Variable-density wind tunnel	dəyişən sıxlıqlı aerodinamik boru	Аэродинамическая труба переменной плотности
Open-circuit wind tunnel	Açıq növlü aerodinamik boru	Аэродинамическая труба разомкнутого типа
Closed-jet wind tunnel	Qapalı işçi hissəli aerodinamik boru	Аэродинамическая труба с закрытой рабочей частью
Open-jet wind tunnel	Açıq işçi hissəli aerodinamik boru	Аэродинамическая труба с открытой рабочей частью
Aerodynamic characteristics	Aerodinamik xarakteristika	Аэродинамическая характеристика
Aerodynamic balance	Aerodinamik tərəzi	Аэродинамические весы
Aerodynamic hearting	Aerodinamik qızma	Аэродинамический нагрев
Aerodynamic wake	Aerodinamik iz	Аэродинамический след
Aerodynamic center	Aerodinamik fokus	Аэродинамический фокус
Lift-drag ratio	Aerodinamik keyfiyyət	Аэродинамическое качество
Aerodynamic resistance	Aerodinamik müqavimət	Аэродинамическое сопротивление
Aerosol	Aerozol	Аэрозоль
Aerolite	Aerolit	Аэролит
Upper-air chart	Aerologik xəritə	Аэрологическая карта
Aerological observatory	Aerologik observatoriya	Аэрологическая обсерватория
Upper-air analysis	Aerologik analiz (təhlil)	Аэрологический анализ
Aerology	Aerologiya	Аэрология
Airborne magnetometer	Aeromaqnitometr	Аэромагнитометр
Aeromechanics	Aeromexanika	Аэромеханика
Aeronaut	Aeronavt	Аэронавт
Aeronautics	Aeronavtika	Аэронавтика
Aeronomy	Aeronomiya	Аэрономия
Airplane	Aeroplan, təyyarə	Аэроплан
Aerial photography	Aeroşəkil	Аэроснимок
Ballon	Aerostat	Аэростат
Aerostatics	Aerostatika	Аэростатика
Aerostatic force	Aerostatik qüvvə	Аэростатическая сила
Aerosphere	Aeromühit	Аэросфера
Aerothermoelasticity	Aerotermoelastiklik	Аэротермоупругость
Aerophotogrametry	Aerofotoqrametriya	Аэрофотограметрия
Aeroelasticity	Aeroelastiklik	Аэроупругость

Аппарат измеритель	Measuring apparatus	Ölçü aparatı
Аппарат кинематографический	Cinema apparatus	Kinomatoqraf aparatı
Аппарат кинопроекционный	Film projection apparatus	Kinoproyeksiya aparatı
Аппарат компенсационный	Compensated apparatus	Kompensasiya aparatı
Аппарат Морзе	Morze's apparatus	Morze aparatı
Аппарат оптический	Optical apparatus	Optik aparat
Аппарат отправитель	Device-sender	Göndərici aparat
Аппарат переносный	Portable apparatus	Köçürücü aparat
Аппарат поляризационный	Polarizing apparatus	Polyarlaşma aparatı
Аппарат приемный	Receiving apparatus	Qəbuledici aparat
Аппарат проекционный	Projection apparatus	Proyeksiya aparatı
Аппарат радио телеграфный	Radio-telegraph apparatus	Radio teleqraf aparatı
Аппарат регулирующий	Regulating apparatus	Tənzimedici aparat
Аппарат рентгеновский	X-ray apparatus	Rentgen aparatı
Аппарат ротационный	Rotation apparatus	Rotasiya aparatı
Аппарат самопишущий	Autographic apparatus	Özüyazan aparat
Аппарат симплексный	Simplex apparatus	Simpleks aparatı
Аппарат слуховой	Hear apparatus	Eşitmə aparatı
Аппарат тепловой	Thermal apparatus	İstilik aparatı
Аппарат отключения тока	Off-state current apparatus	Cərəyanı kəsən aparat
Аппарат точный	Preccise apparatus	Dəqiq aparat
Аппарат чертящий	Drawn apparatus	Cızan aparat
Аппарат Юза	Yuz's apparatus	Yuz aparatı
Аппроксимативная производная	Approximate derivative	Aproksimatik törəmə
Априорная вероятность	Apriori probability	Apriori ehtimal
Апротонный растворитель	Aprotic solvent	Aproton məhlul
Апсида	Apse	Apsid
Апсидная линия	Line of apsides	Apsid xətti
Араго-Френеля опыт	Arago-Frenel experiment	Araqo-Frenel təcrübəsi
Араго явление	Arago effect	Araqo hadisəsi
Аргентометрия	Argentometry	Argentometriya
Аргон	Argon	Arqon
Аргоновая лампа	Argon glow lamp	Arqon lampası
Аргоновый ионный лазер	Argon-ion laser	Arqon ion lazeri
Аргоновый лазер	Argon laser	Arqon lazeri
Аргонная трубка	Argon tube	Arqon borucuğu
Аргумент комплексного числа	Argument	Kompleks ədədin arqumenti
Аргумент перицентра	Argument of perihelion	Perimərkəzin arqumenti
Аргумент широты	Argument of latitude	En dairəsinin arqumenti
Ардометр	Ardometer	Ardometr
Ареометр	Areometer	Areometr
Ареометр процентный	Percentage areometer	Faiz areometri
Ареопикнометр	Areopycnometer	Areopiknometr
Аридная зона	Arid zone	Arid zonası
Арифметизация	Arithmetization	Arifmetikləşmə
Арифметика	Arithmetic	Arifmetika
Арифметическая команда	Arithmetic instruction	Arifmetik komanda
Арифметическая операция с плавающей запятой	Floating-point arithmetic	Üzən (gəzən) vergül ilə arifmetik əməliyyat
Арифметическая операция с фиксированной запятой	Fixed-point arithmetic	Fiksə olunmuş vergül ilə arifmetik əməliyyat
Арифметическая подгруппа	Arithmetic subgroup	Arifmetik alt qrup
Арифметическая прогрессия	Arithmetical progression	Arifmetik proqres
Арифметическая прогрессия высшего порядка	Arithmetic progression of higher order	Yüksək tərtibli arifmetik proqres
Арифметическая сумма	Arithmetic sum	Arifmetik cəm
Арифметический блок	Arithmetic unit	Arifmetik blok
Арифметический оператор	Arithmetic operator	Arifmetik operator
Арифметический ряд	Arithmetic series	Arifmetik sıra
Арифметический сдвиг	Arithmetic shift	Arifmetik dəyişmə
Арифметический треугольник	Arithmetic triangle	Arifmetik üçbucaq
Арифметическое выражение	Arithmetic expression	Arifmetik ifadə
Арифметическое действие	Arithmetic operation	Arifmetik əməliyyat

Арифметическое среднее	Arithmetic mean	Arifmetik orta
Арифметическое устройство	Arithmetic device	Arifmetik quruluş
Арифмометр	1) Adding machine 2) Arithmometer 3) Calculator 4) Desk calculating machine	Arifmometr
Арккосинус	Arc cosine	Arkkosinus
Арккотангенс	Arc cotangent	Arkkotangens
Арксинус	Arc sine	Arksinus
Арктангенс	Arc tangent	Arktangens
Арктический фронт	Arctic front	Arktika cəbhəsi
Арматура	1) Accessories 2) Armature	Armatura
Армиллярная сфера	Armillary sphere	Armilyar dairə (mühit)
Армко-железо	Armco-iron	Armko-dəmir
Ароматические соединения	Aromatic compound	Aromatik birləşmələr
Аррениуса теория	Arrhenius's theory	Arrenius nəzəriyyəsi
Арретир	1) Arrester 2) Arresting lever 3) Caging device 4) Catch 5) Stop	Arretir
Арретировать	1) Cage 2) Rate-cage	Arretirləmək
Артикулирующая способность	Articulating ability	Artikullaşdırma qabiliyyəti
Артикуляция	Articulation	Artikulyasiya
Архимеда закон	Archimedes' principle	Arximed qanunu
Архимедова сила	Buoyancy	Arximed qüvvəsi
Архимедов винт	Archimedes screw	Arximed vinti
Асбест	Asbestos	Asbest
Ассимметрическая молекула	Asymmetrical molecule	Asimmetrik molekul
Асимметрический атом	Asymmetrical atom	Asimmetrik atom
Асимметрический анализ	Asymmetrical analysis	Asimmetrik təhlil
Асимметрический синтез	Asymmetric synthesis	Asimmetrik sintez
Асимметричная волна	Asymmetrical wave	Asimmetrik dalğa
Асимметричная кривая	Asymmetrical curve	Asimmetrik əyri
Асимметричное распределение	Asymmetric distribution	Asimmetrik paylanma
Асимметричные колебания	Asymmetric vibration	Asimmetrik rəqslər
Асимметричный волчок	Asymmetrical top	Asimmetrik fırfıra
Асимметричный ротатор	Asymmetric rotator	Asimmetrik rotator
Асимметрия	Asymmetry	Asimmetriya
Асимметрия восточно-западная	East-West asymmetry	Şərq-Qərb asimmetriyası
Асимметрия северо-южная	North-South asymmetry	Şimal-Cənub asimmetriyası
Асимптота	Asymptote	Asimptota
Асимптотическая сходимость	Asymptotic convergence	Asimptotik yığılma (sıranın)
Асимптотический конус	Asymptotic cone	Asimptotik konus
Асимптотический путь	Asymptotic path	Asimptotik yol
Асимптотический ряд	Asymptotic series	Asimptotik sıra
Асимптотически устойчивый	Asymptotically stable	Asimptotik dayanıqlı
Асимптотическое выражение	Asymptotic expression	Asimptotik ifadə
Асимптотическое значение	Asymptotic value	Asimptotik qiymət
Асимптотическое направление	Asymptotic direction	Asimptotik istiqamət
Асимптотическое разложение	Asymptotic expansion	Asimptotik sıraya ayırma
Асимптотическое решение	Asymptotic solution	Asimptotik həll
Асинхронная вычислительная машина	Asynchronous computer	Asinxron hesablama maşını
Асинхронная машина	Asynchronous machine	Asinxron maşın
Асинхронная обработка	Asynchronous processing	1) Asinxron işləmə 2) Təkmilləşdirmə
Асинхронная операция	Asynchronous operation	Asinxron əməliyyat
Асинхронная передача	Asynchronous transmission	Asinxron ötürmə
Асинхронная работа	Asynchronous working	Asinxron iş
Асинхронная система	Asynchronous system	Asinxron sistem
Асинхронный генератор	Asynchronous generator	Asinxron generator

Асинхронный двигатель	Asynchronous motor	Asinxron mühərrik
Асинхронный режим	Asynchronous mode	Asinxron iş qaydası
Аспиратор	Aspirator	Aspirator
Аспиратор водный	Aque aspirator	Su aspiratoru
Аспиратор двойной	Double aspirator	Qoşa aspirator
Аспирационный психрометр	Aspiration psychrometer	Aspirasion psixrometr
Аспирационный термометр	Aspiration thermometer	Aspirasion termometr
Ассемблер	Assembler	Assembler
Ассимиляция	Assimilation	Assimilyasiya
Ассоциативная память	Associative memory	Assosiativ yaddaş
Ассоциативный регистр	Associative register	Assosiativ qeyd dəftəri
Ассоциация	Association	Assosiasiya
Ассоциация ионов	Association of ions	İonların assosiasiyası
Ассоциация молекул	Molecular association	Molekulların assosiasiyası
Ассоциированная жидкость	Asssociated liquid	Assosiasiya olunmuş maye
Ассоциированная молекула	Asssociated molecule	Assosiasiya olunmuş molekul
Астазирование магнитное	Magnetic astatizing	Maqnit astaziyalaması
Астазировать	Astatize	Astaziyalama
Астазия	Astasia	Astaziya
Астатин	Astatine	Astatin
Астатическая катушка	Astatic coil	Astatik maqara
Астатическая система магнитов	Astatic system of magnets	Astatik maqnitlər sistemi
Астатический	Astatic	Astatik
Астатический гальванометр	Astatic galvanometer	Astatik qalvanometr
Астатический магнитометр	Astatic magnetometer	Astatik maqnitölçən
Астатическое равновесие	1) Astatic balance 2) Astatic equilibrium	Astatik tarazlıq
Астатическое регулирование	Astatic control	Astatik tənzimləmə
Астеносфера	Asthenosphere	Astenosfera
Астеризм	Asterism	Asterizm
Астероид	Planetoid	Asteroid
Астигматизм	Astigmatism	Asiqmatizm
Астигматизм пучка	Astigmatism of pencil	Dəstə asiqmatizmi
Астигматическая разность	Astigmation difference	Asiqmatik fərq
Астигматический пучок лучей	Astigmatic pencil of rays	Şüaların asiqmatik dəstəsi
Астрометрия	Astrometry	Astrometriya
Астрограф	Astrophotometry	Astroqraf
Астроида	Astroid	Astroid
Астрология	Astrology	Astrologiya
Астролябия	Astrolabe	Astrolyabiya
Астролябия с призмой	Astrolabe with prism	Prizma ilə astrolyabiya
Астрометрия	Astrometry	Astrometriya
Астрономическая долгота	Astronomical longitude	Astronomik uzunluq dairəsi
Астрономическая единица	Astronomical unit	Astronomik vahid
Астрономическая единица силы	Astronomical unit of force	Astronomik qüvvə vahidi
Астрономическая обсерватория	Astronomical observatory	Astronomik observatoriya
Астрономическая рефракция	Astronomical refraction	Astronomik refraksiya
Астрономическая широта	Astronomical latitude	Astronomik en dairəsi
Астрономические постоянные	Astronomical constants	Astronomik sabitlər
Астрономические сумерки	Astronomical twilight	Astronomik alaqaranlıqlar
Астрономические часы	Astronomical clock	Astronomik saat
Астрономический климат	Astronomical climate	Astronomik iqlim
Астрономический компас	Astronomical compass	Astronomik kompas
Астрономический символ	Astronomical sign	Astronomik işarə, əlamət
Астрономический телескоп	Astronomical telescope	Astronomik teleskop
Астрономический треугольник	Astronomical triangle	Astronomik üçbucaq
Астрономическое время	Astronomical time	Astronomik vaxt
Астрономия	Astronomy	Astronomiya
Астроспектроскопия	Astronomical triangle	Astrospektroskopiya
Астрофизика	Astrophysics	Astrofizika
Астрофизическая обсерватория	Astrophysical observatory	Astrofiziki observatoriya
Астрофотография	Astrophotography	Astrofotoqrafiya
Астрофотометрия	Celestial photometry	Astrofotometriya

Асферическая линза	Aspherical lens	Asferik linza
Асферическая поверхность	Aspherical surface	Asferik səth
Атаксит	Ataxite	Ataksit
Атактический полимер	Atactic polymer	Ataktik polimer
Атермический раствор	1) Athermal solution 2) Athermic solution	Atermik məhlul
Атвуда машина	Atwood's machine	Atvud maşını
Атлас спектральных линий	1) Spectral atlas 2) Spectral map	Spektral xətlərin atlası
Атмолиз	Atmolysis	Atmoliz
Атмосфера	Atmosphere	Atmosfer
Атмосфера звезды	Stellar atmosphere	Ulduz atmosferi
Атмосфера Земли	Earth atmosphere	Yerin atmosferi
Атмосфера однородная	Homogeneous atmosphere	Bircins atmosfer
Атмосфера равновесия	Atmosphere of equilibrium	Tarazlıq (müvazinət) atmosferi
Атмосфера Солнца	Solar atmosphere	Günəş atmosferi
Атмосфера техническая	Technical atmosphere	Texniki atmosfer
Атмосфера физическая	Physical atmosphere	Fiziki atmosfer
Атмосферики	Atmospherics	Atmosferlər
Атмосферная акустика	1) Atmospheric acoustics 2) Meteorogical acoustics	Atmosfer akustikası
Атмосферная диффузия	Atmospheric diffusion	Atmosfer diffuziyası
Атмосферная коррозия	Atmospheric corrosion	Atmosfer korroziyası
Атмосферная оптика	1) Atmospheric optics 2) Meteorogical optics	Atmosfer optikası
Атмосферная рефракция	Atmosphere refractions	Atmosfer refraksiyası
Атмосферная турбулентность	Atmospheric turbulence	Atmosfer turbiletliyi
Атмосферная циркуляция	Atmospheric circulation	Atmosfer qatlarının dövr etməsi
Атмосферное возмущение	Atmospheric disturbance	Atmosferin həyəcanlanması
Атмосферное давление	Atmospheric pressure, barometric pressure	Atmosfer təzyiqi
Атмосферное излучение	Atmospheric radiation	Atmosferin şüalanması
Атмосферное поглощение	Atmospheric absorption	Atmosferin şüa udması
Атмосферное свечение	Airglow	Atmosferin işıqlanması
Атмосферное электричество	Atmospheric electricity	Atmosfer elektriki
Атмосферные волны	Atmospheric waves	Atmosfer dalğaları
Атмосферные ионы	Atmospheric ions	Atmosfer ionları
Атмосферные колебания	Atmospheric oscillation	Atmosfer rəqsləri
Атмосферные осадки	Precipitation	Atmosfer çöküntüləri
Атмосферные помехи	Atmospheric disturbance	Atmosfer maneələri
Атмосферные приливы	Atmospheric tides	Atmosfer qabarmaları
Атмосферные примеси	Atmospheric impurities	Atmosfer aşqarları
Атмосферные условия	Atmospheric conditions	Atmosfer şəraiti
Атмосферные явления	Atmospheric phenomena	Atmosfer hadisələri
Атмосферный ливень	Air shower	Atmosfer güclü yağışı
Атмосферный озон	Atmospheric ozon	Atmosfer ozonu
Атмосферный разряд	Atmospheric discharge	Atmosfer boşalması
Атмосферный столб	Air column	Atmosfer sütunu
Атмосферный шум	Atmospheric noic	Atmosfer səs-küyü
Атмосферный элемент	Atmophile element	Atmosfer elementi
Атмосферы Коттрелла	Cottrell atmospheres	Kottrell atmosferləri
Атом	Atom	Atom
Атомарный водород	Atomic hydrogen	Atomar hidrogen
Атом вихревой	Eddy atom	Burulğanlı atom
Атом внедрения	Interstitial atom	Tətbiq edilən atom
Атом водородоподобный	Hydrogen-like atom	Hidrogenə bənzər atom
Атом возбужденный	Exited atom	Həyəcanlanmış atom
Атом диамагнитный	Diamagnetic atom	Diamaqnit atom
Атом замещения	1) Atom of substitution 2) Atom of replacement	Əvəzedici atom
Атом ионизированный	Ionization atom	İonlaşmış atom
Атом нейтральный	Neutral atom	Neytral atom
Атом парамагнитный	Paramagnetic atom	Paramaqnit atom

Атом радиоактивный	Radioactive atom	Radioaktiv atom
Атомизм	Atomism	Atomizm
Атомистика	Atomistics	Atomistika
Атомистическое строение	Atomic structure	Atomistik quruluş
Атомная батарея	Atomic battery	Atom batareyası
Атомная бомба	Atomic bomb	Atom bombası
Атомная дисперсия	Atomic dispersion	Atom dispersiyası
Атомная доля	Atomic fraction	Atom hissəsi
Атомная единица	Atomic unit	Atom vahidi
Атомная единица массы	Atomic mass unit	Kütlənin atom vahidi
Атомная магнитная восприимчивость	Atomic magnetic susceptibility	Atom maqnit nüfuzluğu
Атомная масса	Atomic weight	Atom kütləsi
Атомная масса по физической шкале	Physical atomic weight	Fiziki şkalada atom kütləsi
Атомная масса по химической шкале	Chemical atomic weight	Kimyəvi şkalada atom kütləsi
Атомная масса частоты	Atomic mass frequency	Tezliyin atom kütləsi
Атомная модель	Atomic model	Atom modeli
Атомная орбита	Atomic orbit	Atom orbiti
Атомная орбиталь	Atomic orbital	Atom orbitalı
Атомная плоскость	Atomic plane	Atom müstəvisi
Атомная поляризация	Atomic polarization	Atom polyarizasiyası
Атомная рефракция	Atomic refraction	Atom refraksiyası
Атомная решетка	Atomic lattice	Atom qəfəsi
Атомная спектральная линия	Atomic spectral line	Atom spektral xətti
Атомная теория	Atomic theory	Atom nəzəriyyəsi
Атомная теплоемкость	Atomic heat	Atom istilik tutumu
Атомная теплоемкость при постоянном давлении	Atomic heat at constant pressure	Sabit təzyiqdə atom istilik tutumu
Атомная теплоемкость при постоянном объеме	Atomic heat at constant volume	Sabit həcmdə atom istilik tutumu
Атомная тормозная способность	Atomic stopping power	Atom tormozlama qabiliyyəti
Атомная физика	Atomic physics	Atom fizikası
Атомная энергетика	Atomic power engineering	Atom energetikası
Атомная энергия	Atomic energy	Atom enerjisi
Атомно-абсорбционная спектрофотометрия	Atomic absorption spectrophotometry	Atom-absorbsiya spektrofotometriyası
Атомно-абсорбционный спектральный анализ	Atomic absorption spectral analysis	Atom-absorbsiya spektral analiz
Атомно-абсорбционный спектрофотометр	Atomic absorption spectrophotometer	Atom-absorbsiya spektrofotometr
Атомное вращение	Atomic rotation	Atom fırlanması
Атомное время	Atomic time	Atom vaxtı
Атомное сечение	Atomic cross-section	Atom kəsiyi
Атомное состояние	Atomic state	Atomun halı
Атомное ядро	Atomic nucleus	Atom nüvəsi
Атомной коэффициент поляризации	Atomic polarization coefficient	Atom polyarlaşma əmsalı
Атомной тензор поляризации	Atomic polarization tensor	Atom polyarlaşma tenzoru
Атомные модели	Atomic models	Atom modelləri
Атомные часы	Atomic clock	Atom saatı
Атомный вес	Atomic weight	Atom çəkisi
Атомный генератор	Atomic generator	Atom generatoru
Атомный двигатель	Atomic energy engine	Atom mühərriki
Атомный диполь	Atomic dipole	Atom dipolu
Атомный заряд	Atomic charge	Atom yükü
Атомный коэффициент поглощения	Atomic absorption coefficient	Atom udulma əmsalı
Атомный кристалл	Atomic crystal	Atom kristalı
Атомный луч	Atomic ray	Atom şüası
Атомный номер	Atomic number	Atom nömrəsi
Атомный объем	Atomic volume	Atom həcmi
Атомный остаток	Atomic remainder	Atom qalığı
Атомный процент	Atomic percent	Atom faizi
Атомный пучок	Atomic beam	Atom dəstəsi
Атомный радиус	Atomic radius	Atom radiusu
Атомный реактор	Atomic reactor	Atom reaktoru

Атомный слой	Atomic layer	Atom təbəqəsi
Атомный спектр	Atomic spectrum	Atom spektri
Атомный фактор	Atomic factor	Atom faktoru
Атомный фактор рассеяния	Atomic scattering factor	Səpilmənin atom faktoru
Атом отдачи	Recoil atom	İtələmə atomu
Атом решетки	Lattice atom	Qəfəs atomu
Аттенюатор	Attenuator	Attenyuator
Аудиограмма	Audiogram	Audioqram
Аудиометр	Audiometer	Audimetr
Ауксохром	Auxochrome	Auksoxrom
Аустенизация	Austenitizing	Austenizləmə
Аустенит	Austenite	Austenit
Аустенитная структура	Austenitic structure	Austenit quruluşu
Аустенитное зерно	Austenitic grain	Austenit toxumu
Аустина формула	Austina formula	Austin düsturu
Аутооксидация	Autoxidation	Autooksidləşdirmə
Афелий	Aphelion	Afeliy
Афокальная система	Afocal system	Afokal sistem
Аффинная алгебраическая группа	Affine algebraic group	Afin cəbri qrupu
Аффинная геометрия	Affine geometry	Afin həndəsəsi
Аффинная дифференциальная геометрия	Affine differential geometry	Afin differensial həndəsəsi
Аффинная кривизна	Affine curvature	Afin əyriliyi
Аффинная связность	Affine connection	Afin rabitəliyi
Аффинное отображение	Affine mapping	Afin inikası (əks etməsi)
Аффинное преобразование	Affine transformation	Afin çevrilməsi
Аффинное пространство	Affine space	Afin fəzası
Аффинно-конгруэнтный	Affinely congruent	Afin-konqruent
Аффинные координаты	Affine coordinates	Afin koordinatları
Аффинор	Affinor	Afinor
Ахромазия	Achromasia	Axromaziya
Ахромат	Achromat	Axromat
Ахроматизм	Achromatism	Axromatizm
Ахроматическая линза	Achromatic lens	Axromatik linza
Ахроматическая призма	Achromatic prism	Axromatik prizma
Ахроматический цвет	Achromatic color	Axromatik rəng
Ацетилено-кислородное пламя	Oxyacetylene flame	Asetilen-oksigen alovu
Ацетон	Acetone	Aseton
Ацидиметрия	Acidimetry	Asidimetriya
Ациклический	Acyclic	Asiklik
Ациклическое соединение	Acyclic compound	Asiklik birləşmə
Аэрация	1) Aeration 2) Aerification	Aerasiya
Аэрогель	Aerogel	Aerogel
Аэрография	Aerography	Aeroqrafiya
Аэрограмма	Aerogram	Aeroqram
Аэрограф	Aerograph	Aeroqraf
Аэродинамика	Aerodynamics	Aerodinamika
Аэродинамика разряженных газов	Rarefied gas dynamics	Seyrəldilmiş qazların aerodinamikası
Аэродинамика сверхзвуковых скоростей	Supersonic aerodynamics	Səs sürətindən böyük sürətlərin aerodinamikası
Аэродинамическая интерференция	Aerodynamic interference	Aerodinamik interferensiya
Аэродинамическая крутка	Aerodynamic twist	Aerodinamik burma
Аэродинамическая сила	Aerodynamic force	Aerodinamik qüvvə
Аэродинамическая труба	Wind tunnel	Aerodinamik boru
Аэродинамическая труба больших скоростей	High speed wind tunnel	Böyük sürətli aerodinamik boru
Аэродинамическая труба замкнутого типа	Closed-circuit wind tunnel	Qapalı növlü aerodinamik boru
Аэродинамическая труба кратковременного действия	Intermittent wind tunnel	Qısa müddətli işləyən aerodinamik boru
Аэродинамическая труба малой плот-	Low-density wind tunnel	Kiçik sıxlıqlı aerodinamik boru

ности		
Аэродинамическая труба малых скоростей	Low-speed wind tunnel	Kiçik sürətlərə hesablanmış aerodinamik boru
Аэродинамическая труба переменной плотности	Variable-density wind tunnel	dəyişən sıxlıqlı aerodinamik boru
Аэродинамическая труба разомкнутого типа	Open-circuit wind tunnel	Açıq növlü aerodinamik boru
Аэродинамическая труба с закрытой рабочей частью	Closed-jet wind tunnel	Qapalı işçi hissəli aerodinamik boru
Аэродинамическая труба с открытой рабочей частью	Open-jet wind tunnel	Açıq işçi hissəli aerodinamik boru
Аэродинамическая характеристика	Aerodynamic characteristics	Aerodinamik xarakteristika
Аэродинамические весы	Aerodynamic balance	Aerodinamik tərəzi
Аэродинамический нагрев	Aerodynamic hearting	Aerodinamik qızma
Аэродинамический след	Aerodynamic wake	Aerodinamik iz
Аэродинамический фокус	Aerodynamic center	Aerodinamik fokus
Аэродинамическое качество	Lift-drag ratio	Aerodinamik keyfiyyət
Аэродинамическое сопротивление	Aerodynamic resistance	Aerodinamik müqavimət
Аэрозоль	Aerosol	Aerozol
Аэролит	Aerolite	Aerolit
Аэрологическая карта	Upper-air chart	Aerologik xəritə
Аэрологическая обсерватория	Aerological observatory	Aerologik observatoriya
Аэрологический анализ	Upper-air analysis	Aerologik analiz (təhlil)
Аэрология	Aerology	Aerologiya
Аэромагнитометр	Airborne magnetometer	Aeromaqnitometr
Аэромеханика	Aeromechanics	Aeromexanika
Аэронавт	Aeronaut	Aeronavt
Аэронавтика	Aeronautics	Aeronavtika
Аэрономия	Aeronomy	Aeronomiya
Аэроплан	Airplane	Aeroplan, təyyarə
Аэроснимок	Aerial photography	Aeroşəkil
Аэростат	Ballon	Aerostat
Аэростатика	Aerostatics	Aerostatika
Аэростатическая сила	Aerostatic force	Aerostatik qüvvə
Аэросфера	Aerosphere	Aeromühit
Аэротермоупругость	Aerothermoelasticity	Aerotermoelastiklik
Аэрофотограметрия	Aerophotogrametry	Aerofotoqrametriya
Аэроупругость	Aeroelasticity	Aeroelastiklik